UNIVERSIDAD DE CHILE
FACULTAD DE CIENCAS FÍSICAS Y MATEMÁTICAS
DEPARTAMENTO DE GEOLOGÍA

EFFECTS OF HYDROGEOCHEMISTRY ON THE MICROBIAL ECOLOGY FROM GLOBALLY DISTRIBUTED HOT SPRINGS

TESIS PARA OPTAR AL GRADO DE MAGÍSTER EN CIENCIAS, MENCIÓN GEOLOGÍA

CARLA VALENTINA BARBOSA TRONCOSO

PROFESOR GUÍA:
DIEGO MORATA CÉSPEDES

PROFESORA CO-GUÍA:
BEATRIZ DÍEZ MORENO

COMISIÓN:
LINDA DANIELE

Este trabajo ha sido financiado por el Centro de Excelencia en Geotermia de los Andes (CEGA), Proyectos ANID-Fondap 15090013, 15200001 y ACE210005; el Proyecto FONDECYT-CONICYT 1190998 y la Beca de Magíster Nacional ANID 22200311

SANTIAGO DE CHILE

2022

RESUMEN DE LA TESIS PARA OPTAR AL GRADO DE: Magíster en Ciencias, Mención Geología
DE: Carla Valentina Barbosa Troncoso
FECHA: 2022
PROFESOR GUÍA: Diego Morata C.

EFECTO DE LA HIDROQUÍMICA EN LAS COMUNIDADES MICROBIANAS DE FUENTES TERMALES

Las fuentes termales son ecosistemas naturales que albergan una gran diversidad de microrganismos adaptados a vivir a altas temperaturas y, en algunas ocasiones, a valores extremos de pH y elevadas concentraciones de metales. Por su parte, la química de estas fuentes termales depende de los diferentes procesos hidrotermales y geotermales que ocurren en subsuperficie. Cómo pueden influir indirectamente estos procesos a través de la química del agua en la diversidad, identidad y estructura de las comunidades microbianas termales, es una interrogante que hasta la fecha ha sido vagamente abordada.

En esta investigación se analizan secuencias del gen ARN ribosomal 16S y los valores de temperatura, pH, conductividad eléctrica y elementos mayores de 11 fuentes termales del campo geotermal El Tatio (Chile) en conjunto con datos preexistentes de otras 191 fuentes termales de la Zona Volcánica Taupo (Nueva Zelanda), Yellowstone (Estados Unidos) y la zona oriental de la Meseta Tibetana (China). El principal objetivo es comparar las comunidades microbianas termófilas de las cuatro zonas de estudio e identificar posibles relaciones entre ellas, la hidroquímica, el contexto geodinámico y los procesos geotermales a los que se ven sometidos los fluidos termales.

Dentro de los principales resultados, se obtiene que la riqueza de las comunidades microbianas es menor en aguas de tipo ácido-sulfatadas y que ésta no depende de la temperatura. Además, mediante un análisis de componentes principales (PCA) de los parámetros químicos, un escalado multidimensional de las secuencias analizadas (MDS) y un análisis de varianza multivariante permutacional (PERMANOVA), se obtiene que los parámetros químicos que mayormente se relacionan a la estructura de las comunidades microbianas son temperatura, concentraciones de Mg^{2+} y Si (PC4) que explican un 7.4% de la varianza y pH, y concentraciones de SO_4^- y Mg^+ (PC2), que explican un 5%. Por otro lado, los parámetros que mayormente condicionan las comunidades a nivel de *Phylum* y familias específicas son el pH y las concentraciones de SO_4^-. Como la varianza de estos de parámetros se explica principalmente por la formación de aguas vapor calentada, se propone que este mecanismo de generación de acidez tiene especial relevancia en la diversidad, identidad y estructura de las comunidades termales, condicionando en parte la disponibilidad de energía como compuestos inorgánicos. Sin embargo, teniendo en cuenta que todos los factores químicos considerados sólo explican el 25% de la varianza de los datos, se plantea que las comunidades microbianas son modeladas por complejas interacciones bióticas y abióticas que van más allá de los parámetros analizados. Además, se obtiene que la distancia geográfica no explica los cambios en la composición de las comunidades microbianas analizadas y que dichas comunidades se encuentran relacionadas taxonómicamente. Lo anterior da cuenta del gran potencial que tienen estos ecosistemas para resolver interrogantes asociadas a la teoría de nichos.

Se concluye que esta investigación aporta en el entendimiento de la ecología microbiana a escala global y es una primera aproximación al estudio de la historia evolutiva de las comunidades microbianas termales en sintonía con los procesos geológicos que han ido ocurriendo desde el origen de la vida. Este enfoque tiene además potenciales repercusiones en la búsqueda de la vida más allá de la Tierra.

AGRADECIMIENTOS

En primer lugar, quiero agradecer al Dr. Diego Morata por motivarme a “hacer cosas nuevas” como me dijo un día cuando comenzamos con esta investigación. Gracias por la oportunidad brindada y por la confianza depositada en mi trabajo. En segundo lugar, le agradezco a la Dra. Linda Daniele por su buena disposición y constante apoyo en asuntos académicos y no académicos. En tercer lugar, agradezco profundamente a la Dra. Beatriz Diez por todo lo que he aprendido de microorganismos en ambientes extremos. Gracias por abrirme las puertas de su grupo de investigación y por el tremendo ejemplo de liderazgo, talento, vocación y entrega hacia sus alumnos. Gracias a los tres profesores miembros de la comisión por sus contribuciones y correcciones que permitieron que esta tesis fuera posible.

Por otro lado, quiero agradecer al proyecto Centro de Excelencia en Geotermia de los Andes (CEGA) Proyectos ANID-Fondap 15090013, 15200001 y ACE210005, al proyecto “El Tatio geysers field as a model system to study virus-host interactions and local adaptations” (FONDECYT-CONICYT 1190998) y a la Agencia Nacional de Investigación y Desarrollo (ANID, Becas de Magíster Nacional 22200311) por financiar esta investigación. Agradezco también a la Iniciativa de Investigación UnACh 2020-132-Unach por el apoyo en la publicación del manuscrito fruto de esta tesis.

De manera muy especial quiero agradecer a las comunidades de Toconce y Caspana que permitieron el acceso al campo geotermal el Tatio, autorizando la realización de este estudio.

Gracias a todos los miembros del BDLab de quienes he aprendido muchísimo en las reuniones de los martes y en los terrenos al Tatio. Gracias por sus buenas ideas y consejos amistosos, ha sido un placer conocerlos a todas y a todos. En particular quiero agradecerle a Javier, un excelente compañero de trabajo y mentor. Gracias también a Jaime por sus sabios consejos y su excelente disposición a resolver mis dudas en todo momento. Los admiro a ambos. A Oscar, Sergio y Christina por el trabajo y buenas conversaciones en terreno y a todos quienes participaron del muestreo de octubre 2021, que fue una gran instancia de aprendizaje y compartir. Finalmente, le agradezco a Johanna por todo el trabajo logístico que significaron mis muestras, sobre todo por las extracciones en tiempos de cuarentena y a Pablo por su apoyo con los servidores.

A todos quienes me ayudaron en el desafiante proceso de escritura de esta tesis: Sebastián y Catalina del Centro de Escritura Armadillo Lab de la FCFM; a Cristian, Nancy y Violeta que amablemente se ofrecieron a apoyarme con el inglés. También quiero agradecerles a Verónica, Erika y Samuel del Laboratorio de Geoquímica de Fluidos del CEGA por los análisis químicos. Muchas gracias también a Maritza del Departamento de Geología por su constante preocupación y ayuda.

Por último, quiero agradecerle a mi familia y amigos. A mi mamá Carla, mi papá Iván, mi hermana Paulina, a Anita, Lorena, Marcos, Daniel y Claudio. A mis amigos y amigas incondicionales y a aquellos que han ido apareciendo en el camino. A mis tías y primos. Gracias por todo el apoyo, las palabras de aliento, los abrazos cálidos en momentos oportunos, el cariño y tiempo compartido con Amaro, la comida rica, los momentos gratos y el amor recibido, que muchas veces fue a la distancia. Y gracias también a muchas personas a quienes podría estar agradeciéndoles durante hojas, porque esta tesis de magíster fue posible gracias al tiempo y cariño de muchos seres de luz.

No me queda más que darle las gracias a Alejandro y a Amaro, los chinitos. Son lo máximo.

TABLE OF CONTENT

FIGURES INDEX

Supplementary Figures

TABLES INDEX

Supplementary Tables

CHAPTER 1: INTRODUCTION

1.1. Motivation

The interaction of microorganisms with geological processes, known as geomicrobiology, has a tremendous potential to provide comprehensive answers to questions posed by the geosciences. The link between both areas of knowledge was recognized in 1887 when Winogradsky proposed two metabolisms that use inorganic compounds to obtain energy: chemolithotrophy and autotrophy (Bender et al., 2019a; Winogradsky, 1887). However, it was not until the beginning of the 1980s that geomicrobiology took on greater relevance (Lutz et al., 2016) contributing to numerous topics such as the study of biogeochemical cycles, sedimentology, mineralogy, mining, astrobiology, and bioremediation.

Studying the impact of the geosphere in microbial life, which is turning this perspective 180º (Druschel and Kappler, 2015), has been mainly focused on the understanding of the origin of life and on elucidating how geological processes affect biogeochemical cycles (geobiochemistry) (Shock and Boyd, 2015). Nevertheless, the more we know about the interactions of biotic and abiotic components of an environment, the more interrelations we observe between Earth and biological sciences. Along this line, if environmental parameters influence the composition of a microbial community and these parameters are explained through geological processes, a connection between microbial life and Earth's processes is identified.

Terrestrial hot springs are ecosystems where relevant biotic-abiotic interactions occur. Temperature and water chemistry lead to environmental conditions that limit life in many of its forms. However, the last few decades have shown how diverse thermophilic communities can be. Thermal water become a source of chemical energy that some microorganisms can use by developing specific metabolic pathways based on the available chemical compounds. The chemistry of terrestrial hot springs is determined by the origin of water, the lithology of the reservoir, and secondary geothermal processes, which yield thermal features of diverse compositions in the same geothermal systems. Therefore, looking at hot springs' geochemistry caused by geological processes represents an opportunity to link microbial ecology with geothermal processes.

Thermal ecosystems can host thermophiles, hyperthermophiles and in some cases provide the conditions for polyextremophiles microorganisms to develop. The relevance of extremophiles inhabiting hydrothermal systems lies in their multiple biotechnological applications, not to mention that they are believed to be the microorganisms from which life began. The present study aims to (1) elucidate how microbial communities respond to geochemical changes in thermal water, (2) relate those geochemical changes to hydrothermal processes, and (3) compare microbial communities from geothermal areas located thousands of kilometers apart, which is also an opportunity to evaluate their geographic distribution with an ecological approach.

1.2. Objective

The main purpose of this thesis is to determine if there is an influence of the geological setting and local geothermal processes on the structure and composition of the microbial communities inhabiting terrestrial hot springs, through their physicochemical parameters and the concentration of their major elements.

Specific

1. Describe the analyzed hot springs in terms of physicochemical parameters and major ion concentrations.
2. Identify the main geothermal processes involved in the chemistry of thermal waters.
3. Characterize the thermal microbial communities populating the analyzed hot springs in terms of their alpha diversity, beta diversity, and composition.
4. Statistically compare the hydrochemistry of the hot springs and their microbial communities.
5. Establish whether the diversity and composition of the microbial communities respond to certain geological elements through hydrochemistry.

1.3. Hypotheses

Geological settings and local geothermal processes regulate the chemistry of hot springs and have an influence in the structure and composition of the microbial communities that inhabit them.

1.4. Thesis structure

This thesis is divided into four chapters: Chapter 1 contains the introduction of the scientific problem addressed. Then, a theoretical framework is presented in Chapter 2 which briefly introduces the reader to geothermal systems and microbial life from terrestrial hot springs. Chapter 3 consists of a draft of the manuscript titled “Effects of hydrogeochemistry on the microbial ecology of terrestrial hot springs” which will be submitted for publication in the following weeks. The main conclusions of the study are presented in Chapter 4.

CHAPTER 2: THEORETICAL FRAMEWORK

2.1. Geothermal systems

The Earth's internal heat is a renewable source of energy that can be exploited due to the circulation of fluids through the upper kilometers of its crust. The Earth's heat comes from (1) the gravitational energy released in the formation of Earth commonly called primordial heat and (2) from the decay of radioactive elements such as potassium, uranium, and thorium (Gupta and Roy, 2005; White, 2005). Geothermal provinces are preferentially located in tectonically or volcanically active zones where geothermal gradients are anomalously elevated. They are found associated with magmatic arcs, hotspots, transtensional pull-apart basins, and magmatic or non-magmatic rifts (Jolie et al., 2021).

The formation of natural geothermal systems involves the local availability of the following elements (Gupta and Roy, 2005; Moeck, 2014):

1. A source of heat. The classic and most intuitive example is a magma body. However, it is also possible to attribute the origin of the heat to a cooling plutonic body or to the elevated geothermal gradient of the zone.

2. Fluid recharge. Fluids that circulate and favor the heat transfer from the heat source to the shallowest levels of the crust. It is known -from stable isotopes- that these cold fluids are mainly meteoric water and/or seawater.

3. Permeable rocks. Sequences that allow the displacement of fluids and their cumulation, fulfilling the role of a geothermal reservoir.

4. A caprock. Impermeable rock that isolates the reservoir trapping hot fluids rising from deep zones, and it is a barrier against cold water infiltration. This capping structure usually contains impermeable minerals such as clays formed by hydrothermal alteration.

Geothermal fluids occur as liquid, steam, or as a combination of these two phases. They have been classified by many authors into primary and secondary fluids. The former is defined as the ones found at the bottom of the convection cell (Arnórsson et al., 2007). The composition of these fluids depends on their source, the proportion of magmatic fluids in zones of active magmatism (Giggenbach, 1988a; Stewart and Hulston, 1975), and the type of rock through which it circulates. On the other hand, secondary fluids form due to depressurization boiling and the mixing of rising primary fluids. The leading processes during this ascent are the following (Arnórsson et al., 2007; W F Giggenbach, 1991; Kaasalainen and Stefánsson, 2012; Nicholson, 1993; Nordstrom et al., 2009):

- Despressuration boiling
- Phase separation
- Vapor condensation
- Mixing with other fluids. When these fluids are shallower and cooler groundwater, the process is called dilution.
- Water-rock interaction as primary mineral dissolution or precipitation of alteration mineralogy (Daniele et al., 2020; Hedenquist, 1991; Roulleau et al., 2016; Wrage et al., 2017).

Fluid geochemistry of surficial thermal features is an important piece of geothermal exploration in all stages (Nicholson, 1993). Water chemistry and stables isotopes are used to determine the source of the

fluids, establish the equilibrium of the fluids with the aquifer rock, estimate the temperature in the reservoir (geothermometry), define the main water-rock interactions in the system and the dominant secondary processes taking place.

2.2. Microorganisms in terrestrial hot springs

Glaciers, water bodies with extremely high salinities, terrestrial hot springs, hydrothermal vents in the deep sea, or courses of acid mine drainage are examples of extreme environments where temperature, pH, redox potential, salinity, hydrostatic pressure, toxic compounds, nutrient concentration, radiation, or a combination of these parameters limit the existence of a particular group of organisms. Many times, microorganisms are the only forms of life that can thrive under these environments, thanks to different mechanisms of adaptation. Furthermore, for every extreme condition a variety of microorganisms not only tolerate this harsh condition, but they often require it to survive (Rampelotto, 2010) and what could represent an extreme condition for one group may not be for another.

To date, the molecular basis for adaptation at high temperatures is the most studied mechanism of survival in extreme conditions. Extremely high temperatures can be naturally found in terrestrial hot springs and hydrothermal vents which also provide the most ancient continuously inhabited ecosystem on Earth (Reysenbach and Shock, 2002). Hydrothermal ecosystems are home to thermophiles, whose growth temperature optimum is over 45°C, and hyperthermophiles, whose optimum exceeds 80°C (Bender et al., 2019b). To date, the most resistant known bacterial and archaeal microorganisms can grow at temperatures as high as 95°C and 122°C (Takai et al., 2008) respectively. By comparison, *Eukarya* can't survive temperatures over 65ºC. This fact explains that thermophiles are mostly from *Bacteria* and *Archaea* domains and hyperthermophiles belong mainly to the *Archaea* domain. These temperatures are handled by microorganisms due to a variety of cellular adaptations. Their membrane lipids contain more saturated and straight-chain fatty acids that provide the right fluidity to the membrane and prevent the cell to disrupt (Bender et al., 2019b). Proteins of thermophiles are also heat-stable by being smaller, more basic, or even through the action o chaperones which help to refold denatured proteins (Rampelotto, 2010).

Terrestrial hot springs are a particular environment where extremely high temperatures are found. Beside hot, thermal water can be very acidic due to gases discharges from the geothermal reservoir or by biogeochemical processes. Two examples are the production of sulfuric acid from hydrogen sulfide in oxidating conditions and the extraction of energy from hydrogen sulfur by chemoautotrophic microorganisms (Brock, 1978). Consequently, many thermophiles are also adapted to highly acid conditions. In that case, they are called acidophiles if their growth pH optimum is below 3 (Baker-Austin and Dopson, 2007). In terrestrial hot springs, acidophiles are commonly related to the sulfur, hydrogen, iron, or arsenic cycles (Urbieta et al., 2015). The most extreme acidophiles living at high temperatures were isolated from volcanically heated soils in Japan. They were two species of the *Picrophilus* genus that were able to grow at pH 0.7 (Schleper et al., 1995).

Salinity may also be a limitation to the development of life in terrestrial hot springs, especially in geothermal systems influenced by marine water or evaporitic rock sequences. Microorganisms whose optimally growth in high salinity waters are classified as slight (0.2-0.5 NaCl M), moderate (0.5-2.0 NaCl M), borderline extreme (2.0-3.0 NaCl M) and extreme (3.0-4.0 NaCl M) halophiles (Wakai, 2019). Moderate to extreme halophiles are more commonly found in marine than in terrestrial hot springs because of the salinity of the latter does not normally exceed 0.5 M.

2.2.1. Metabolic pathways

Cells maintain homeostasis through biochemical reactions which are referred collectively to as the metabolism. Catabolism is all the energy-yielding reactions that require chemicals or light (**Figure 2.1**). When microorganisms tap the energy available from the oxidation of organic compounds, they are called chemoorganotrophs. If they take advantage of inorganic compounds, they are called chemolithotrophs. On the other side, if the source of energy is light, microorganisms receive the name of phototrophs. Phototrophs contain pigments that convert light energy into ATP in a reaction that can produce O_2 or not. The former is called oxygenic photosynthesis, which is characteristic of cyanobacteria and algae. The latter is called anoxygenic photosynthesis and is carried out mainly by purple bacteria, green bacteria, and heliobacteria.

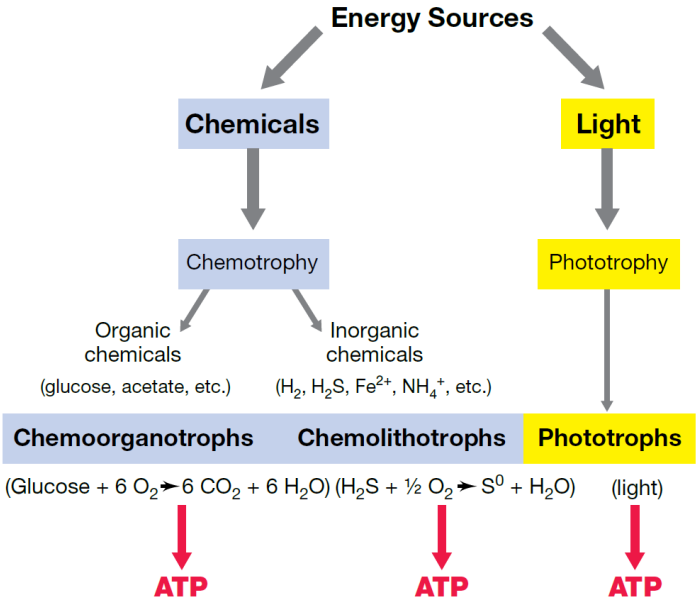

Figure 2.1 Energy sources that microorganisms can use. Obtained from (Bender et al., 2019b)

The metabolic strategies in natural ecosystems are highly determined by the physical and geochemical properties of the environment (Alsop et al., 2014). Particularly, chemical sources of energy have a protagonist role in hot spring ecosystems, especially at temperatures >75 ºC where photosynthesis may not occur (Cox et al., 2011). Examples of metabolic strategies used by chemolithotrophs in these ecosystems are hydrogen oxidation, sulfur oxidation, ferric ion reduction, and sulfate reduction. Microorganisms catalyze oxidation-reduction reactions that are out of equilibrium (Shock et al., 2005) to obtain energy. This chemical energy can be quantified using the Gibbs energy of the study system to calculate the amount of energy that can be released from every feasible reaction. Using this principle, Shock et al. (2005) proved that hydrogen oxidation was the most favorable strategy to support life in a hot spring in Yellowstone National Park.

2.2.2. Biogeography and environmental factor

Populations of thermal microorganisms have unique properties that differentiate them from non-thermal environment microbiomes (Inskeep et al., 2013b, 2013a; Li and Ma, 2019; Li et al., 2014). 'Everything is everywhere, and nature selects' has been best applied to microbial biogeographic in marine environments (e.g., Ionescu et al., 2010), while genetic speciation seems to dominate in isolated environments, such as terrestrial hot springs. In the latter, microorganisms are adapted to conditions that are different from the surrounding air or water through which they would have to disperse. Thus,

geographic isolation may be relevant in the survival and diversification of these microorganisms (Papke et al., 2003).

On the other hand, environmental parameters such as temperature, pH, and chemical composition have been shown to have great influence in shaping hot springs microbial communities (e.g., Massello et al., 2020; Power et al., 2018; Zhang et al., 2018). This influence is subjected to the studied system and the analyzed samples, implying that there is no general rule as to how these microorganisms are influenced by these environmental factors. However, it has been showed that extremely high temperatures and acidic pH values limit diversity in terrestrial hot springs (Chan et al., 2017; Inskeep et al., 2013a, 2013c; Podar et al., 2020; Power et al., 2018; Sharp et al., 2014).

The role of geographic isolation and environmental variables in specific thermal taxa has been also analyzed. Papke et al. (2003) studied the influence of geographic isolation in hot spring populations of the cyanobacterium *Synechococcus.* These authors did not find any correspondence between these cyanobacteria and the 20 hydrochemical variables analyzed. They concluded that geographic isolation had a role in the observed evolutionary divergences. Similarly, Whitaker et al. (2003) showed that populations of *Sulfolobus* hyperthermophilic archaea located at different sites differ between them, implying differentiation and divergence due to geographic isolation.

Despite no clear relationship exists between environmental parameters and the structure and composition of thermal microbial communities worldwide, some taxa seem to be related to certain temperature and pH ranges. In near-neutral to alkaline pH and temperatures below 75ºC, the most found phyla are *Cyanobacteria*, *Chloroflexi*, and *Proteobacteria* (Alcamán et al., 2015; Alcorta et al., 2018a; Amin et al., 2017; Cole et al., 2013; Hamilton et al., 2019; Wang et al., 2013). Similarly, other phyla such as *Planctomycetes* and *Firmicutes* also increase in abundance at pH above 4.5 (Sharp et al., 2014). At these physicochemical conditions, microorganisms can form phototrophic mats. Above 75 ºC and neutral pH, *Aquificae*, *Crenarchaeaota, Deinococcus-Thermus*, *Thermodesulfobacteria*, and *Thermotogae* are the dominant phyla (Cole et al., 2013; Hou et al., 2013; Inskeep et al., 2013b; Podar et al., 2020; Wang et al., 2013; Zhang et al., 2018).

In contrast, hot springs with low pH values harbor thermoacidophilic Bacteria and Archaea that use chemical sources of energy such as members of the *Acidithiobacillus, Sulfolobales, Thermoproteales*, and *Desulfurococcales* genus (Inskeep et al., 2013a; Kozubal et al., 2012). Members of the *Acidithiobacillus* bacteria genus have the capability of oxidizing various reduced inorganic sulfur compounds and, in some cases, ferrous iron to obtain energy for carbon dioxide fixation (Quatrini and Johnson, 2019). Likewise, members of the *Sulfolobales* genus obtain energy by oxidizing sulfide, sulfur, thiosulfate, and ferrous iron and *Firmicutes* and *Thermales*, grow chemoorganotrophically in acidic environments on several organic substrates (Hou et al., 2013).

2.2.3. Habitat

Thermal ecosystems support microorganisms living associated with sediments, water columns, or forming filaments to more complex microbial mats. It has been observed ecological differentiation in the microbial communities inhabiting sediments, water, and biofilms (Cole et al., 2013; Colman et al., 2016; Uribe-Lorío et al., 2019).

Adherence is a strategy that many microorganisms use to form microbial biofilms with different levels of complexity, which impacts their preservation potential. Microbial mats are complex biofilms that comprise communities of different species embedded in a matrix of exopolysaccharides and nutrients (Prieto-Barajas et al., 2018). These vertically layered structures involve microorganisms from the *Bacteria* domain, but *Archaea* and *Eukarya* can also be present. The most ancient microbial mats discovered dated

to 3.5 Ga (Djokic et al., 2017; Seckbach and Oren, 2010), which convert them to the first evidence of visible life on Earth preserved in the geological record, as stromatolites.

Phototrophic microbial mats can grow in terrestrial hot springs. These communities are limited to temperatures below 75 °C, which is the temperature of chlorophyll degradation. The most abundant phylum that form these mats are *Cyanobacteria*, *Proteobacteria*, *Chloroflexi*, *Bacteroidetes*, and *Deinococcus-Thermus* (Alcorta et al., 2018a; Mackenzie et al., 2013; Prieto-Barajas et al., 2018). On the other hand, acid microbial mats can be formed by non-photosynthetic groups and have communities that oxidate iron and sulfur minerals (Prieto-Barajas et al., 2018). These mats are mostly found in courses of acid mine drainage, but they can also grow in acidic springs as have been observed in Yellowstone National Park (Inskeep et al., 2013a, 2013b; Kozubal et al., 2012).

2.2.4. Metagenomics

One of the main sources of current information in the study of microorganisms is their genetic material. The early development of DNA sequencing started with the Sanger method proposed by Frederick Sanger in 1977 who won a Novel Prize for this accomplishment (Bender et al., 2019b). This method was limited to around 800 nucleotides per reaction so large DNA molecules must be cut and cloned to be sequenced (Bender et al., 2019b). New technologies of sequencing have been developed in the last years, known as Next-Generations Sequencing (NGS), that can sequence hundreds to thousands of genes at one time.

Genomics is the study of the complete genetic complement of a single organism. In contrast, metagenomics involves the total present DNA of a sample. It has become a basic technology to the understanding of microbial ecology and evolution in many environments, including terrestrial hot springs. Typically, two sequencing strategies have been used to identify and compare microbial communities: (1) amplicon sequencing which captures a phylogenetic marker, and (2) shotgun sequencing which captures the totality of DNA within a sample.

Amplicon sequencing obtains the sequence of a PCR fragment that targets a specific region of a chosen gene, which depends on the study of microorganisms. The 16S ribosomal RNA gene has been extensively used for bacterial recognition, making great contributions to the characterization of microbial community structure over the past decades (Tringe and Hugenholtz, 2018). This gene contains nine hypervariable regions (V1-V9) that have the information to establish the taxonomy and phylogeny of a microbial community. However, it does not provide clues to the functional capacity of a community. The main steps to sequence with this strategy are:

1. Sampling microbial communities
2. DNA extractions
3. Amplification of the 16S rRNA targeted region
4. Sequencing
5. Grouping similar sequences in operational taxonomic units (OTUs) or detection of single DNA sequences in amplicon sequence variants (ASVs). The latter method provides more reusability, reproducibility and comprehensiveness that the former. Thus, it has been proposed that ASVs should replace OTUs as unit of marker-gene analysis (Callahan et al., 2017).
6. Identification of OTUs or ASVs using databases.

CHAPTER 3:EFFECTS OF HYDROGEOCHEMISTRY ON THE MICROBIAL ECOLOGY OF TERRESTRIAL HOT SPRINGS

Carla Barbosa †, Javier Tamayo-Leivab,c,d †, Jaime Alcortab, Oscar Salgadob,e, Linda Danielea, Diego Morataa, Beatríz Díezb,c,d *

[1] *Department of Geology and Andean Geothermal Center of Excellence (CEGA-Fondap), Santiago, Chile.*
[3] *Department of Molecular Genetics and Microbiology, Pontifical Catholic University of Chile, Santiago, Chile.*
[4] *Center for Climate and Resilience Research (CR)2, University of Chile, Santiago, Chile.*
[5] *Center of Genome Regulation (CGR), University of Chile, Santiago, Chile.*
[6] *Laboratorio de Bioinformática, Facultad de Educación, Universidad Adventista de Chile, Chillán, Chile.*

***** Correspondence: Beatriz Diez (bdiez@bio.puc.cl)
† These authors have contributed equally to this work

Keywords: 16S rRNA gene, Geothermal field, Alpha and beta diversity, thermal water, co-occurrence networking.

3.1. Abstract

Temperature, pH and hydrochemistry of terrestrial hot springs play a critical role in shaping thermal microbial communities. However, the interactions of biotic and abiotic factors at this terrestrial-aquatic interface are still not well understood on a global scale, and the question of how underground events influence microbial communities remains open. To answer this, 11 new samples obtained from the El Tatio geothermal field (Chile) were analyzed by 16S rRNA amplicon sequencing (V4 region), along with 191 samples from previous publications obtained from the Taupo Volcanic Zone (New Zealand), the Yellowstone Plateau Volcanic Field (United States of America), and the Eastern Tibetan Plateau (China), with their temperature, pH, and major ion concentration.

Microbial alpha diversity was lower in acid-sulfate waters than in chloride and bicarbonate waters, and no significant correlations were found with temperature. However, moderate correlations were observed between chemical parameters such as pH (mostly constrained to temperatures below 70 ºC), SO42- and abundances of members of the phyla Armatimonadota, Deinococcota, Chloroflexota, Campilobacterota, and Thermoplasmatota. pH and SO42- gradients were explained by phase separation of sulfur-rich hydrothermal fluids and oxidation of reduced sulfur in the steam phase, which were identified as key processes shaping these communities. No significant geographic distance decay was detected on the microbial communities according to Bray-Curtis, Jaccard, unweighted and weighted Unifrac similarity/dissimilarity indices. Instead, an ancient potential divergence in the same taxonomic groups is suggested between globally distant thermal zones. Ordination and permutational analysis of variance (PERMANOVA) showed that temperature, pH, and major element hydrochemistry explains only 25% of the microbial community structure. Therefore, most of the variance of the thermophilic community remained unexplained, suggesting that other environmental or biotic factors are also involved, and highlighting the environmental complexity of the ecosystem and its great potential to test niche theory ecological associated questions.

3.2. Introduction

Geothermal regions are globally distributed in zones of elevated crustal heat flow, preferentially concentrated in areas of active magmatism and/or crustal thinning (Jolie et al., 2021; Moeck, 2014). Crustal heat transfer is locally enhanced by circulating water, which can reach the surface and form geothermal features. The chemistry of these waters represents an opportunity to explore the processes that occur before the fluids reach the surface. These fluids form primarily from meteoric water and/or seawater (Arnórsson et al., 2007; Chambefort and Stefánsson, 2020) that is heated in the upper first few kilometers of the Earth's crust. Aquifer fluids may undergo compositional changes by depressurization boiling, phase separation, mixing, precipitation or dissolution of minerals or by contributions of magmatic fluids (Arnórsson et al., 2007; Giggenbach, 1991; Kaasalainen and Stefánsson, 2012; Nicholson, 1993).

According to pH and major ion concentrations, hot springs are usually classified into i) NaCl waters, ii) acid-sulfate waters, and iii) HCO3 or CO2-rich waters (Arnórsson et al., 2007; Hedenquist, 1991; Kaasalainen and Stefánsson, 2012; Nicholson, 1993; Nordstrom et al., 2009; Sheppard and Lyon, 1984; White, 1957; Wrage et al., 2017). NaCl waters are distinguished by their near-neutral pH and high concentrations of Cl-. Their major element composition is considered to reflect fluid-mineral equilibrium in the reservoir, except for highly mobile components such as Cl-(Arnórsson and Andrésdóttir, 1995; Giggenbach, 1988). In contrast, acid-sulfate waters are characterized by high concentrations of SO_4^{2-} and low pH values. The acidity is caused by contributions of HCl and SO2 derived from magmatic/volcanic sources or by the joint action of phase separation and mixing of geothermal fluids (Nordstrom et al., 2009; Taran and Kalacheva, 2020). In the latter, reservoir fluids boil during ascent and separate into an H_2S-CO_2-rich steam phase and a liquid-saline phase. The steam phase rises and mixes with shallow or surface groundwater and the available H_2S is oxidized to form SO_4^{2-}. According to geothermal reservoirs conceptual models (Moeck, 2014), the third type of water consists of near-neutral pH bicarbonate-rich waters, preferentially located at the periphery of geothermal systems. These waters may originate from the boiling of a CO_2-rich geothermal fluid, followed by condensation of the steam phase and fluid interaction with the surrounding rocks.

These aqueous environments provided by hydrothermal activity are colonized by microorganisms that overcome extreme conditions such as high temperature, extreme pH values, and high concentration of dissolved mineral species (Inskeep et al., 2013b; Power et al., 2018). These microorganisms take advantage of specific local hydrochemistry through various metabolic pathways (Alcamán-Arias et al., 2018; Dick and Shock, 2013). Complex interactions between the local environmental conditions of the hot springs and their microbial communities have been previously described. In particular, the impact of water temperature, pH, and chemistry on the microbial community structure differs depending on the system studied. It has been suggested that temperature would be the factor that modulates the microbial communities inhabiting hot springs in the Tibetan Plateau (Guo et al., 2020; Wang et al., 2013; Zhang et al., 2018) and Malaysia (Chan et al., 2017). In contrast, pH has been found to be the most critical parameter structuring microbial life in the Taupo Volcanic Zone (Power et al., 2018), and its contribution along with temperature has been shown to strongly influence microbial beta diversity in hot springs in Yellowstone National Park (Colman et al., 2016) and Costa Rica (Uribe-Lorío et al., 2019). In addition to these factors, other chemical parameters such as total and dissolved organic carbon, redox potential, dissolved sulfide, and elemental sulfur have also been shown to impact specific taxa in thermal communities (Inskeep et al., 2013a; Zhang et al., 2018).

However, on a global scale, much less has been studied overall on how thermal microbial communities are structured. Massello et al. (2020) reanalyzed novel and previous data obtained for

geothermal areas in Argentina and Malaysia, New Zealand, India, China, Russia and USA, and were unable to demonstrate a significant effect of temperature and pH on microbial communities, possibly explained by the effect of other multiple factors involved (Massello et al., 2020). Among these other factors, the hydrochemistry of thermal features has been suggested to influence the community due to varied physicochemical drivers (Alsop et al., 2014; Mathur et al., 2007), leading to the question of how geothermal processes such as water-rock interactions, boiling or water mixing affect microbial communities in terrestrial hot springs environments.

Yet, little investigation has been conducted to understand the role of hydrogeochemical processes on the ecology of terrestrial hot springs. Colman et al. (2019a) studied chemosynthetic hot spring communities in Yellowstone National Park and proposed that water acidification generated by phase separation controls the availability of nutrients, which influences the microbial ecology o thermophilic communities. In addition, Colman et al. (2019b) analyzed a chemosynthetic microbial community in Yellowstone National Park and suggested that subsurface and near-surface water mixing play a key role in promoting chemosynthetic biodiversity in geothermal systems. Similarly, Guo et al., (2021) investigated the role of hydrogeochemical processes on the microbial ecology of hot springs in Yunnan Province (China). The authors proposed that shallow circulation and sulfur oxidation accounted for the hydrochemistry of moderate-temperature acidic springs while high-temperature alkaline springs hydrochemistry was the result of deeper fluid circulation. This distinction was recognized as the main contributor to the environmental variations modulating microbial communities in Yunnan.

In the present study, we investigated the influence of hydrothermal processes on the microbial communities inhabiting hot springs at four emblematic geothermal sites worldwide. We carried out this identification by comparing the hydrochemistry and respective microbial communities of 152 hot springs from the Taupo Volcanic Zone (New Zealand), 25 from the Yellowstone Plateau Volcanic Field (The United States of America), 11 from the Altiplano-Puna Volcanic Complex (Chile), and 14 from the Eastern Tibetan Plateau Geothermal Belt (China).

3.3. Study zones

3.3.1. Taupo Volcanic Zone (TVZ)

The TVZ (**Figure 3.1A**) is an active zone of calc-alkaline volcanism and intra-arc rifting derived from westward subduction of the Pacific Plate beneath the North Island (DeMets et al., 1990). As a result, within this approximately 30 km x 150 km extensional basin, voluminous rhyolitic volcanism has been active since 1.6 My ago (Wilson et al., 1995) and hydrothermal activity is concentrated in its central part. Abundant andesitic sequences overlay the basement due to the volcanic activity that started 2 My ago. Rhyolitic pyroclasts and lava flow, mainly discharged by caldera-type volcanoes and Quaternary sediments cover the area (Hochstein, 1995). Structures are NNE-trending faults that extended from Mt. Ruapehu to the Bay of Plenty with a 15-20 km wide rift zone, known as Taupo Fault Belt or Taupo Rift (Cole and Spinks, 2015).

The total geothermal heat flux in the zone has been estimated to be 4.2 ± 0.5 GW (Bibby et al., 1995) and is released mainly in its central part by 23 high-temperature (>250 ºC) geothermal fields (Milicich et al., 2020). These fields occur in specific zones of the TVZ characterized by 1) a strongly fractured subsurface consisting of deep fractures through the greywacke basement that are the preferential pathways for rising fluids, 2) a low-permeability cap overlying the reservoir, and 3) low-topographic terrain (Wilson and Rowland, 2016). The fluid chemistry of the thermal features greatly varies between

and within geothermal systems. Deep geothermal fluids, which reach over 300ºC (Millot et al., 2012), consist of water, carbon dioxide, and chloride as their most important components (Giggenbach, 1995). This water is predominantly of meteoric origin with proportions of magmatic inputs. Giggenbach (1995) defined one group of fluids linked to arc-type magma while another linked to rift-type magmas. The first group is likely to receive inputs from gas-depleted melts and includes geothermal fields in the western part of the TVZ. The second is more likely to be associated with highly volatile-charged magmas in the eastern part of the TVZ. However, (Bégué et al., 2017) proposed that fluids linked to arc-type magmas were actually derived from a rhyolitic melt in equilibrium with a highly crystalline andesitic magma.

3.3.2. Yellowstone Plateau Volcanic Field (YPVF)

The YPVF (**Figure 3.1B**), located in Yellowstone National Park (YNP) in Wyoming, Idaho, and Montana (United States of America), has been formed over the past 2.1 Ma due to intraplate hotspot activity. Three cataclysmic volcanic eruptions have been reported in that period (Christiansen, 2001) producing mainly rhyolitic lava flows, sequences of ash-flow tuffs, and basaltic lava flows without intermediate-composition rocks (Hildreth et al., 1991). The latter event, dated to 0.64 Ma, gave rise to the Lava Creek Tuff and the Yellowstone Caldera (Christiansen, 2001).

The YPVF hosts the largest geothermal region in the world. Its surficial manifestations are found primarily within or near to the margin of the Yellowstone caldera or along north-south-trending faults outside the caldera (Rye and Truesdell, 2007). They comprise more than 10000 features, including thermal pools, mud pots, fumaroles, and frying pan (Hurwitz et al., 2020). Geothermal manifestations vary in gas and water composition, having pH values between 1.5 and 10. According to their chemistry and location, two main groups have been proposed by Fournier (Fournier, 1989): 1) neutral to alkaline chloride waters concentrated in low-elevation zones or along the edge of rhyolite flows and 2) acid waters emitted preferentially at high elevations, often in the eastern part of the caldera, where gases such as CO_2, H_2S, H_2, and CH_4 have already been exsolved from alkaline water at greater depths (Hurwitz and Lowenstern, 2014). From hot springs' hydrochemical analyses, deep fluids are known to reach 340 to 370 ºC, which ascend through successively shallower and colder reservoirs (Dobson et al., 2003) where changes in physicochemical conditions lead to water-gas-rock chemical reactions (Hurwitz and Lowenstern, 2014). Mixing water has been also described to produce intermediate-composition manifestations (Fournier, 1989; Nordstrom et al., 2009).

3.3.3. El Tatio (at Altiplano-Puna Volcanic Complex (APVC))

The Andes is an orogenic belt formed due to the subduction of the oceanic Nazca plate under the continental upper South America plate. The APVC located in the Central Volcanic Zone of the Andes, is one of the largest silicic volcanic fields in the world (De Silva, 1989) formed since the Miocene (Salisbury et al., 2011). This area covers more than 50,000 km^2 with an average elevation of 4.4 km (Ward et al., 2014). Quaternary volcanism, active fractures and fault systems in this zone have given the natural conditions to develop high-temperature geothermal systems (Lahsen, 1988; Sanchez-Alfaro et al., 2015), such as El Tatio.

El Tatio (**Figure 3.1C**) is one of the largest and most well-studied geothermal fields in the world. It is located over 4200 meters above sea level, where extreme atmospheric conditions are due to low precipitation and high evaporation rates, high daily temperature oscillations (Nicolau et al., 2014), and high rates of ultraviolet radiation (Phoenix et al., 2006). The local geology is characterized by ignimbrite sequences and Neogene to Quaternary dacitic/andesitic lavas overlaid by glacial, lacustrine, and colluvial quaternary deposits (Marinov and Lahsen, 1984). Structural features contemplate N-striking west verging

thrust faults and NW-striking sinistral faults concentrated to the southeast of the field (Letelier et al., 2021; Veloso et al., 2020). Most of the thermal features are located between these structures and lineaments (Veloso et al., 2020). The geothermal area encloses about 200 thermal features including geysers, fumaroles, hot springs, and mud volcanoes (Glennon and Pfaff, 2003; Letelier et al., 2021); and extensive sinter deposits. The temperature of the thermal fluids can reach 86°C at the surface, which is the boiling point at this altitude, while the pH ranges from 5.5 to 8.2. Fluid's chemistry of the thermal features has shown a particularly saline thermal water due to high concentrations of Cl^- and Na^+. Concentrations of SiO_2, and arsenic can be extremely high as well (Cortecci et al., 2005; Cusicanqui et al., 1975; Giggenbach, 1978; Letelier et al., 2021; Munoz-Saez et al., 2018; Tassi et al., 2010, 2005). Conceptual implications of the system have been deduced: meteoric water recharge at higher altitudes, ~15 to 20 km east of El Tatio (Munoz-Saez et al., 2018), with the Tocorpuri caldera as the main catchment area (Letelier et al., 2021). Two local reservoirs, one deeper and hotter (260-270 ºC) and one shallower and cooler (160-170 ºC) accumulate hot fluids and feed thermal features. In addition, a larger-scale model has been recently proposed (Letelier et al., 2021), that integrates El Tatio into a regional geothermal system that also comprises La Torta dome 10 km southeast of El Tatio. In this model, a third hotter reservoir is proposed below La Torta dome, from which fluids flow sub-horizontally across NW-striking faults and rise at the intersection between the N- and NW-striking faults found in El Tatio (**Figure 3.1C**).

3.3.4. Eastern Tibetan Plateau Geothermal Belt

The Tibetan-Himalayan Plateau has been formed by the collision between the Indian and Eurasian tectonic plates since the early Cenozoic (Yin and Harrison, 2000). The Tibetan Plateau is the largest plateau on Earth (Zhang et al., 2012) and is composed of tectonic terranes accreted to the southern margin of Asia throughout the Phanerozoic (Dewey et al., 1988). In its eastern region, ~4000 m above sea level is located the Songpan-Ganzi complex, a triangular fold belt containing multiple lithospheric-scale strike-slip and thrust fault zones (Tang et al., 2017b). This area is covered by granitic rocks, dated between the Middle Triassic and Cenozoic, and it is bounded to the west by the Yidun arc across the Ganzi Suture (Tang et al., 2017a). The Yidun arc consists of Triassic felsic volcanic rocks overlying Paleozoic passive margin-type sediments (Tang et al., 2017b; Zhang et al., 2002).

In the ETPGB (**Figure 3.1D**) about 250 thermal manifestations are distributed in three geothermal belts, each spatially related to a fault system (Zhang et al., 2017). From west to east (1) the Dege-Batang-Xiangcheng geothermal belt is related to the Dege-Xiangcheng fault system, (2) the Ganzi-Xinlong-Litang geothermal belt to the Ganzi-Litang fault zone, and (3) the Luhuo-Daofu-Kangding geothermal belt to the Xianshuihe fault zone (Zhao et al., 2021). It is believed that reservoir fluids upwelling is favored by the permeability given by these fault systems (Zhang et al., 2017). Tang et al. (2017) proposed two types of geothermal systems. The Kangding-type is characterized by a mantle-derived heat source from the radioactive decay of Cenozoic granite. The main reservoirs are granitic intrusive bodies and Triassic sandstones. On the other hand, the Batang-type systems have a crust-derived heat source that heats Mesozoic intrusive bodies. In both types of systems, the recharge has a meteoric origin.

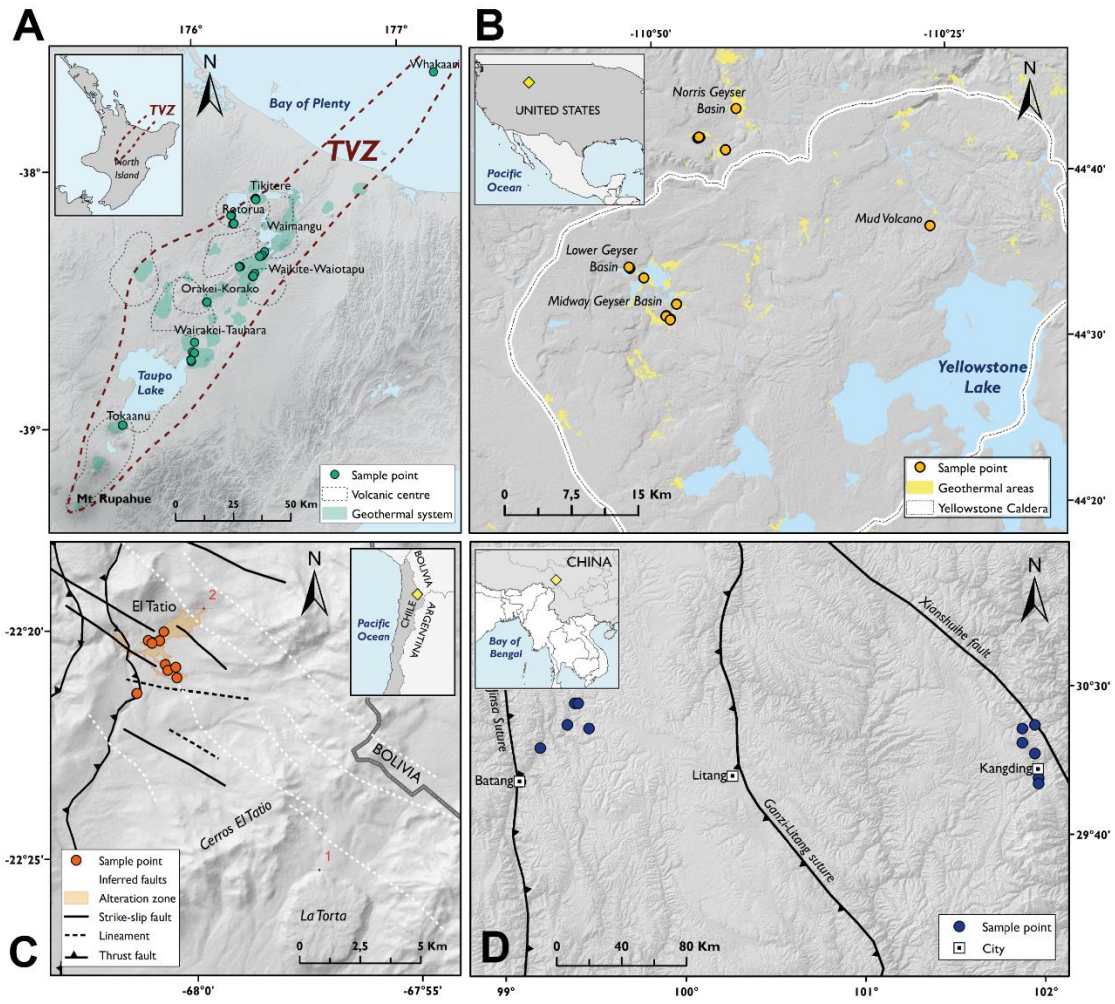

Figure 3.1 Location of the analyzed hot springs. A. Taupo Volcanic Zone (TVZ), B. Yellowstone Plateau Volcanic Field, C. El Tatio at the Altiplano-Puna Volcanic Complex, D. Eastern Tibetan Plateau Geothermal Belt.

3.4. Methodology

3.4.1. El Tatio hot springs sampling and analysis

Water and microbial mat samples were obtained from 11 hot springs of the El Tatio geothermal field in January 2020 (**Figure 3.1A**). Temperature and pH were measured in situ with a WTW Multi340i multiparameter analyzer. Water from the hot springs was collected in 125 mL polyethylene bottles previously rinsed with ultra-pure water and HNO_3 for cation measurements. Water was filtered through 0.45 µm Millipore membrane filters (Merck; Darmstadt, Germany), except the samples for bicarbonate analysis. Samples for cation measurements were acidified with HNO_3 4 N and samples for silica quantification were diluted to 10% v/v. All samples were stored at 4ºC until analysis. Cation concentrations were obtained by Flame Atomic Absorption Spectroscopy (Perkin Elmer Pinaacle 900F) at the Andean Geothermal Center of Excellence (CEGA) of the Geology Department of the University of Chile. Anion quantifications were performed with Ion Chromatography (Thermo Scientific Dionex ICS-2100) and carbonate speciation was carried out by titration with the Giggenbach method (Giggenbach and Goguel, 1989). Chemical analyses were validated by the electroneutrality condition of the solution. The

admitted ionic balance was ± 5 % according to the electrical conductivity of the samples (Custodio and Llamas, 1983).

To sample the microbial communities of the mat, approximately 2 ml of the mat was recovered in duplicate with a cork borer. Samples were preserved in cryogenic vials with RNAlater reagent (Thermo Fisher Scientific) and stored at -80°C until analysis. DNA extractions were carried out according to Alcorta et al. (2018). Briefly, samples were immersed in xanthogenate buffer (1% potassium ethyl xanthogenate (Sigma-Aldrich, USA), 100 mM Tris-HCl (pH 7.4), 20 mM EDTA (pH 8), 800 mM ammonium acetate) and then mechanically shaken (TissueLyzer II, Qiagen) for one minute at 30 revolutions per second. Next, samples were incubated for two hours at 65°C with 10% SDS. After being mixed in a vortex, the samples were immersed in ice for 30 minutes. DNA extraction was performed with phenol-chloroform-isoamyl alcohol (25:24:1), while residual phenol was removed with chloroform-isoamyl alcohol (25:1). Nucleic acid precipitation was carried out within two hours at -80°C with cold absolute isopropanol and 0.4M ammonium acetate. The pellet was washed successively with 70% ethanol. The quality and quantity of the recovered nucleic acids were monitored using 1% agarose gel electrophoresis, Qubit (LifeTechnologies, Carlsbad, California, USA), and Nanodrop (Thermo Fisher Scientific, Waltham Massachusetts, USA). Finally, universal primers 515F (5'-GTGYCAGCMGCCGCGGTAA-3') and 926R (5'-CCGYCAATTYMTTTRAGTTT-3') were used to amplify the V4-V5 hypervariable region of the 16S rRNA gene (Parada et al., 2016). Sequencing of the 22 samples was performed on the Illumina MiSeq platform (Argonne National Laboratory; Lemont, IL, USA). The 16S rRNA sequences of the 11 new samples at El Tatio were submitted to the NCBI Sequence Read Archive (SRA) database under the Bioproject accession number PRJNA825489.

3.4.2. Worldwide hot springs collection data

16S rRNA amplicon sequences from hot springs water (166) and mat (25) samples were retrieved from public databases along with their hydrochemical metadata as follows: the initial 758 16S rRNA amplicon samples found were reduced to 414 due to the large heterogeneity of sampling methods and measured variables. A minimum of 3 and a maximum of 25 sampling points per geothermal field were then imposed, randomly removing samples from sub- and over-represented geothermal systems. The final data set consisted of 191 terrestrial hot springs amplicon samples with their respective geographic location, temperature, pH, and concentrations of Ca^{2+}, Mg^{2+}, Na^{+}, K^{+}, Cl^{-}, HCO_3^{-}, SO_4^{2-}, and SiO_2. This data set belonged to 3 previous publications (Guo et al., 2020; Hamilton et al., 2019; Power et al., 2018) that analyzed 13 geothermal fields (Table 3 1) distributed over 3 zones in New Zealand (TVZ), the United States of America (YPVF), and China (ETPGB). Raw sequences were obtained from the Sequence Read Archive (SRA) database of the National Center for Biotechnology Information (NBCI). The YPVF and the ETPGB metadata were obtained from their respective articles and the TVZ metadata was recovered from the One Thousand Spring project website (https://1000springs.org.nz/). HCO_3^{-} concentrations for the YPVF samples were calculated with the USGS geochemical speciation code PHREEQC (Parkhurst and Appelo, 1999).

3.4.3. Taxonomic assignation

Each set of sequences was individually imported according to their local source into Qiime2 (Bokulich et al., 2018; Bolyen et al., 2019) as demultiplexed sequences. Denoising and resolving the amplicon sequence variants (ASVs) were performed with the DADA2 pipeline (Callahan et al., 2016) yielding a total of 7,505,257 sequences after filtering (**Table 3.4-1**). At this stage, primers were also removed where necessary. Next, sequences were constrained to the V4 region of the 16S rRNA gene with

the cutadapt tool and then taxonomic classification was assigned using the q2-feature-classifier (Bokulich et al., 2018) against the SILVA-138 99% Operational Taxonomic Unit (OTU) reference sequences of the V4 region. After removing the mitochondria and chloroplast sequences, a rooted phylogenetic tree was constructed with fasttree2 (Price et al., 2010). Counts of each ASV and associated taxonomic tables were exported for subsequent statistical and ecological analyses. For the samples that were in duplicates, those with the highest number of reads were chosen for these analyses.

Table 3.4-1 Number of 16S rRNA amplicon sequences from each set of samples before and after filtering.

Source	Country	Study zone	Samples	Geothermal systems	Total sequences	Filtered sequences	Median filtered sequences
Power et al. (2018)	New Zealand	Taupo Volcanic Zone	152	Rotorua (RO), Orakei Koraro (OK), Tokaanu (TK), Tikitere (TT), Waiotapu (WP), Waimangu (WG) Waikite (WK), Wairakei-Tahura (WT), White Island (WI)	9,254,997	6,348,970	26,467
Hamilton et al. (2019)	The United States of America	Yellowstone Plateau Volcanic Field	25	Yellowstone (YE)	1,187,293	843,032	32,110
Guo et al. (2020)	China	Eastearn Tibetan Plateau Geothermal Belt	14	Batang (BT), Kangding (KD)	427,442	360,291	26,041
This paper	Chile	Altiplano Puna Volcanic Complex	11	El Tatio (TT)	389,044	256,760	24,063

3.4.4. Statistical and ecological analysis

An exploratory data analysis was performed on the hydrochemical variables of the 13 geothermal systems. After scaling the data to zero mean and unit variance, Spearman's rank correlation coefficients between these variables were calculated (Kendall, 1948). Next, dimensional reduction of the variables was obtained with principal component analysis (PCA) using the stats package (R Core Team, 2013).

Sequence analyses were conducted in R with the packages phyloseq (McMurdie and Holmes, 2013) and ampvis2 (Andersen et al., 2018). Prior to alpha diversity analyses, rarefaction curves were constructed with the vegan package (Oksanen et al., 2019). Community alpha diversity for all samples was obtained using observed richness and Shannon index (Shannon, 1948). These indices were grouped and displayed according to habitat (water or mat), study zone, and geothermal field. They were then tested for statistical significance using the Kruskal-Wallis test (Kruskal and Wallis, 1952). Spearman's correlation index between richness and hydrochemical variables was calculated for all samples and by study zone. The significant and highest correlations between chemical parameters and alpha diversity in each study zone were then plotted in two-component diagrams.

Prior to beta diversity analyses, read counts were normalized using the DESeq2 package (Anders and Huber, 2010). A multidimensional Metric Scaling (MDS) was performed based on weighted Unifrac distances (Lozupone et al., 2007) which were then used in a permutational analysis of variance (PERMANOVA) (Anderson, 2001) using the adonis2 function of the vegan package with 9,999 permutations using observed richness, habitat (mat or water), and PCA-eigenvectors as explanatory variables.

In addition, to assess the effect of hydrochemical gradients on selected taxa, Spearman's correlation index was calculated between physicochemical parameters and taxa whose relative abundance in their study zone exceeded 0.1% at the phylum and family level. Only taxa with significant correlations ($p < 0.05$) greater than 0.3 were selected and plotted on a heatmap. Then, microbial co-occurrences networks were performed per study zone with the Sparse Inverse Covariance Estimation for Ecological Association Inference method (SPIEC-EASI; Kurtz et al., 2015) and plotted with ggnet (Briatte, 2020).

Finally, a distance decay analysis was conducted based on similarity/dissimilarity indexes: Jaccard (Real and Vargas, 1996), Bray-Curtis (Bray et al., 1957), unweighted Unifrac (Lozupone and Knight, 2005), and weighted Unifrac (Lozupone et al., 2007). Geodesic distances between samples were obtained through the geosphere package (Hijmans et al., 2017) and then, these distances were used to define spatial scales (local: 0 - 58 km; regional: 58 - 279 km; global: 280 – 8,576 km). A linear regression on the logarithmic scale was performed for the 4 indexes and the geodesic distances between samples at each of the three spatial scales, and then their R^2, p-value, and slope were used for further discussion.

3.5. Results and Discussions

According to the criteria applied in the literature search, 9 geothermal fields in the TVZ were included in this study. From south to north these fields were Tokaanu, Wairakei-Tahura, Orakei-Korako, Waikite, Waiotapu, Waimangu, Roturua, Tikitere, and Whakaari (White Island) (**Figure 3.1A**). Likewise, the fields included in the ETPGB were Batang and Kanding (**Figure 3.1D**), the one included in the APVC was El Tatio (**Figure 3.1C**), and the YPVF geothermal system, which is called Yellowstone thereafter (**Figure 3.1B**). The 4 study zones are placed in different tectonic settings, which have fundamental implications for the characteristics of their geothermal systems. Some of them are their thermal regime, heat flow, hydrogeologic regime, fluid dynamics, faults and fractures, stress regime, and lithological sequences. All these properties also influence their fluid chemistry as well as local conditions (Moeck, 2014). This permits the detection of thermal manifestations of very different compositions in the same geothermal field and, at the same time, surface manifestations of different geothermal fields with similar chemical compositions

3.5.1. Hot spring hydrochemistry

Physicochemical parameters and major ion concentrations of the analyzed hot springs covered a broad hydrochemical spectrum (**Supplementary Table 3-2**), which opened the possibility of analyzing microbial communities in different hydrochemical scenarios. Temperatures ranged between 31.5 and 99 °C, pH between 1.5 and 9.9, and electrical conductivity between 236 and 21,000 µS/cm (**Figure 3.2A-C**). Ionic concentrations varied as much as 5 orders of magnitude, such as Cl^-, which ranged from 0.05 mg/l to 7,061 mg/l. SO_4^{2-} concentrations ranged from 1.6 mg/l to 2,418 mg/l and HCO_3^- values ranged from 0 to 1,228 mg/l. As for cationic concentrations, Na^+ values reported the broadest range among the samples ranging from 1.7 mg/l and 4,580 mg/l, followed by K^+ with concentrations between 1.6 mg/l to 508 mg/l. Ca^{2+} and Mg^{2+} values ranged from 0.36 mg/l to 381 mg/l and from 0 to 173 mg/l respectively, and Si

concentrations ranged from 14.06 mg/l to 368 mg/l. Zonal dependence was observed for the hydrochemical ranges, with greater homogeneity in El Tatio and ETPGB samples than in YPVF and TVZ, although ETPGB samples covered a wide temperature range between 37.4°C and 88.2°C.

Samples were plotted on a Piper diagram (Piper, 1944; **Figure 3.2D)** according to their major ions concentration. Cl^- was the dominant anion in 71% of the samples and Na^+ was the dominant cation in 92%, meaning that most of the waters were classified as Na-Cl type. Looking at the scale of the study zone, it was noticed that waters in the APVC were all Na-Cl type, while in the ETPGB there were only HCO_3-type waters. Furthermore, most of the Na-HCO_3 and Ca-HCO_3 samples in the dataset belonged to the ETPGB. As for the YPVF and the TVZ samples, they comprised Na-Cl and Na-SO_4 waters, and a reduced number of Na-HCO_3.

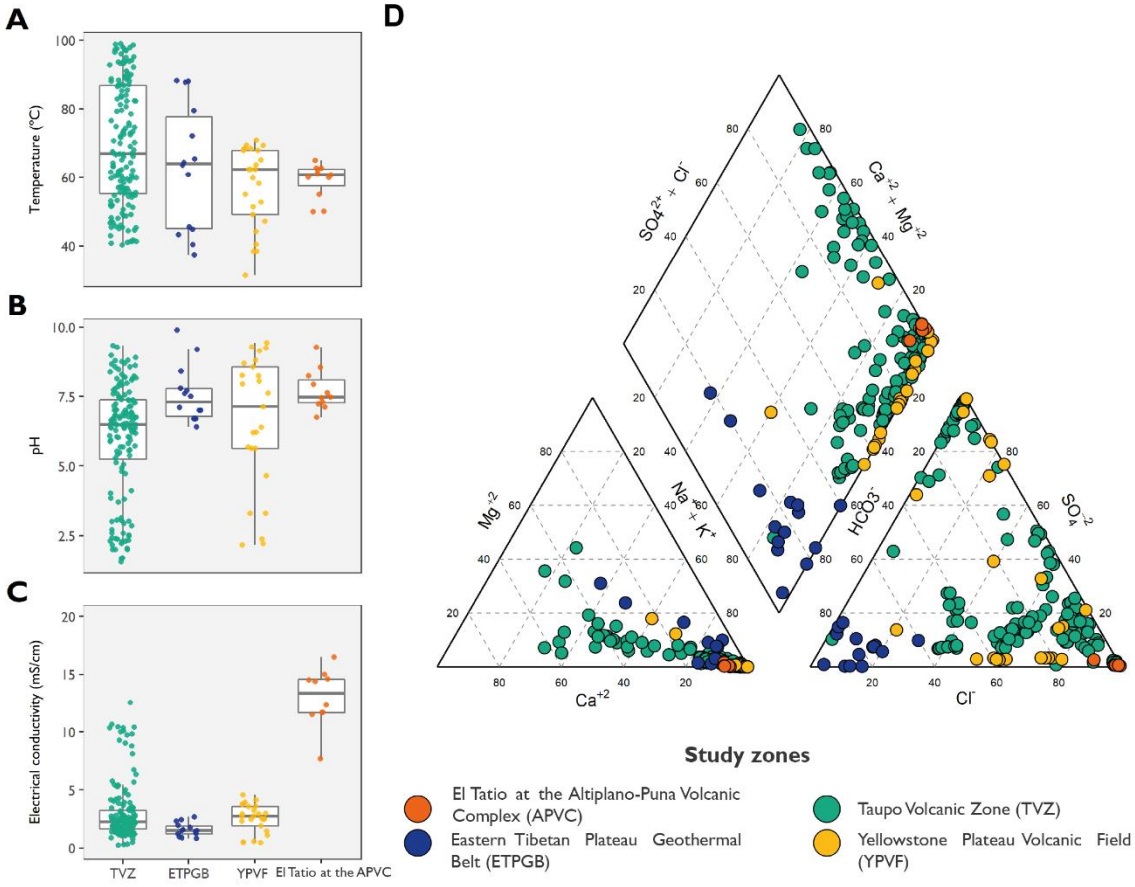

Figure 3.2 Distribution of temperature (A), pH (B) and electrical conductivity (C) of the samples at each study zone. D. Piper Diagram of the analyzed samples by study zone.

3.5.1.1. NaCl water

Most of the variance in the water chemistry was explained by Cl^-, Na^+, and K^+ concentrations (**Supplementary Figure 3-1**). Of the samples analyzed, 107 were classified as NaCl waters (**Figure 3.2**). Cl^- concentrations at El Tatio were the highest of all samples, reaching 7,062 mg/l. Tokaanu's Cl^- concentrations reached 3,234 mg/l and were the highest in the TVZ, which is consistent with previous studies (Bernal et al., 2014; Soto et al., 2019). High salinities in Tokaanu have been interpreted as a cause of steam loss and surface evaporation processes (Bégué et al., 2017; Robinson and Sheppard, 1986;

Simpson and Bignall, 2016). Also, both processes have been described as two of the most important secondary events at El Tatio (Munoz-Saez et al., 2018; Nicolau et al., 2014), which probably contribute to concentrate the Cl^- and many other compounds in the rising water. At El Tatio, water-rock interactions between thermal fluids and Mesozoic to Quaternary volcanic rocks have been proposed (Munoz-Saez et al., 2018) and the concentrations of Na^+ and Cl^- are more than an order of magnitude higher than those of other ions. In contrast, NaCl waters from Wairakei-Tauhara, Waimangu, Rotorua, Orakei-Korako, and Yellowstone had Cl^- concentrations below 1,314 mg/l and higher ratios of HCO_3^- to Cl^- and SO_4^{2-} to Cl^-, which may suggest that other secondary processes are controlling their major element chemistry.

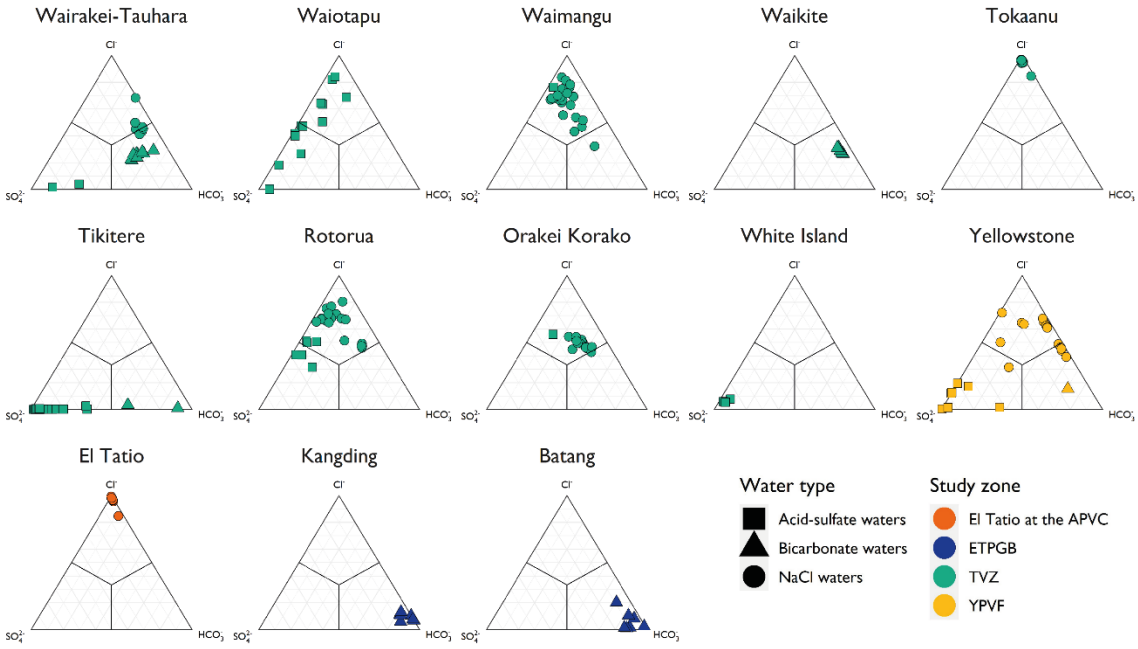

Figure 3.3 Ternary SO_4-Cl-HCO_3 diagrams for each geothermal field. Samples are represented according to the geothermal area and water type

3.5.1.2. Acid-sulfate waters

Of the 60 acid-sulfate water samples, 3 of them were taken at the active White Island volcano. The 3 analyzed samples had pH values between 3.05 and 5.41, and SO_4^{2-} concentrations between 804 and 1,969 mg/l. Surface fluids of this geothermal system have been shown to contain extremely low pH reaching negative values (Christenson et al., 2017). Fluids sources identified include meteoric water, seawater, and magmatic steam (Christenson et al., 2017; Marty and Giggenbach, 1990; Tedesco and Toutain, 1991). The latter has been shown to contribute sulfur more as SO_2 and less as H_2S (Christenson et al., 2017) and these inputs are responsible for the low pH values reported (Giggenbach et al., 2003).

The remaining 57 samples belonged to Yellowstone, Waiotapu, Wairakei-Tauhara, and Tikitere, and their acidity has previously been interpreted as the result of S-rich fluid phase separation and condensation of the steam phase followed, in many cases, by mixing with shallower water (Giggenbach et al., 1994; Henley and Stewart, 1983; Hunt et al., 1994; Lowenstern et al., 2015; Nordstrom et al., 2009). In addition, Nordstrom et al. (2009) deduced many mixing processes in the YPVF that can explain the SO_4^{2-} and Cl^- concentrations in the analyzed waters. These authors proposed two end members for meteoric water: one consisting of meteoric water only (MO) and another formed by mixing meteoric water with sulfate-rich

steam (MG) (**Figure 3.4A**). They also proposed three hydrothermal waters: hydrothermal water only (HO), hydrothermal water with subsurface boiling (HB), and hydrothermal water with subsurface boiling and hot gas discharge (HBG). Thus, the highest concentrations of SO_4^{2-} included in this study (200 mg/l < SO_4^{2-} < 645 mg/l) could have formed due to mixing of MO and MG (**Figure 3.4A**). Intermediate SO_4^{2-} concentrations (40 mg/l < SO_4^{2-} < 200 mg/l) may have been HBG or could have been produced due to the mixing of MG with MO. The lowest SO_4^{2-} concentration (SO_4^{2-} < 40 mg/l) could have been formed by mixing MO with HO.

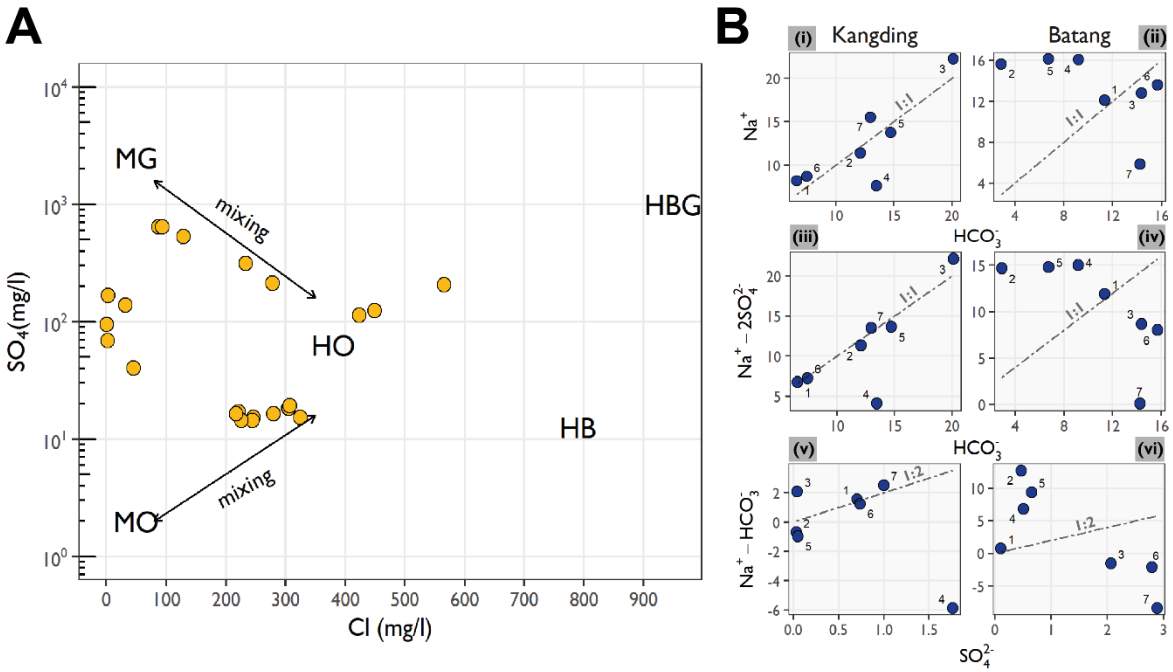

Figure 3.4 A. SO_4^{2-} concentrations of the YPVF samples plotted against its Cl^- concentrations. HO: hydrothermal only, HB: hydrothermal with subsurface boiling, MO: meteoric only, MG: meteoric water with hot gas discharges, HBG: hydrothermal with subsurface boiling hot gas discharge. Proposed by Nordstrom et al. (2009). B. Molar concentrations of Na^+, SO_4^{2-} and HCO_3^- in samples from Batang and Kangding geothermal fields. Dashed lines show the stoichiometric ratios of dissolution of albite in presence of CO_2 (i-ii) and dissolution of albite in presence of CO_2 and H_2S (iii-vi).

On the other hand, hydrochemical trends were observed at Tikitere and Waiotapu, where samples displayed between the SO_4^{2-} and HCO_3^- vertex of the ternary diagram in Tikitere, and the SO_4^{2-} and Cl^- vertex in Waiotapu (**Figure 3.3**). These samples exhibited pH values of 1.57 to 6.48 and 2.31 to 5.55 respectively. Lower pH values were observed to be correlated with higher Eh values (**Supplementary Figure 3-2**), leading to relate acidity to shallower fluid circulation. High concentrations of sulfate in these acidic samples also contribute to consider oxidation of reduced S as an important mechanism of acidity. More information on water chemistry would be needed to evaluate the role of water-rock interactions in the formation of these acid-sulfate waters.

At El Tatio, steam-heated waters have been reported (Cortecci et al., 2005; Giggenbach, 1978; Letelier et al., 2021; Munoz-Saez et al., 2018; Tassi et al., 2010) as well as at Tokaanu (Robinson and Sheppard, 1986; Soto et al., 2019), but these samples were not included in the present study.

3.5.1.3. HCO_3^- or CO_2-rich waters

For Batang, Kangding, Waikite, Waimangu, Tikitere, Wairakei-Tauhara, and Yellowstone, 35 samples were classified as HCO_3^- or CO_2-rich water. The highest HCO_3^- concentrations were found in the ETPGB (412 mg/l > HCO_3^- > 1,228 mg/l). Ratios of Na^+ to Cl^- in these samples were above unity, suggesting that Na^+ originated from the dissolution of silicate minerals (Hounslow, 1995). Previous studies have shown that surface thermal fluids in Kangding contain a volume percentage of CO_2 greater than 95% (Guo et al., 2017). This compound favors the dissolution of silicate minerals, which are widely distributed in intrusive and metamorphic rocks in the ETPGB (Zhao et al., 2021). If isochemical dissolution of albite had occurred, Na^+ and HCO_3^- would have been incorporated into the water in the same molar ratios as they were in the rock (Daniele et al., 2020).

$$NaAlSi_3O_8 + CO_2 + 2H_2O \leftrightarrow Na^+ + Al(OH)_3 + HCO_3^-$$

As seen in **Figure 3.4B (i-ii)**, Kangding samples and Batang's sample 1 located close to the equimolar line, but none of them adjusted completely. Since H_2S may also have favored albite dissolution by producing Na^+ and SO_4^{2-} in 2:1 molar ratio, the joint action of CO_2 and H_2S was evaluated.

$$NaAlSi_3O_8 + H_2S + 2O_2 \leftrightarrow 2Na^+ + 6SiO_2 + 2AlO(OH) + SO_4^-$$

Although H_2S concentrations are low in the ETPGB (Guo et al., 2017, 2014), the Kangding waters conformed better to the equimolar line with the addition of SO_4^{2-} (**Figure 3.4B (iii)**). However, as **Figure 3.4B (iv)** illustrates, Kangding's samples 2, 3, and 5 deviate from the equimolar line, which may be explained by analytical errors that could have been more evident at low concentrations of SO_4^{2-}. In contrast, ionic concentrations in the remaining Batang samples and sample 4 from Kangding did not appear to be dominated by albite dissolution.

Turning to the TVZ, Waikite bicarbonate waters have been interpreted as peripheral waters, being an outflow from the Waiotapu geothermal field (Giggenbach et al., 1994; Kaya et al., 2014). In that case, bicarbonate may have originated from the interaction of CO_2 with the surrounding rocks. This same origin is believed to have the bicarbonate-rich waters of Wairakei-Tauhara.

3.5.2. Microbial communities

The 16S rRNA gene is a universal genetic marker for Bacteria and Archaea that allows us to compare the microbial structure of the communities between hot springs and analyze the biological response against the metadata of interest. Standardized sequence processing was performed on the 11 samples from El Tatio and the 191 pre-existing samples in the NCBI SRA database from the other 3 study zones. A total of 7,505,257 clean sequences were recovered from these 202 hot springs samples, representing 950 Archaea and 16,398 Bacteria ASVs. Of these clean sequences, 6,348,970 belonged to the TVZ (median = 26,467), 843,032 to the YPVF (median = 32,110), 360,291 to the ETPGB (median = 26,041), and 256,760 to the APVC (median = 24,063; **Table 3.4-1**).

Table 3.5-1 Number of 16S rRNA amplicon sequences from each set of samples before and after filtering.

Source	Country	Study zone	Samples	Geothermal systems	Total sequences	Filtered sequences	Median filtered sequences

Source	Country	Study zone	Samples	Geothermal systems	Total sequences	Filtered sequences	Median filtered sequences
Power et al. (2018)	New Zealand	Taupo Volcanic Zone	152	Rotorua (RO), Orakei Koraro (OK), Tokaanu (TK), Tikitere (TT), Waiotapu (WP), Waimangu (WG) Waikite (WK), Wairakei-Tahura (WT), White Island (WI)	9,254,997	6,348,970	26,467
Hamilton et al. (2019)	The United States of America	Yellowstone Plateau Volcanic Field	25	Yellowstone (YE)	1,187,293	843,032	32,110
Guo et al. (2020)	China	Eastearn Tibetan Plateau Geothermal Belt	14	Batang (BT), Kangding (KD)	427,442	360,291	26,041
This paper	Chile	Altiplano Puna Volcanic Complex	11	El Tatio (TT)	389,044	256,760	24,063

3.5.2.1. Alpha and Beta diversity

Rarefaction curves analysis showed that ASVs saturation was reached beyond 15,000 reads per sample (**Supplementary Figure 3-3**). Analysis of microbial community diversity in each hot spring showed a wide range of observed richness between 9 and 904 ASVs, while the Shannon index ranged from 0.14 to 5.6 (**Supplementary Table 3-3**). Diversity values were calculated by habitat (water or mat), study zone (4), and geothermal field (13). No statistically significant differences in observed richness ($p > 0.05$) were found grouping by habitat or study zone. However, the Shannon index showed significantly ($p < 0.05$) lower diversity in water communities (2.6 in the ETPGB and 2.77 in the TVZ) compared to microbial mat communities (3.24 in El Tatio and 3.54 in the YPVF, **Supplementary Figure 3-4**). In contrast, when looking at the scale of the geothermal field, a greater contrast was observed in both metrics. The highest Shannon indexes (3.5-3.9) were found at Wairakei-Tahura (TVZ), Waikite (TVZ), and Yellowstone (YPVF), which also had the highest observed richness along with Batang (ETPGB) and Waimangu (TVZ; 118-200). In contrast, the least diverse communities were found at Tikitere (TVZ), Waiotapu (TVZ), and White Island (TVZ; 1.3-2.3; 23-42).

To further analyze the influence of water chemistry on alpha diversity, correlations between chemical parameters and diversity indexes were calculated for each study zone (**Supplementary Figure 3-5**). No statistically significant correlations were found between temperature and alpha diversity in any study zone, which support the findings of (Hamilton et al., 2019; Power et al., 2018) but contrasts with two previous intercontinental studies that correlated hot spring temperature with alpha diversity (Podar et al., 2020; Sharp et al., 2014). On the other hand, observed richness and Shannon index correlated with pH ($R = 0.49, 0.3$; $p < 0.05$) and SO_4^{2-} concentrations ($R = -0.51, -0.34$; $p < 0.05$) in the TVZ microbial communities, which was already detected by Power et al. (2018). The authors also showed that this effect of pH on alpha diversity was constrained to specific temperature ranges. Thus, samples from all zones were grouped by temperature, which showed that the correlation between pH and alpha diversity was limited to temperatures below 70 ºC (**Supplementary Figure 3-6**). This led to the establishment that acid-sulfate waters have lower diversity indexes compared to bicarbonate and NaCl water at temperatures below 70 ºC (**Figure 3.5**).

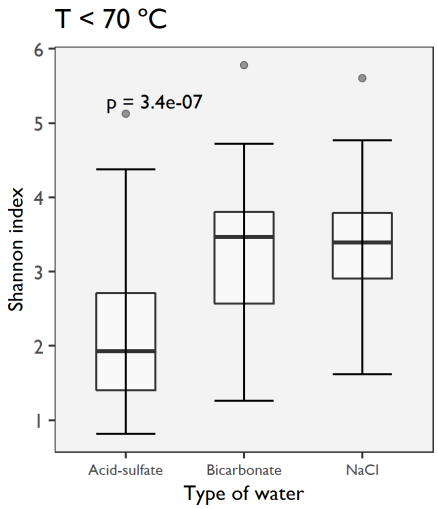

Figure 3.5 Shannon index for microbial communities inhabiting acid-sulfate, bicarbonate and chloride waters at temperature below 70º C.

To analyze the variation in species composition among different hot springs, geothermal fields and zones, an ordinate analysis was performed on the weighted Unifrac Beta diversity index. Axis 1 (36.3%) and Axis 2 (14.1%) generated with the MDS analysis explained a total of 50.53% of the variance (**Figure 3.6A**). The results did not show a clear distribution of the samples according to their study zone in the ETPGB and TVZ microbial communities. On the contrary, samples from El Tatio showed small phylogenetic distances with most of the YPVF samples.

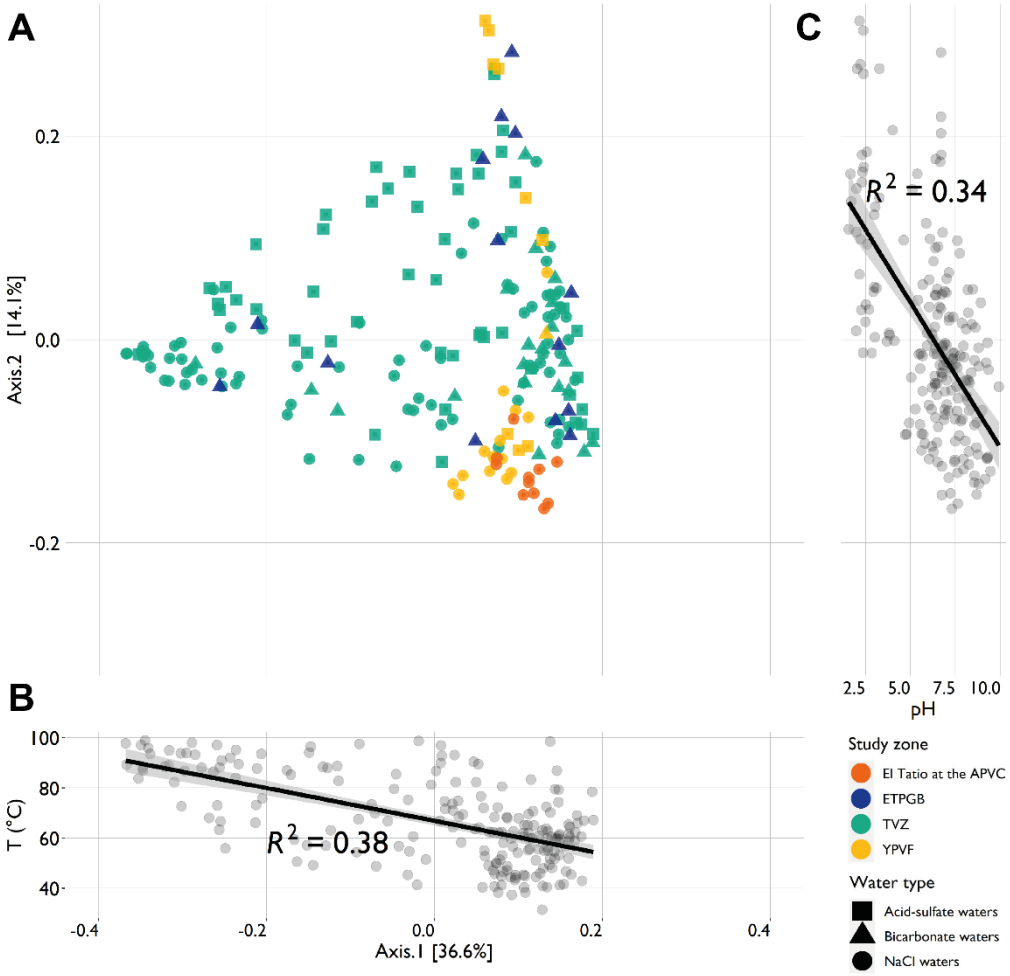

Figure 3.6 A. Axis 1 and 2 resulted from the MDS analysis performed on the weighted Unifrac distances between microbial communities. B. Correlation of Axis 1 with temperature. C. Correlation of Axis 2 with pH.

3.5.2.2. Multiple variables as conditioning factors of thermal microbial taxonomic composition

Microbial communities in the TVZ and the ETPGB were mainly composed of Aquificota and Proteobacteria phyla, comprising 55% and 56% of their abundance, respectively (**Supplementary Figure 3-7A**). More specifically, the dominant families in the TVZ were Aquificaceae, Hydrogenothermaceae and Hydrogenobaculaceae (**Supplementary Figure 3-7B**). The two former Aquificota families also dominated in the ETPGB along with the Thermaceae and Comamonadaceae families. In contrast, the El Tatio communities were mainly composed of the phyla Chloroflexota, Bacteroidota, and Cyanobacteria, covering 62% of its relative abundance. The dominant families in this field were Chloroflexaceae, an uncultured member of Armatimonadota, Roseiflexaceae, and Nostocaceae. At El Tatio a previous study showed that Chloroflexota accounts for the majority of microbial mat and sediment sequences between 38 ºC and 54 ºC, whereas Deinococcota dominated at higher temperatures (Engel et al., 2013). Similarly, Chloroflexota, Bacteroidota, and Cyanobacteria, together with Proteobacteria, comprised 55% of the relative abundance of YPVF communities. The dominant families in the YPVF were Leptococcaceae, Roseiflexaceae, and Thermaceae.

Since temperature and pH have traditionally been considered to have a strong influence on shaping microbial community structures in hot springs, this correlation was tested with the MDS axes in the different samples. The results showed that temperature correlated moderately with Axis 1 (R^2= 0.36, $p < 0.05$), and pH with Axis 2 ($R^2 = 0.34$, $p < 0.05$) (**Figure 3.6**). Therefore, it is suggested that the structure of the analyzed samples was partially influenced by temperature and pH gradients. No ordering by water type was observed in the distribution of microbial communities, except for communities of the YPVF acid-sulfate waters that were preferentially distributed along Axis 2.

To further assess potential drivers of community composition, temperature, pH, and major ion concentrations were subjected to PCA analysis (**Supplementary Figure 3-1**). The resulting principal components, together with observed richness and microbial community habitat (water or mat), were used as explanatory variables in a PERMANOVA analysis. Results showed small contributions from each variable, rather than a single principal explainer (**Table 3.5-2**). The highest linear correlation of the hydrochemical factors was 8.3% given by PC4, which was highly related to temperature, $Mg^{2+,}$ and Si concentrations ($p < 0.001$). PC2, mostly associated with pH, SO_4^{2-}, and Mg^{2+}, as well as PC3 associated with HCO_3^- and Si also showed a significant influence on beta diversity, each explaining less than 5% of the total variance ($R^2 = 0.045$, $p < 0.001$). Microbial community habitat contributed to explaining 3.8%, while observed richness explained 2.1%. Hence, 63.19% of the variance remained unexplained, suggesting other environmental variables involved in structuring these communities, such as humidity, solar radiation (Phoenix et al., 2006), or other hydrochemical variables not considered in the present study. In the literature, it has been suggested that microbial community variance is better constrained with hydrochemistry where photosynthesis is absent (Inskeep et al., 2013a; Shock et al., 2005). In these cases, the concentrations of dissolved species regulate the metabolic pathways that microorganisms can resort to (Shock et al., 2005). On the other hand, the influence of the biological component, such as the interaction between taxa, could also play a role in shaping these thermal communities.

Table 3.5-2 PERMANOVA results using as explanatory variables observed richness, habitat (water/microbial mat) and the principal components of the PCA constructed with hydrochemical variables. Distances were based on weighted Unifrac metric. Pr(>F): p-value associated with the F statistic.

	R^2	F-model	Pr(>F)
Observed richness	0.0212	6.37	P < 0.001
Habitat	0.0376	11.26	P < 0.001
PC1	0.0211	6.32	P < 0.01
PC2	0.0453	13.56	P < 0.001
PC3	0.0449	13.44	P < 0.001
PC4	0.0834	24.95	P < 0.001
PC5	0.0205	6.13	P < 0.001
PC6	0.0103	3.10	P < 0.01
PC7	0.0090	2.71	P < 0.05
PC8	0.0051	1.55	P > 0.1
PC9	0.0099	2.95	P < 0.05
PC10	0.0032	0.97	P > 0.1
Residual	0.6320		-
Total	0.944		-

Furthermore, when assessing the effect of hydrochemical gradients on dominant taxa (>0.1%), only weak to moderate correlations ($\rho = 0.2$ to 0.7; $p < 0.05$) were identified with the relative abundances of these taxa (**Figure 3.7**). Chloroflexota, Bacteroidota, and Cyanobacteria, the most abundant phyla of the YPVF and the APVC, were moderately positively correlated with pH and moderately negatively correlated with SO_4^{2-}. These correlations confirm the circumneutral to alkaline pH at which members of Chloroflexota and Cyanobacteria grow optimally in terrestrial hot springs, forming phototrophic mats (e.g., Alcamán et al., 2015; Inskeep et al., 2013b; Mackenzie et al., 2013; Sharp et al., 2014; Uribe-Lorío et al., 2019; Zhang et al., 2018).

Chloroflexaceae family showed the highest correlation with pH (**Supplementary Figure 3-8**), as reported for the genus *Chloroflexus* (Hamilton et al., 2019). However, the highest correlations of pH and SO_4^{2-} were observed for members of the family Thermaceae (Deinococcota) and a family with uncultured members of Armatimonadota. Power et al. (2019) and Hamilton et al. (2019) previously recognize this positive correlation between pH and the *Thermus* genus of the Thermaceae family in YPVF and TVZ, respectively. Similarly, thermophilic members of Armatimonadota have only been found at neutral or alkaline pH (Lee, 2015). In contrast, the abundances of Thermoplasmatota and Campilobacterota increased with SO_4^{2-} and decreased with pH, as observed for Desulfurellaceae and a family with uncultured members of the phylum Thermoplasmatota. The family Acidithiobacillaceae (Proteobacteria) was similarly related to the above parameters, being the only family of Proteobacteria correlated with temperature, which are preferentially present at lower temperatures. This family and in particular its best-known genus, *Acidithiobacillus*, have been extensively reported in acidic terrestrial hot springs and acid mine drainage courses (e.g., Gagliano et al., 2016; Mahmoud et al., 2005; Willis et al., 2019).

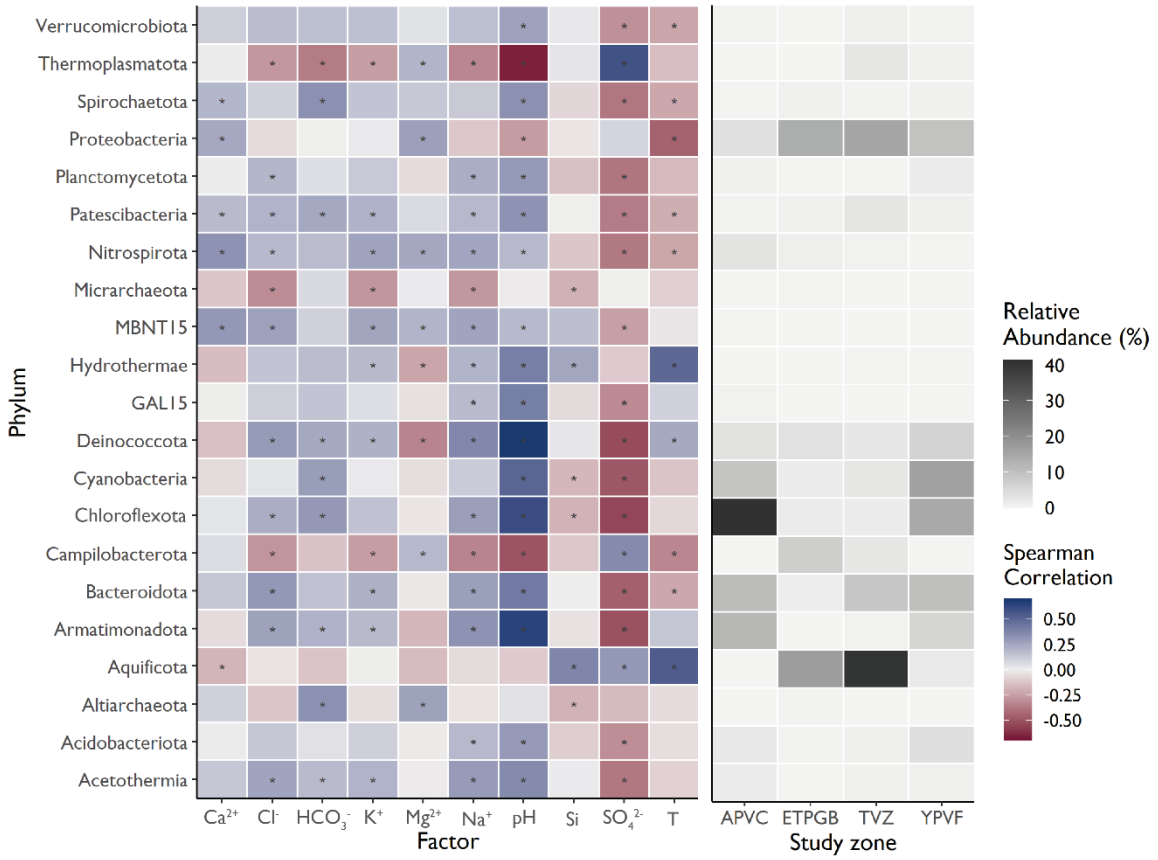

Figure 3.7 Highest Spearman correlations ($\rho > 0.3$; $p > 0.01$) between phylum abundance and hydrochemical variables. Sequences were previously filtered by relative abundance (<0.1%).

Members of Aquificota, a dominant phylum in ETPGB, were correlated with different chemical parameters. Aquificacea, were preferentially distributed at high temperatures, as previously reported for the genus *Aquificae* on the Tibetan Plateau, Yellowstone, and Iceland (Inskeep et al., 2013b; Podar et al., 2020; Zhang et al., 2018). Members of Hydrogenobaculaceae were not affected by temperature but were negatively correlated with pH and HCO_3, and positively correlated with SO_4^{2-} . The genus *Hydrogenobaculum* has been isolated from sites with pH values between 1.02 and 5.75 and high concentrations of H_2, H_2S, and CO_2 (Romano et al., 2013). Members of this genus have been found to grow on these chemical species and use them together with thiosulfate as energy sources (Romano et al., 2013), illustrating their dependence on hot spring chemistry (**Supplementary Figure 3-8**). In addition, Hydrothermae and Bathyarchaeia (Ca. Bathyarchaeota) also showed a moderately positive correlation with temperature.

Weaker correlations were found between pH, SO_4^{2-}, temperature, Cl^-, Na^+, Ca^{2+}, and Mg^{2+}, and some other taxa ($\rho < 0.4$; $p < 0.05$). This again suggests that the action of environmental conditions on microbial communities in thermal environments is not limited to the individual effects of one or a couple of parameters, but to a set of complex interactions between biotic and abiotic elements, as described by the niche theory (Hirzel and Le Lay, 2008)

In that sense, and to analyze biotic interactions between those phyla that were more correlated with water chemistry, microbial co-occurrence networks were also performed by geothermal zone (**Figure 3.8**).

This analysis showed higher modularity and lower betweenness in El Tatio and ETPGB than in YPVF and TVZ, probably due to the difference in the number of samples analyzed for each zone, which allowed more significant connections in the latter two. Furthermore, as inferred from their correlations between chemical factors, positive connections were found between some phyla that are affected by the same environmental factors. This was observed in the Armatimonadota and Chloroflexota nodes, and in the Cyanobacteria, Chloroflexota, and Bacteroidota nodes, which correlated similarly with pH and SO_4^{2-}. Many interactions between microorganisms forming photoautotrophic mats have been already described (Alcamán et al., 2015; Kim et al., 2015; Steinke et al., 2020).

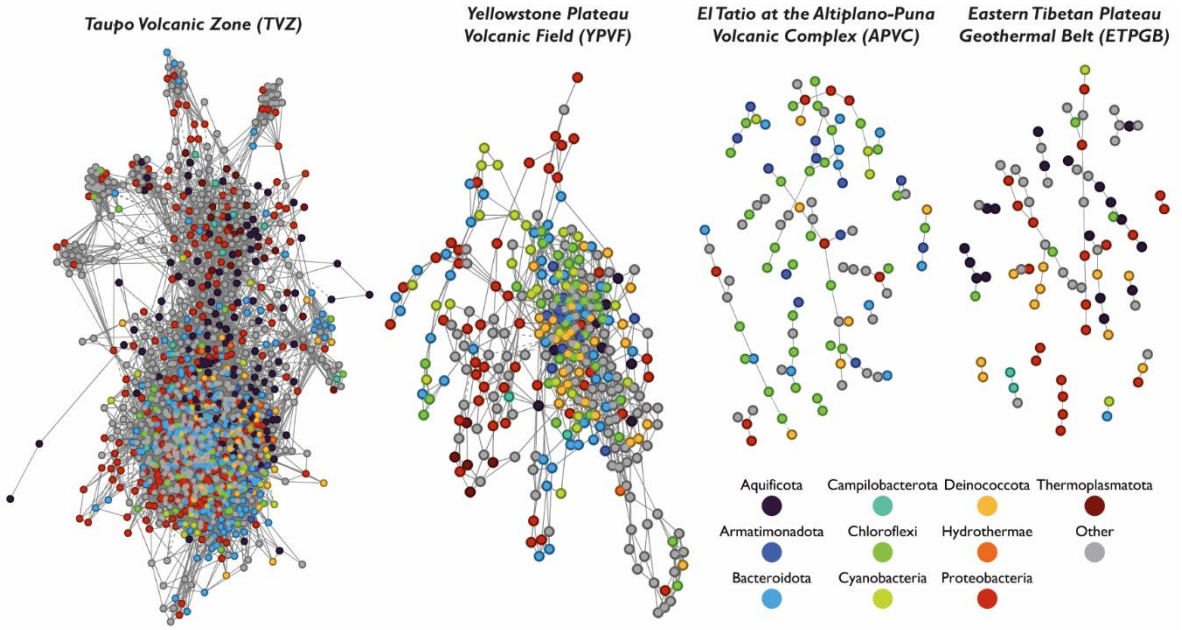

	TVZ		YPVF		APVC		ETPGB	
Modularity	0.002 (35 modules)		0.598 (21 modules)		0.915 (17 modules)		0.855 (13 modules)	
Betweenness	Median	SD	Median	SD	Median	SD	Median	SD
	620.928	2,371.486	329.479	945.164	0.500	8.400	6.000	31.082

Figure 3.8 Microbial co-occurrence network of the 4 study zones. Nodes (ASVs) are colored by phylum. Colored nodes represent those phyla with the highest correlations with chemical parameters. Positive connections between nodes are displayed with continuous lines and negative interactions with segmented lines.

3.5.2.3. Role of geothermal processes on chemistry and microbial communities

PERMANOVA results indicated that the eigenvectors PC4 (temperature, $Mg^{2+,}$ and Si) and PC2 (pH, SO_4^{2-}, and Mg^{2+}) were the most important explanatory factors of community structure. However, Mg^{2+} and Si concentrations did not show other relevant correlations with the community as did temperature, pH, and SO_4^{2-}. In addition, pH and SO_4^{2-} were negatively correlated (**Supplementary Figure 3-9**), which is probably because the main source of acidity in geothermal waters is the oxidation of H_2S that produces SO_4^{2-} (Nordstrom et al., 2009). These and other correlations between pH and chemical variables (**Supplementary Figure 3-9**) make it difficult to determine what the actual influence of each parameter is on the microbial communities. Moreover, many water-rock interaction rates are favored at low pH values, such as the dissolution of Ca-bearing minerals (Palandri and Kharaka, 2004) that increase the

concentration of Ca^{2+} and Mg^{2+} in the water. This interaction could explain the low to moderate correlations between certain taxa and Ca^{2+} and Mg^{2+} (**Figure 3.7, Supplementary Figure 3-8**).

On the other hand, the availability of reduced sulfur in surface manifestations is linked to regional and local conditions that shape the entire geothermal system, such as its tectono-magmatic setting, and geological and hydrogeological mechanisms (Moeck, 2014). The regional conditions that allow the formation of steam-heated water have been evaluated by Guo et al., 2014 in the Tibetan Plateau. These studies explained the absence of acid-sulfate waters in this geothermal zone by (1) the lack of a confining layer separating the underlying NaCl waters from steam after phase separation, and (2) the depth of magmatic chambers that could play a role in the low H_2S concentrations in geothermal fluids. Moreover, it has been shown that microbial communities on the Tibetan Plateau are modulated by temperature (Guo et al., 2020; Wang et al., 2013; Zhang et al., 2018), which might be explained to some extent by the absence of acidic springs. In fact, Guo et al. (2021) found and analyzed a thermal spring with pH<5 and demonstrated that its microbial community structure differed from the rest of hot springs in this geothermal zone.

In addition to the mechanisms proposed by Guo et al. (2014), local processes also affect the acidity of this steam-heated water, such as the dissolution/precipitation of certain minerals or the ratio of shallow water and S-rich steam in the fluid. Hot springs fed by concentrated H_2S-CO_2-rich fluid would have higher SO_4^{2-} concentrations and lower pH values than those with a higher shallow component. These local variations can be evidenced in Tikitere, where samples showed a wide pH range. As shown in **Supplementary Figure 3-10**, 51.9% of the community structure at Tikitere was explained by Axis 1, which was moderately correlated with pH ($R^2 = 0.48$). Thus, the community structure of Tikitere responds to the pH gradient. However, no correlation was found between pH, SO_4^{2-} and alpha diversity in this geothermal field, which could be attributed to the temperature variations experienced by the hot springs (from 44.4 to 86.8 ºC), which probably also affect the communities. Additionally, deep geothermal fluids may precipitate alunite, anhydrite, or pyrite at different depths and decrease their sulfur concentrations, as occurs in Yellowstone (Giggenbach, 1988; Nordstrom et al., 2009). This would prevent the formation of acid-sulfate waters (Nordstrom et al., 2009).

In contrast to the mentioned processes, no clear influence of Na^+, K^+, and Cl^- concentrations was detected on the analyzed microbial communities. Therefore, water-rock interactions that incorporate Na^+, K^+, and Cl^- to the water or secondary processes that concentrate them do not appear to play a critical role in modeling alpha diversity, community structure, or the taxonomy of thermophile microbial communities, but rather there are other environmental factors that shape these communities, which might occur in El Tatio and Tokaanu geothermal fields.

3.5.2.4. Influence of geographic distance on beta diversity

To evaluate whether geographic distance influences the similarity among microbial communities, its effect was determined at three different spatial scales defined as local, regional, and global. The local scale includes samples within the same geothermal system (< 58 km) while the regional scale defines the maximum distance between samples from the same study zone (< 279 km). Finally, the global scale comprises distances between different study zones (< 8,576 km). As there is no data between 279 km and 8,576 km, this scale was defined as a continental scale.

At the local scale, all beta diversity indexes showed significant ($p < 0.01$) negative relationships with distance (**Figure 3.9**). Jaccard and Bray-Curtis indexes showed weak correlations with distance ($R^2 =$

0.11, $p < 0.01$), but still higher than phylogeny-based relationships ($R^2 < 0.01$, $p < 0.01$). At the regional scale, only unweighted Unifrac similarities were significant ($p < 0.01$), but with almost zero correlation with geographic distance ($R^2 = 0.003$). Similarly, on a global scale, unweighted and weighted Unifrac showed almost absent correlations with geographic distance ($R^2 = 0.0033$, $R^2 = 0.013$, $p < 0.01$). From these results, no distance-decay on microbial communities' similarity was inferred based on Jaccard and Bray-Curtis indexes nor unweighted and weighted Unifrac distances. Thus, it is shown that geography does not explain the change in community composition across hydrothermal regions, at least for the four indices tested here. However, as the microbial communities tested were taxonomically related on a global scale, this might suggest for a potential ancient divergence in the same taxonomic groups between globally distant thermal zones and thus with the time, some endemic character in each of them appeared as previously reported in the literature for some specific taxa (Erikstad et al., 2019; Miller et al., 2007; Papke et al., 2003; Valverde et al., 2012; Whitaker et al., 2003).

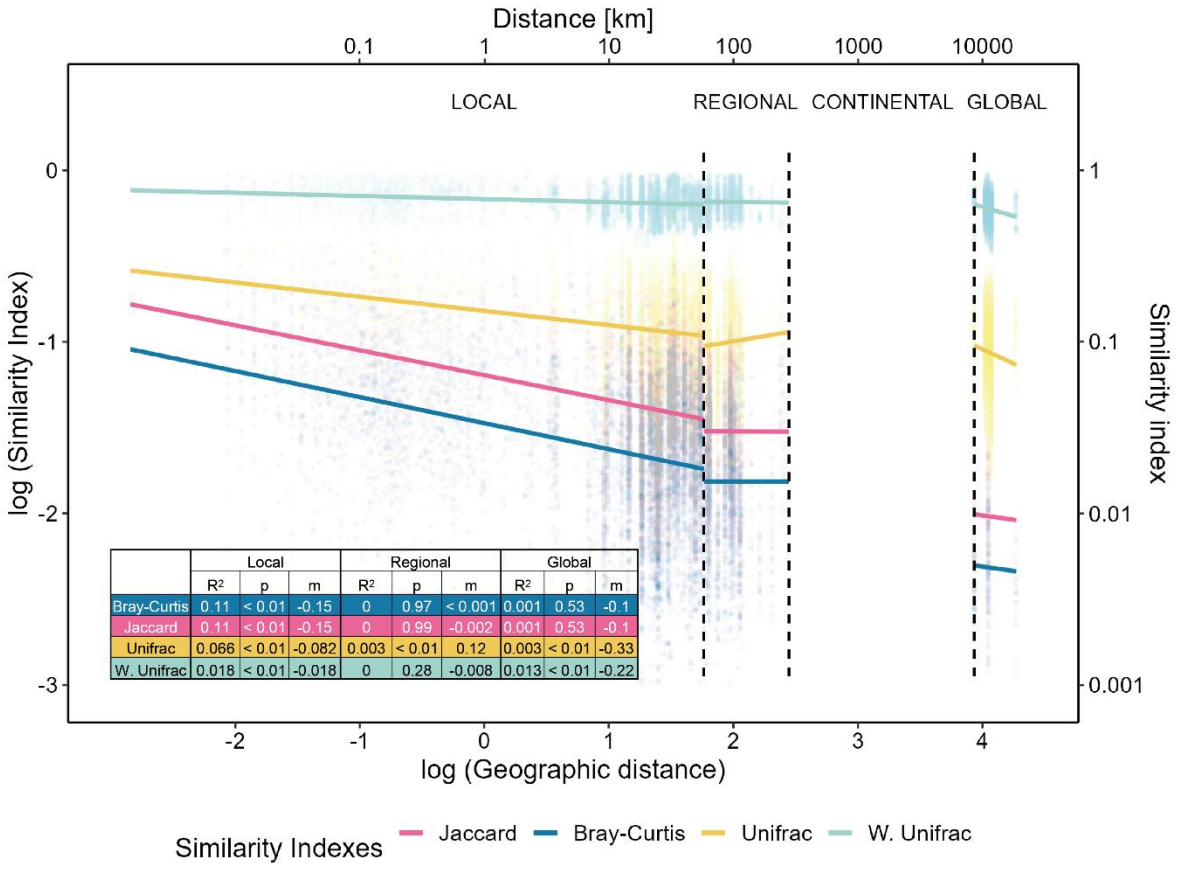

	Local			Regional			Global		
	R^2	p	m	R^2	p	m	R^2	p	m
Bray-Curtis	0.11	< 0.01	-0.15	0	0.97	< 0.001	0.001	0.53	-0.1
Jaccard	0.11	< 0.01	-0.15	0	0.99	-0.002	0.001	0.53	-0.1
Unifrac	0.066	< 0.01	-0.082	0.003	< 0.01	0.12	0.003	< 0.01	-0.33
W. Unifrac	0.018	< 0.01	-0.018	0	0.28	-0.008	0.013	< 0.01	-0.22

Figure 3.9 Jaccard, Bray-Curtis indexes and unweighted Unifrac and weighted unifrac distances of the microbial communities according to their geographic distance.

3.6. Conclusions

Worldwide hot springs have a wide hydrochemical composition resulting of deep and shallow geothermal processes. In this study, statistical analyses were used to determine the influence of physicochemical parameters, major ion concentration, and geographic distance on 202 microbial communities in hot springs from New Zealand, the United States of America, Chile, and China. Ordination and PERMANOVA analyses showed that temperature and pH play a key role in shaping

microbial communities, which is in line of previous studies. Similarly, SO_4^{2-} concentrations, mostly determined by phase separation, also showed correlations with taxonomy, alpha and beta diversity of the microbial communities, highlighting the potential relevance of geochemical processes in the microbial ecology of thermophilic communities. In addition, geographic distance showed no effect on community composition changes across hydrothermal regions. Moreover, the results indicate that the intercontinental microbial communities inhabiting the studied terrestrial hot springs are taxonomically related. It will now be necessary to include more water/gas chemical and biotic variables as well as other metagenomic tools and a larger number of samples to better understand the role of hydrochemical gradients and water origin in the structure and metabolism of the microbial communities of hot springs on the local and global scales.

Author Contributions

CB: Conceptualization, methodology, formal analysis, writing – original draft, writing – review & editing. **JTL**: Conceptualization, methodology, formal analysis, writing – original draft, writing – review & editing. **JA**: Conceptualization, methodology, writing – original draft, writing – review & editing. **DM**: Conceptualization, supervision, resources, funding acquisition. **OS**: Methodology, funding acquisition. **LD**: Writing – review & editing. **BD**: Conceptualization, writing – original draft, supervision, resources, funding acquisition.

Acknowledgment

This work was financially supported by the Chilean National Agency of Research and Development (ANID) through the Andean Geothermal Center of Excellence (CEGA, ANID-FONDAP 15090013, 15200001 & ACE210005), Millennium Institute Center for Genome Regulation (ICN2021_044), FONDECYT 1190998, a National Master Scholarship granted to CB (22200311), and a National Doctoral Scholarship granted to JTL (21171048) during the analysis and writing of this manuscript. Additional support was provided by the research effort Iniciativa de Investigación UnACh 2020-132-Unach. The authors acknowledge Johanna Saldías for her logistical support in the BD Lab during this research and Verónica Rodríguez for helping with the hydrochemical analyses. The authors also acknowledge Caspana and Toconce Aymara Communities for the permission to the fieldwork performed at El Tatio geothermal field.

References

Alcamán-Arias, M.E., Pedrós-Alió, C., Tamames, J., Fernández, C., Pérez-Pantoja, D., Vásquez, M., Díez, B., 2018. Diurnal changes in active carbon and nitrogen pathways along the temperature gradient in porcelana hot spring microbial mat. Front. Microbiol. 9, 1–17. https://doi.org/10.3389/fmicb.2018.02353

Alcamán, M.E., Fernandez, C., Delgado, A., Bergman, B., Díez, B., 2015. The cyanobacterium Mastigocladus fulfills the nitrogen demand of a terrestrial hot spring microbial mat. ISME J. 9, 2290–2303. https://doi.org/10.1038/ismej.2015.63

Alcorta, J., Espinoza, S., Viver, T., Alcamán-Arias, M.E., Trefault, N., Rosselló-Móra, R., Díez, B., 2018. Temperature modulates Fischerella thermalis ecotypes in Porcelana Hot Spring. Syst. Appl. Microbiol. 41, 531–543. https://doi.org/10.1016/j.syapm.2018.05.006

Alsop, E.B., Boyd, E.S., Raymond, J., 2014. Merging metagenomics and geochemistry reveals environmental controls on biological diversity and evolution. BMC Ecol. 14, 1–12. https://doi.org/10.1186/1472-6785-14-16

Anders, S., Huber, W., 2010. Differential expression analysis for sequence count data. Genome Biol. 11. https://doi.org/10.1186/gb-2010-11-10-r106

Andersen, Kirkegaard, Karst, Albertsen, 2018. ampvis2: an R package to analyse and visualise 16S rRNA amplicon data. bioRxiv. https://doi.org/https://doi.org/10.1101/299537

Anderson, M.J., 2001. A new method for non-parametric multivariate analysis of variance. Austral Ecol. 26, 32–46. https://doi.org/10.1046/j.1442-9993.2001.01070.x

Arnórsson, S., Andrésdóttir, A., 1995. Processes controlling the distribution of boron and chlorine in natural waters in Iceland. Geochim. Cosmochim. Acta 59, 4125–4146. https://doi.org/10.1016/0016-7037(95)00278-8

Arnórsson, S., Stefánsson, A., Bjarnason, J.Ö., 2007. Fluid-fluid interactions in geothermal systems. Rev. Mineral. Geochemistry 65, 259–312. https://doi.org/10.2138/rmg.2007.65.9

Bégué, F., Deering, C.D., Gravley, D.M., Chambefort, I., Kennedy, B.M., 2017. From source to surface: Tracking magmatic boron and chlorine input into the geothermal systems of the Taupo Volcanic Zone, New Zealand. J. Volcanol. Geotherm. Res. 346, 141–150. https://doi.org/10.1016/j.jvolgeores.2017.03.008

Bernal, N.F., Gleeson, S.A., Dean, A.S., Liu, X.M., Hoskin, P., 2014. The source of halogens in geothermal fluids from the Taupo Volcanic Zone, North Island, New Zealand. Geochim. Cosmochim. Acta 126, 265–283. https://doi.org/10.1016/j.gca.2013.11.003

Bibby, H.M., Caldwell, T.G., Davey, F.J., Webb, T.H., 1995. Geophysical evidence on the structure of the Taupo Volcanic Zone and its hydrothermal circulation. J. Volcanol. Geotherm. Res. 68, 29–58. https://doi.org/10.1016/0377-0273(95)00007-H

Bokulich, N.A., Kaehler, B.D., Rideout, J.R., Dillon, M., Bolyen, E., Knight, R., Huttley, G.A., Gregory Caporaso, J., 2018. Optimizing taxonomic classification of marker-gene amplicon sequences with QIIME 2's q2-feature-classifier plugin. Microbiome 6, 1–17. https://doi.org/10.1186/s40168-018-0470-z

Bolyen, E., Rideout, J.R., Dillon, M.R., Bokulich, N.A., Abnet, C.C., Al-Ghalith, G.A., Alexander, H., Alm, E.J., Arumugam, M., Asnicar, F., Bai, Y., Bisanz, J.E., Bittinger, K., Brejnrod, A., Brislawn, C.J., Brown, C.T., Callahan, B.J., Caraballo-Rodríguez, A.M., Chase, J., Cope, E.K., Da Silva, R.,

Diener, C., Dorrestein, P.C., Douglas, G.M., Durall, D.M., Duvallet, C., Edwardson, C.F., Ernst, M., Estaki, M., Fouquier, J., Gauglitz, J.M., Gibbons, S.M., Gibson, D.L., Gonzalez, A., Gorlick, K., Guo, J., Hillmann, B., Holmes, S., Holste, H., Huttenhower, C., Huttley, G.A., Janssen, S., Jarmusch, A.K., Jiang, L., Kaehler, B.D., Kang, K. Bin, Keefe, C.R., Keim, P., Kelley, S.T., Knights, D., Koester, I., Kosciolek, T., Kreps, J., Langille, M.G.I., Lee, J., Ley, R., Liu, Y.X., Loftfield, E., Lozupone, C., Maher, M., Marotz, C., Martin, B.D., McDonald, D., McIver, L.J., Melnik, A. V., Metcalf, J.L., Morgan, S.C., Morton, J.T., Naimey, A.T., Navas-Molina, J.A., Nothias, L.F., Orchanian, S.B., Pearson, T., Peoples, S.L., Petras, D., Preuss, M.L., Pruesse, E., Rasmussen, L.B., Rivers, A., Robeson, M.S., Rosenthal, P., Segata, N., Shaffer, M., Shiffer, A., Sinha, R., Song, S.J., Spear, J.R., Swafford, A.D., Thompson, L.R., Torres, P.J., Trinh, P., Tripathi, A., Turnbaugh, P.J., Ul-Hasan, S., van der Hooft, J.J.J., Vargas, F., Vázquez-Baeza, Y., Vogtmann, E., von Hippel, M., Walters, W., Wan, Y., Wang, M., Warren, J., Weber, K.C., Williamson, C.H.D., Willis, A.D., Xu, Z.Z., Zaneveld, J.R., Zhang, Y., Zhu, Q., Knight, R., Caporaso, J.G., 2019. Reproducible, interactive, scalable and extensible microbiome data science using QIIME 2. Nat. Biotechnol. 37, 852–857. https://doi.org/10.1038/s41587-019-0209-9

Bray, J.R., Curtis, J.T., Roger, J., 1957. This content downloaded from 147.8.31.43 on Mon. Source Ecol. Monogr. 27, 325–349.

Briatte, F., 2020. Ggnet: Functions to Plot NetworksWith ggplot2. R package version 0.1.0. Available online at: https://github.com/briatte/ggnet.

Callahan, B.J., McMurdie, P.J., Rosen, M.J., Han, A.W., Johnson, A.J.A., Holmes, S.P., 2016. DADA2: High-resolution sample inference from Illumina amplicon data. Nat. Methods 13, 581–583. https://doi.org/10.1038/nmeth.3869

Chambefort, I., Stefánsson, A., 2020. Fluids in geothermal systems. Elements 16, 407–411. https://doi.org/10.2138/GSELEMENTS.16.6.407

Chan, C.S., Chan, K.G., Ee, R., Hong, K.W., Urbieta, M.S., Donati, E.R., Shamsir, M.S., Goh, K.M., 2017. Effects of physiochemical factors on prokaryotic Biodiversity in Malaysian circumneutral hot springs. Front. Microbiol. 8. https://doi.org/10.3389/fmicb.2017.01252

Christenson, B.W., White, S., Britten, K., Scott, B.J., 2017. Hydrological evolution and chemical structure of a hyper-acidic spring-lake system on Whakaari/White Island, NZ. J. Volcanol. Geotherm. Res. 346, 180–211. https://doi.org/10.1016/j.jvolgeores.2017.06.017

Christiansen, R.L., 2001. The Quaternary and Pliocene Yellowstone Plateau volcanic field of Wyoming, Idaho, and Montana, US Geological Survey Professional Paper. https://doi.org/10.3133/pp729G

Cole, J.W., Spinks, K.D., 2015. Caldera volcanism and rift structure in the Taupo Volcanic Zone, New Zealand. Geol. Soc. Spec. Publ. 327, 9–29. https://doi.org/10.1144/SP327.2

Colman, D.R., Feyhl-Buska, J., Fecteau, K.M., Xu, H., Shock, E.L., Boyd, E.S., 2016. Ecological differentiation in planktonic and sediment-associated chemotrophic microbial populations in Yellowstone hot springs. FEMS Microbiol. Ecol. 92. https://doi.org/10.1093/femsec/fiw137

Colman, D.R., Lindsay, M.R., Amenabar, M.J., Boyd, E.S., 2019a. The Intersection of Geology, Geochemistry, and Microbiology in Continental Hydrothermal Systems. Astrobiology 19, 1505–1522. https://doi.org/10.1089/ast.2018.2016

Colman, D.R., Lindsay, M.R., Boyd, E.S., 2019b. Mixing of meteoric and geothermal fluids supports hyperdiverse chemosynthetic hydrothermal communities. Nat. Commun. 10. https://doi.org/10.1038/s41467-019-08499-1

Cortecci, G., Boschetti, T., Mussi, M., Lameli, C.H., Mucchino, C., Barbieri, M., 2005. New chemical and

original isotopic data on waters from El Tatio geothermal field, northern Chile. Geochem. J. 39, 547–571. https://doi.org/10.2343/geochemj.39.547

Cusicanqui, H., Mahon, W.A.J., Ellis, A.J., 1975. The Geochemistry of the El Tatio Geothermal Field, Northern Chile. Proc. Second United Nations Symp. Dev. Use Geotherm. Resour. 1, 703–711.

Custodio, E., Llamas, M.R., 1983. Hidrología Subterránea [Groundwater hydrology], Second Edi. ed. Editorial Omega, Barcelona.

Daniele, L., Taucare, M., Viguier, B., Arancibia, G., Aravena, D., Roquer, T., Sepúlveda, J., Molina, E., Delgado, A., Muñoz, M., Morata, D., 2020. Exploring the shallow geothermal resources in the Chilean Southern Volcanic Zone: Insight from the Liquiñe thermal springs. J. Geochemical Explor. 218, 106611. https://doi.org/10.1016/j.gexplo.2020.106611

De Silva, S.L., 1989. Altiplano-Puna volcanic complex of the central Andes. Geology 17, 1102–1106. https://doi.org/10.1130/0091-7613(1989)017<1102:APVCOT>2.3.CO;2

DeMets, C., Gordon, R.G., Argus, D.F., Stein, S., 1990. Current plate motions. Geophys. J. Int. 101, 425–478. https://doi.org/10.1111/j.1365-246X.1990.tb06579.x

Dewey, J., Shackleton, R., Chengfa, C., Yiyin, S., 1988. The tectonic evolution of the Tibetan Plateau. Philos. Trans. R. Soc. London. Ser. A, Math. Phys. Sci. 327, 379–413. https://doi.org/10.1098/rsta.1988.0135

Dick, J.M., Shock, E.L., 2013. A metastable equilibrium model for the relative abundances of microbial phyla in a hot spring. PLoS One 8. https://doi.org/10.1371/journal.pone.0072395

Dobson, P.F., Kneafsey, T.J., Hulen, J., Simmons, A., 2003. Porosity, permeability, and fluid flow in the Yellowstone geothermal system, Wyoming. J. Volcanol. Geotherm. Res. 123, 313–324. https://doi.org/10.1016/S0377-0273(03)00039-8

Engel, A.S., Johnson, L.R., Porter, M.L., 2013. Arsenite oxidase gene diversity among Chloroflexi and Proteobacteria from El Tatio Geyser Field, Chile. FEMS Microbiol. Ecol. 83, 745–756. https://doi.org/10.1111/1574-6941.12030

Erikstad, H.A., Ceballos, R.M., Smestad, N.B., Birkeland, N.K., 2019. Global biogeographic distribution patterns of thermoacidophilic verrucomicrobia methanotrophs suggest allopatric evolution. Front. Microbiol. 10, 1–11. https://doi.org/10.3389/fmicb.2019.01129

Fournier, R.O., 1989. Geochemistry and dynamics of the Yellowstone National Park Hydrothermal System. Annu. Rev. Earth Planet. Sci. 17, 13–53.

Gagliano, A.L., Tagliavia, M., D'Alessandro, W., Franzetti, A., Parello, F., Quatrini, P., 2016. So close, so different: geothermal flux shapes divergent soil microbial communities at neighbouring sites. Geobiology 14, 150–162. https://doi.org/10.1111/gbi.12167

Giggenbach, W., Sheppard, D., Robinson, B., Stewart, M., Lyon, G., 1994. Geochemical structure and position of the Waiotapu geothermal field, New Zealand. Geothermics 23, 599–644. https://doi.org/10.1016/0375-6505(94)90022-1

Giggenbach, W.F., 1995. Variations in the chemical and isotopic composition of fluids discharged from the Taupo Volcanic Zone, New Zealand. J. Volcanol. Geotherm. Res. 68, 89–116. https://doi.org/10.1016/0377-0273(95)00009-J

Giggenbach, W.F., 1991. Applications of geochemistry in geothermal reservoir development.

Giggenbach, W.F., 1988. Geothermal solute equilibria. Derivation of Na-K-Mg-Ca geoindicators.

Geochim. Cosmochim. Acta 52, 2749–2765. https://doi.org/10.1016/0016-7037(88)90143-3

Giggenbach, W.F., 1978. The isotopic composition of waters from the El Tatio geothermal field, Northern Chile. Geochim. Cosmochim. Acta 42, 979–988. https://doi.org/10.1016/0016-7037(78)90287-9

Giggenbach, W.F., Goguel, R.L., 1989. Collection and analysis of geothermal and volcanic water and gas discharges. Rep. No. CD 2401. Chem. Div. DSIR, Petone, New Zeal.

Giggenbach, W.F., Shinohara, H., Kusakabe, H., Ohba, T., 2003. Formation of acid volcanic brines through interaction of magmatic gases, seawater, and rock within the White Island volcanic-hydrothermal system, New Zealand. Geochmica Cosmochim. Acta Special Pu, 19–40. https://doi.org/10.5382/sp.10.02

Glennon, J.A., Pfaff, R.M., 2003. The extraordinary thermal activity of El Tatio Geyser Field, Antofagasta Region, Chile. GOSA Trans. 8, 31–78.

Guo, L., Wang, G., Sheng, Y., Sun, X., Shi, Z., Xu, Q., Mu, W., 2020. Temperature governs the distribution of hot spring microbial community in three hydrothermal fields, Eastern Tibetan Plateau Geothermal Belt, Western China. Sci. Total Environ. 720, 137574. https://doi.org/10.1016/j.scitotenv.2020.137574

Guo, Q., Kirk Nordstrom, D., Blaine McCleskey, R., 2014. Towards understanding the puzzling lack of acid geothermal springs in Tibet (China): Insight from a comparison with Yellowstone (USA) and some active volcanic hydrothermal systems. J. Volcanol. Geotherm. Res. 288, 94–104. https://doi.org/10.1016/j.jvolgeores.2014.10.005

Guo, Q., Pang, Z., Wang, Y., Tian, J., 2017. Fluid geochemistry and geothermometry applications of the Kangding high-temperature geothermal system in eastern Himalayas. Appl. Geochemistry 81, 63–75. https://doi.org/10.1016/j.apgeochem.2017.03.007

Hamilton, T.L., Bennett, A.C., Murugapiran, S.K., Havig, J.R., 2019. Anoxygenic Phototrophs Span Geochemical Gradients and Diverse Morphologies in Terrestrial Geothermal Springs. mSystems 4, 1–25. https://doi.org/10.1128/msystems.00498-19

Hedenquist, J.W., 1991. Boiling and dilution in the shallow portion of the Waiotapu geothermal system, New Zealand. Geochim. Cosmochim. Acta 55, 2753–2765. https://doi.org/10.1016/0016-7037(91)90442-8

Henley, R.W., Stewart, M.K., 1983. Chemical and isotopic changes in the hydrology of the tauhara geothermal field due to exploitation at wairakei. J. Volcanol. Geotherm. Res. 15, 285–314. https://doi.org/10.1016/0377-0273(83)90104-X

Hijmans, R.J., Williams, E., Vennes, C., Hijmans, M.R.J., 2017. Package 'geosphere'. Spherical trigonometry 1.

Hildreth, W., Halliday, A.N., Christiansen, R.L., 1991. Isotopic and chemical evidence concerning the genesis and contamination of basaltic and rhyolitic magma beneath the yellowstone plateau volcanic field. J. Petrol. 32, 63–138. https://doi.org/10.1093/petrology/32.1.63

Hirzel, A.H., Le Lay, G., 2008. Habitat suitability modelling and niche theory. J. Appl. Ecol. 45, 1372–1381. https://doi.org/10.1111/j.1365-2664.2008.01524.x

Hochstein, M.P., 1995. Crustal heat transfer in the Taupo Volcanic Zone (New Zealand): comparison with other volcanic arcs and explanatory heat source models. J. Volcanol. Geotherm. Res. 68, 117–151. https://doi.org/10.1016/0377-0273(95)00010-R

Hou, W., Wang, S., Dong, H., Jiang, H., Briggs, B.R., Peacock, J.P., Huang, Q., Huang, L., Wu, G., Zhi,

X., Li, W., Dodsworth, J.A., Hedlund, B.P., Zhang, C., Hartnett, H.E., Dijkstra, P., Hungate, B.A., 2013. A Comprehensive Census of Microbial Diversity in Hot Springs of Tengchong, Yunnan Province China Using 16S rRNA Gene Pyrosequencing. PLoS One 8. https://doi.org/10.1371/journal.pone.0053350

Hounslow, A.W., 1995. Water quality data analysis and interpretation.

Hunt, T., Glover, R., Wood, C., 1994. Waimangu, Waiotapu, and Waikite geothermal systems, New Zealand: background and history. Geothermics 23, 379–400. https://doi.org/10.1016/0375-6505(94)90010-8

Hurwitz, S., Lowenstern, J.B., 2014. Dynamics of the Yellowstone hydrothermal system. Eos, Trans. Am. Geophys. Union 69, 849–849. https://doi.org/10.1029/88EO01108

Hurwitz, S., McCleskey, R.B., Bergfeld, D., Peek, S.E., Susong, D.D., Roth, D.A., Hungerford, J.D.G., White, E.B., Harrison, L.N., Hosseini, B., Vaughan, R.G., Hunt, A.G., Paces, J.B., 2020. Hydrothermal Activity in the Southwest Yellowstone Plateau Volcanic Field. Geochemistry, Geophys. Geosystems 21, 1–27. https://doi.org/10.1029/2019GC008848

Inskeep, W.P., Jay, Z.J., Herrgard, M.J., Kozubal, M.A., Rusch, D.B., Tringe, S.G., Macur, R.E., Jennings, R. de M., Boyd, E.S., Spear, J.R., Roberto, F.F., 2013a. Phylogenetic and functional analysis of metagenome sequence from high-temperature archaeal habitats demonstrate linkages between metabolic potential and geochemistry. Front. Microbiol. 4. https://doi.org/10.3389/fmicb.2013.00095

Inskeep, W.P., Jay, Z.J., Tringe, S.G., Herrgård, M.J., Rusch, D.B., 2013b. The YNP metagenome project: Environmental parameters responsible for microbial distribution in the yellowstone geothermal ecosystem. Front. Microbiol. 4, 1–15. https://doi.org/10.3389/fmicb.2013.00067

Jolie, E., Scott, S., Faulds, J., Chambefort, I., Axelsson, G., Gutiérrez-Negrín, L.C., Regenspurg, S., Ziegler, M., Ayling, B., Richter, A., Zemedkun, M.T., 2021. Geological controls on geothermal resources for power generation. Nat. Rev. Earth Environ. 2, 324–339. https://doi.org/10.1038/s43017-021-00154-y

Kaasalainen, H., Stefánsson, A., 2012. The chemistry of trace elements in surface geothermal waters and steam, Iceland. Chem. Geol. 330–331, 60–85. https://doi.org/10.1016/j.chemgeo.2012.08.019

Kaya, E., O'Sullivan, M.J., Hochstein, M.P., 2014. A three dimensional numerical model of the Waiotapu, Waikite and Reporoa geothermal areas, New Zealand. J. Volcanol. Geotherm. Res. 283, 127–142. https://doi.org/10.1016/j.jvolgeores.2014.07.008

Kendall, 1948. Rank Correlation Methods, Oxford: Griffin.

Kim, Y.M., Nowack, S., Olsen, M., Becraft, E.D., Wood, J.M., Thiel, V., Klapper, I., Kühl, M., Fredrickson, J.K., Bryant, D.A., Ward, D.M., Metz, T.O., 2015. Diel metabolomics analysis of a hot spring chlorophototrophic microbial mat leads to new hypotheses of community member metabolisms. Front. Microbiol. 6. https://doi.org/10.3389/fmicb.2015.00209

Kruskal, W.H., Wallis, W.A., 1952. Use of Ranks in One-Criterion Variance Analysis. J. Am. Stat. Assoc. 47, 583–621. https://doi.org/10.1080/01621459.1952.10483441

Kurtz, Z.D., Müller, C.L., Miraldi, E.R., Littman, D.R., Blaser, M.J., Bonneau, R.A., 2015. Sparse and Compositionally Robust Inference of Microbial Ecological Networks. PLoS Comput. Biol. 11, 1–25. https://doi.org/10.1371/journal.pcbi.1004226

Lahsen, A., 1988. Chilean geothermal resources and their possible utilization. Geothermics 17, 401–410. https://doi.org/10.1016/0375-6505(88)90068-5

Lee, C.-Y.K., 2015. The First Insights into the Phylogeny, Genomics, and Ecology of the Novel Bacterial Phylum Armatimonadetes. University of Waikato.

Letelier, J.A., O'Sullivan, J., Reich, M., Veloso, E., Sánchez-Alfaro, P., Aravena, D., Muñoz, M., Morata, D., 2021. Reservoir architecture model and heat transfer modes in the El Tatio-La Torta geothermal system, Central Andes of northern Chile. Geothermics 89. https://doi.org/10.1016/j.geothermics.2020.101940

Lowenstern, J.B., Bergfeld, D., Evans, W.C., Hunt, A.G., 2015. Origins of geothermal gases at Yellowstone. J. Volcanol. Geotherm. Res. 302, 87–101. https://doi.org/10.1016/j.jvolgeores.2015.06.010

Lozupone, C., Knight, R., 2005. UniFrac: A new phylogenetic method for comparing microbial communities. Appl. Environ. Microbiol. 71, 8228–8235. https://doi.org/10.1128/AEM.71.12.8228-8235.2005

Lozupone, C.A., Hamady, M., Kelley, S.T., Knight, R., 2007. Quantitative and qualitative β diversity measures lead to different insights into factors that structure microbial communities. Appl. Environ. Microbiol. 73, 1576–1585. https://doi.org/10.1128/AEM.01996-06

Mackenzie, R., Pedrós-Alió, C., Díez, B., 2013. Bacterial composition of microbial mats in hot springs in Northern Patagonia: Variations with seasons and temperature. Extremophiles 17, 123–136. https://doi.org/10.1007/s00792-012-0499-z

Mahmoud, K.K., Leduc, L.G., Ferroni, G.D., 2005. Detection of Acidithiobacillus ferrooxidans in acid mine drainage environments using fluorescent in situ hybridization (FISH). J. Microbiol. Methods 61, 33–45. https://doi.org/10.1016/j.mimet.2004.10.022

Marinov, N., Lahsen, A., 1984. Carta geológica de Chile, Hoja Calama, Escala 1: 250.000. Serv. Nac. Geol. y Minería 58.

Marty, B., Giggenbach, W.F., 1990. Major and rare gases at White Island volcano, New Zealand: origin and flux of volatiles. Geophys. Res. Lett. 17, 247–250.

Massello, F.L., Chan, C.S., Chan, K.G., Goh, K.M., Donati, E., Urbieta, M.S., 2020. Meta-analysis of microbial communities in hot springs: Recurrent taxa and complex shaping factors beyond ph and temperature. Microorganisms 8, 1–18. https://doi.org/10.3390/microorganisms8060906

Mathur, J., Bizzoco, R.W., Ellis, D.G., Lipson, D.A., Poole, A.W., Levine, R., Kelley, S.T., 2007. Effects of abiotic factors on the phylogenetic diversity of bacterial communities in acidic thermal springs. Appl. Environ. Microbiol. 73, 2612–2623. https://doi.org/10.1128/AEM.02567-06

McMurdie, P.J., Holmes, S., 2013. Phyloseq: An R Package for Reproducible Interactive Analysis and Graphics of Microbiome Census Data. PLoS One 8. https://doi.org/10.1371/journal.pone.0061217

Milicich, S.D., Chambefort, I., Wilson, C.J.N., Alcaraz, S., Ireland, T.R., Bardsley, C., Simpson, M.P., 2020. A zircon U-Pb geochronology for the Rotokawa geothermal system, New Zealand, with implications for Taupō Volcanic Zone evolution. J. Volcanol. Geotherm. Res. 389, 106729. https://doi.org/10.1016/j.jvolgeores.2019.106729

Miller, S.R., Castenholz, R.W., Pedersen, D., 2007. Phylogeography of the thermophilic cyanobacterium Mastigocladus laminosus. Appl. Environ. Microbiol. 73, 4751–4759. https://doi.org/10.1128/AEM.02945-06

Millot, R., Hegan, A., Négrel, P., 2012. Geothermal waters from the Taupo Volcanic Zone, New Zealand: Li, B and Sr isotopes characterization. Appl. Geochemistry 27, 677–688. https://doi.org/10.1016/j.apgeochem.2011.12.015

Moeck, I.S., 2014. Catalog of geothermal play types based on geologic controls. Renew. Sustain. Energy Rev. 37, 867–882. https://doi.org/10.1016/j.rser.2014.05.032

Munoz-Saez, C., Manga, M., Hurwitz, S., 2018. Hydrothermal discharge from the El Tatio basin, Atacama, Chile. J. Volcanol. Geotherm. Res. 361, 25–35. https://doi.org/10.1016/j.jvolgeores.2018.07.007

Nicholson, K., 1993. Geothermal fluids: Chemistry and exploration techniques, Journal of Geochemical Exploration. https://doi.org/10.1016/0375-6742(95)90013-6

Nicolau, C., Reich, M., Lynne, B., 2014. Physico-chemical and environmental controls on siliceous sinter formation at the high-altitude El Tatio geothermal field, Chile. J. Volcanol. Geotherm. Res. 282, 60–76. https://doi.org/10.1016/j.jvolgeores.2014.06.012

Nordstrom, K.D., Blaine McCleskey, R., Ball, J.W., 2009. Sulfur geochemistry of hydrothermal waters in Yellowstone National Park: IV Acid-sulfate waters. Appl. Geochemistry 24, 191–207. https://doi.org/10.1016/j.apgeochem.2008.11.019

Oksanen, A.J., Blanchet, F.G., Friendly, M., Kindt, R., Legendre, P., Mcglinn, D., Minchin, P.R., Hara, R.B.O., Simpson, G.L., Solymos, P., Stevens, M.H.H., Szoecs, E., 2019. Vegan. Encycl. Food Agric. Ethics 2395–2396. https://doi.org/10.1007/978-94-024-1179-9_301576

Palandri, Kharaka, 2004. A Compilation of Rate Parameters of Water-Mineral Interaction Kinetics. Geol. Surv. Menlo Park CA.

Papke, R.T., Ramsing, N.B., Bateson, M.M., Ward, D.M., 2003. Geographical isolation in hot spring cyanobacteria. Environ. Microbiol. 5, 650–659. https://doi.org/10.1046/j.1462-2920.2003.00460.x

Parada, A.E., Needham, D.M., Fuhrman, J.A., 2016. Every base matters: Assessing small subunit rRNA primers for marine microbiomes with mock communities, time series and global field samples. Environ. Microbiol. 18, 1403–1414. https://doi.org/10.1111/1462-2920.13023

Parkhurst, D.L., Appelo, C.A.J., 1999. User's guite to PHREEQC (Version 2)- A computer program for speciation, batch-reaction, one-dimensonal transport, and inverse geochemical calculations. Water-Resources Investig. Rep. https://doi.org/10.2307/3459821

Phoenix, V.R., Bennett, P.C., Engel, A.S., Tyler, S.W., Ferris, F.G., 2006. Chilean high-altitude hot-spring sinters: A model system for UV screening mechanisms by early Precambrian cyanobacteria. Geobiology 4, 15–28. https://doi.org/10.1111/j.1472-4669.2006.00063.x

Piper, A.M., 1944. A graphic procedure in the geochemical interpretation of water-analyses. Am. Geophys. union 914–928.

Podar, P.T., Yang, Z., Björnsdóttir, S.H., Podar, M., 2020. Comparative Analysis of Microbial Diversity Across Temperature Gradients in Hot Springs From Yellowstone and Iceland. Front. Microbiol. 11, 1–16. https://doi.org/10.3389/fmicb.2020.01625

Power, J.F., Carere, C.R., Lee, C.K., Wakerley, G.L.J., Evans, D.W., Button, M., White, D., Climo, M.D., Hinze, A.M., Morgan, X.C., McDonald, I.R., Cary, S.C., Stott, M.B., 2018. Microbial biogeography of 925 geothermal springs in New Zealand. Nat. Commun. 9. https://doi.org/10.1038/s41467-018-05020-y

Price, M.N., Dehal, P.S., Arkin, A.P., 2010. FastTree 2 - Approximately maximum-likelihood trees for large alignments. PLoS One 5. https://doi.org/10.1371/journal.pone.0009490

Quatrini, R., Johnson, D.B., 2019. Acidithiobacillus ferrooxidans. Trends Microbiol. 27, 282–283. https://doi.org/10.1016/j.tim.2018.11.009

R Core Team, 2013. R: A language and environment for statistical computing. R Found. Stat. Comput. Vienna, Austria.

Real, R., Vargas, J.M., 1996. The probabilistic basis of Jaccard's index of similarity. Syst. Biol. 45, 380–385. https://doi.org/10.1093/sysbio/45.3.380

Robinson, B.W., Sheppard, D.S., 1986. A chemical and isotopic study of the Tokaanu-Waihi geothermal area, New Zealand. J. Volcanol. Geotherm. Res. 27, 135–151. https://doi.org/10.1016/0377-0273(86)90083-1

Romano, C., D'Imperio, S., Woyke, T., Mavromatis, K., Lasken, R., Shock, E.L., McDermott, T.R., 2013. Comparative genomic analysis of phylogenetically closely related Hydrogenobaculum sp. isolates from yellowstone national park. Appl. Environ. Microbiol. 79, 2932–2943. https://doi.org/10.1128/AEM.03591-12

Rye, R.O., Truesdell, A.H., 2007. The Question of Recharge to the Deep Thermal Reservoir Underlying the Geysers and Hot Springs of Yellowstone National Park. U.S. Geol. Surv. Prof. Pap. 1717 205–234.

Salisbury, M.J., Jicha, B.R., de Silva, S.L., Singer, B.S., Jiménez, N.C., Ort, M.H., 2011. 40Ar/39Ar chronostratigraphy of Altiplano-Puna volcanic complex ignimbrites reveals the development of a major magmatic province. Bull. Geol. Soc. Am. 123, 821–840. https://doi.org/10.1130/B30280.1

Sanchez-Alfaro, P., Sielfeld, G., Campen, B. Van, Dobson, P., Fuentes, V., Reed, A., Palma-Behnke, R., Morata, D., 2015. Geothermal barriers, policies and economics in Chile - Lessons for the Andes. Renew. Sustain. Energy Rev. 51, 1390–1401. https://doi.org/10.1016/j.rser.2015.07.001

Shannon, C.E., 1948. A Mathematical Theory of Communication. Bell Syst. Tech. J. 27, 623–656. https://doi.org/10.1002/j.1538-7305.1948.tb00917.x

Sharp, C.E., Brady, A.L., Sharp, G.H., Grasby, S.E., Stott, M.B., Dunfield, P.F., 2014. Humboldt's spa: Microbial diversity is controlled by temperature in geothermal environments. ISME J. 8, 1166–1174. https://doi.org/10.1038/ismej.2013.237

Sheppard, D.S., Lyon, G.L., 1984. Geothermal fluid chemistry of the Orakeikorako field, New Zealand. J. Volcanol. Geotherm. Res. 22, 329–349. https://doi.org/10.1016/0377-0273(84)90008-8

Shock, E.L., Holland, M., Meyer-Dombard, D.R., Amend, J.P., 2005. Geochemical sources of energy for microbial metabolism in hydrothermal ecosystems: Obsidian Pool, Yellowstone National Park. Geotherm. Biol. Geochemistry Yellowstone Natl. Park 95–112.

Simpson, M.P., Bignall, G., 2016. Undeveloped high-enthalpy geothermal fields of the Taupo Volcanic Zone, New Zealand. Geothermics 59, 325–346. https://doi.org/10.1016/j.geothermics.2015.08.006

Soto, M.F., Hochstein, M.P., Campbell, K., Keys, H., 2019. Sporadic and waning hot spring activity in the Tokaanu Domain, Hipaua-Waihi-Tokaanu geothermal field, Taupo Volcanic Zone, New Zealand. Geothermics 77, 288–303. https://doi.org/10.1016/j.geothermics.2018.10.005

Steinke, L., Slysz, G.W., Lipton, M.S., Klatt, C., Moran, J.J., Romine, M.F., Wood, J.M., Anderson, G., Bryant, D.A., Ward, D.M., 2020. Short-term stable isotope probing of proteins reveals taxa incorporating inorganic carbon in a hot spring microbial mat. Appl. Environ. Microbiol. 86. https://doi.org/10.1128/AEM.01829-19

Tang, X., Zhang, J., Pang, Z., Hu, S., Tian, J., Bao, S., 2017a. The eastern Tibetan Plateau geothermal belt, western China: Geology, geophysics, genesis, and hydrothermal system. Tectonophysics 717, 433–448. https://doi.org/10.1016/j.tecto.2017.08.035

Tang, X., Zhang, J., Pang, Z., Hu, S., Wu, Y., Bao, S., 2017b. Distribution and genesis of the eastern Tibetan Plateau geothermal belt, western China. Environ. Earth Sci. 76, 1–15. https://doi.org/10.1007/s12665-016-6342-6

Taran, Y., Kalacheva, E., 2020. Acid sulfate-chloride volcanic waters; Formation and potential for monitoring of volcanic activity. J. Volcanol. Geotherm. Res. 405, 107036. https://doi.org/10.1016/j.jvolgeores.2020.107036

Tassi, F., Aguilera, F., Darrah, T., Vaselli, O., Capaccioni, B., Poreda, R.J., Delgado Huertas, A., 2010. Fluid geochemistry of hydrothermal systems in the Arica-Parinacota, Tarapacá and Antofagasta regions (northern Chile). J. Volcanol. Geotherm. Res. 192, 1–15. https://doi.org/10.1016/j.jvolgeores.2010.02.006

Tassi, F., Martinez, C., Vaselli, O., Capaccioni, B., Viramonte, J., 2005. Light hydrocarbons as redox and temperature indicators in the geothermal field of El Tatio (northern Chile). Appl. Geochemistry 20, 2049–2062. https://doi.org/10.1016/j.apgeochem.2005.07.013

Tedesco, D., Toutain, J., 1991. Chemistry and emission rate of volatiles from White Island volcano (New Zealand). Geophys. Res. Lett. 18, 113–116.

Uribe-Lorío, L., Brenes-Guillén, L., Hernández-Ascencio, W., Mora-Amador, R., González, G., Ramírez-Umaña, C.J., Díez, B., Pedrós-Alió, C., 2019. The influence of temperature and pH on bacterial community composition of microbial mats in hot springs from Costa Rica. Microbiologyopen 8. https://doi.org/10.1002/mbo3.893

Valverde, A., Tuffin, M., Cowan, D.A., 2012. Biogeography of bacterial communities in hot springs: A focus on the actinobacteria. Extremophiles 16, 669–679. https://doi.org/10.1007/s00792-012-0465-9

Veloso, E.E., Tardani, D., Elizalde, D., Godoy, B.E., Sánchez-Alfaro, P.A., Aron, F., Reich, M., Morata, D., 2020. A review of the geodynamic constraints on the development and evolution of geothermal systems in the Central Andean Volcanic Zone (18–28°Lat.S). Int. Geol. Rev. 62, 1294–1318. https://doi.org/10.1080/00206814.2019.1644678

Wang, S., Hou, W., Dong, H., Jiang, H., Huang, L., Wu, G., Zhang, C., Song, Z., Zhang, Y., Ren, H., Zhang, J., Zhang, L., 2013. Control of Temperature on Microbial Community Structure in Hot Springs of the Tibetan Plateau. PLoS One 8. https://doi.org/10.1371/journal.pone.0062901

Ward, K.M., Zandt, G., Beck, S.L., Christensen, D.H., McFarlin, H., 2014. Seismic imaging of the magmatic underpinnings beneath the Altiplano-Puna volcanic complex from the joint inversion of surface wave dispersion and receiver functions. Earth Planet. Sci. Lett. 404, 43–53. https://doi.org/10.1016/j.epsl.2014.07.022

Whitaker, R.J., Grogan, D.W., Taylor, J.W., 2003. Geographic barriers isolate endemic populations of hyperthermophilic archaea. Science (80-.). 301, 976–978. https://doi.org/10.1126/science.1086909

White, D.E., 1957. Thermal water of volcanic origin. Bull. Geol. Soc. Am. 68, 1637–1658.

Willis, G., Nancucheo, I., Hedrich, S., Giaveno, A., Donati, E., Johnson, D.B., 2019. Enrichment and isolation of acid-tolerant sulfate-reducing microorganisms in the anoxic, acidic hot spring sediments from Copahue volcano, Argentina. FEMS Microbiol. Ecol. 95, 1–11. https://doi.org/10.1093/femsec/fiz175

Wilson, C.J.N., Houghton, B.F., McWilliams, M.O., Lanphere, M.A., Weaver, S.D., Briggs, R.M., 1995. Volcanic and structural evolution of Taupo Volcanic Zone, New Zealand: a review. J. Volcanol. Geotherm. Res. 68, 1–28. https://doi.org/10.1016/0377-0273(95)00006-G

Wilson, C.J.N., Rowland, J. V., 2016. The volcanic, magmatic and tectonic setting of the Taupo Volcanic

Zone, New Zealand, reviewed from a geothermal perspective. Geothermics 59, 168–187. https://doi.org/10.1016/j.geothermics.2015.06.013

Wrage, J., Tardani, D., Reich, M., Daniele, L., Arancibia, G., Cembrano, J., Sánchez-Alfaro, P., Morata, D., Pérez-Moreno, R., 2017. Geochemistry of thermal waters in the Southern Volcanic Zone, Chile – Implications for structural controls on geothermal fluid composition. Chem. Geol. 466, 545–561. https://doi.org/10.1016/j.chemgeo.2017.07.004

Yin, A., Harrison, T.M., 2000. Evolution of the Himalayan-Tibetan Orogen. Annu. Rev. Earth Planet. Sci. 28, 211–280.

Zhang, J., Li, W.Y., Tang, X.C., Tian, J., Wang, Y.C., Guo, Q., Pang, Z.H., 2017. Geothermal data analysis at the high-temperature hydrothermal area in Western Sichuan. Sci. China Earth Sci. 60, 1507–1521. https://doi.org/10.1007/s11430-016-9053-2

Zhang, K.-J., Zhang, Y.-X., Tang, X.-C., Xia, B., 2012. Late Mesozoic tectonic evolution and growth of the Tibetan plateau prior to the Indo-Asian collision. Earth-Science Rev. 114, 236–249. https://doi.org/10.1016/j.earscirev.2012.06.001

Zhang, K.J., Xia, B., Liang, X., 2002. Mesozoic-Paleogene sedimentary facies and paleogeography of Tibet, western China: Tectonic implications. Geol. J. 37, 217–246. https://doi.org/10.1002/gj.911

Zhang, Y., Wu, G., Jiang, H., Yang, J., She, W., Khan, I., Li, W., 2018. Abundant and rare microbial biospheres respond differently to environmental and spatial factors in tibetan hot springs. Front. Microbiol. 9, 1–16. https://doi.org/10.3389/fmicb.2018.02096

Zhao, J., Wang, G., Zhang, C., Xing, L., Man, L.I., Zhang, W., 2021. Genesis of Geothermal Fluid in Typical Geothermal Fields in Western Sichuan, China. Acta Geol. Sin. 95, 873–882. https://doi.org/10.1111/1755-6724.14715

Supplementary Material

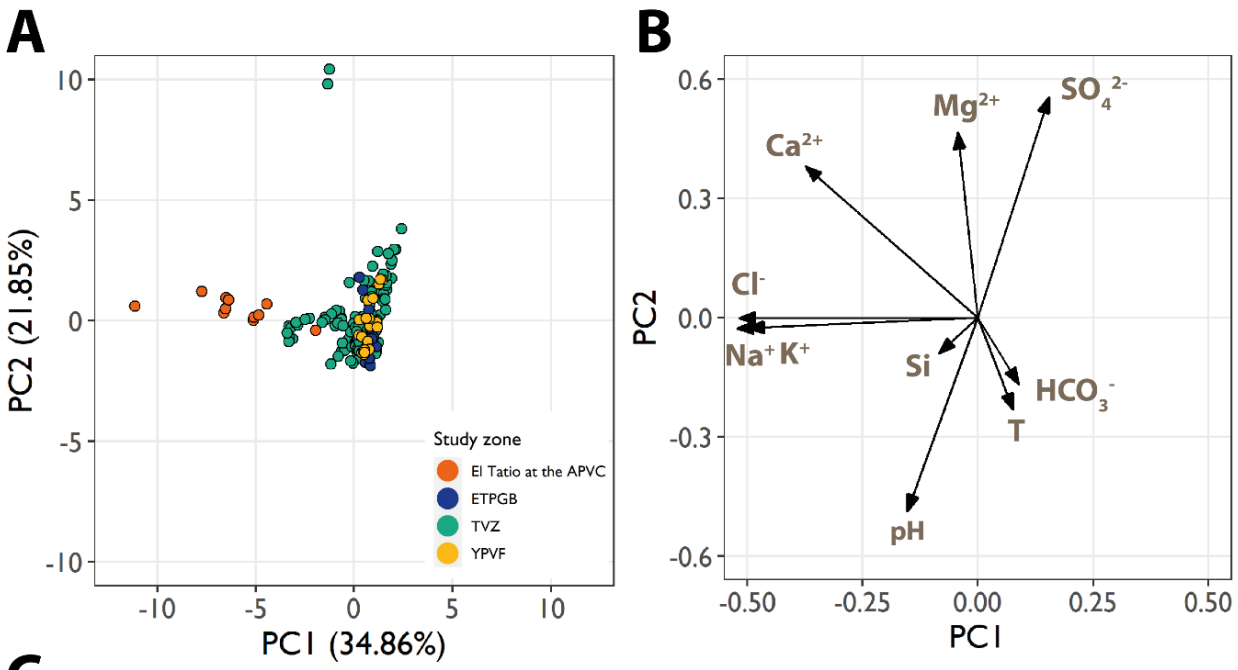

C

	PC1	PC2	PC3	PC4	PC5	PC6	PC7	PC8	PC9	PC10
T	0.08	-0.23	0.30	**0.60**	**0.64**	0.14	-0.25	0.06	-0.01	0.01
pH	-0.15	**-0.49**	-0.27	0.31	0.01	**-0.50**	**0.57**	0.01	0.03	0.01
Cl^-	**-0.52**	0.00	0.06	-0.14	0.16	0.07	0.03	-0.22	**-0.41**	0.68
SO_4^{2-}	0.15	**0.56**	0.21	0.06	0.28	0.17	**0.72**	-0.04	-0.01	-0.02
HCO_3^-	0.09	-0.17	**-0.63**	0.18	-0.04	0.71	0.12	-0.11	0.02	0.06
Na^+	**-0.52**	-0.03	0.03	-0.08	0.13	0.12	0.01	-0.34	-0.25	-0.71
K^+	**-0.50**	-0.03	0.09	-0.04	-0.04	0.25	0.10	**0.79**	0.20	-0.04
Mg^{2+}	-0.04	**0.47**	-0.33	**0.48**	-0.17	-0.21	-0.18	0.26	-0.52	-0.06
Ca^{2+}	-0.38	0.38	-0.20	0.25	0.04	-0.15	-0.16	-0.29	**0.68**	0.11
Si	-0.09	-0.09	**0.50**	**0.45**	**-0.66**	0.22	0.10	-0.20	0.00	0.05

Supplementary Figure 3-1 Principal component analysis (PCA) of the 11 hydrochemical variables including the 202 analyzed hot springs. A) Distribution of the analyzed samples in PC1 and PC2 B) Eigenvectors in PC1 and PC2 C) Table with the resulted eigenvalues.

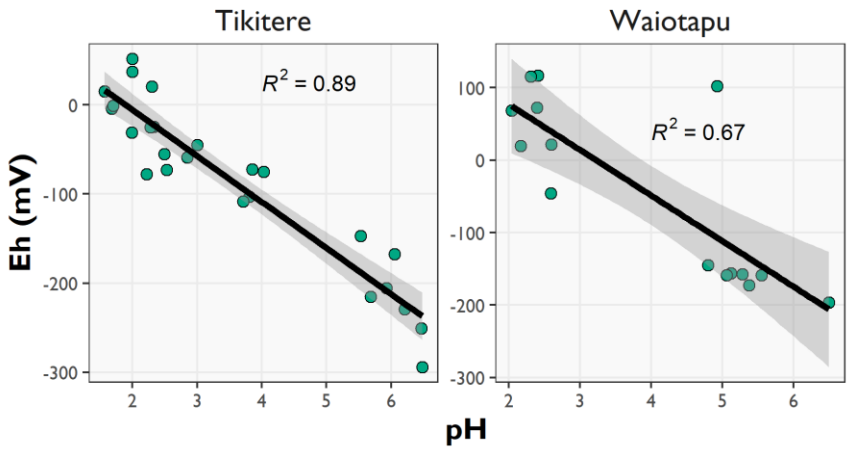

Supplementary Figure 3-2 Eh vs pH values of samples in Tikitere and Waiotapu geothermal fields. Eh values were obtained from the One Thousand Spring project website (https://1000springs.org.nz/).

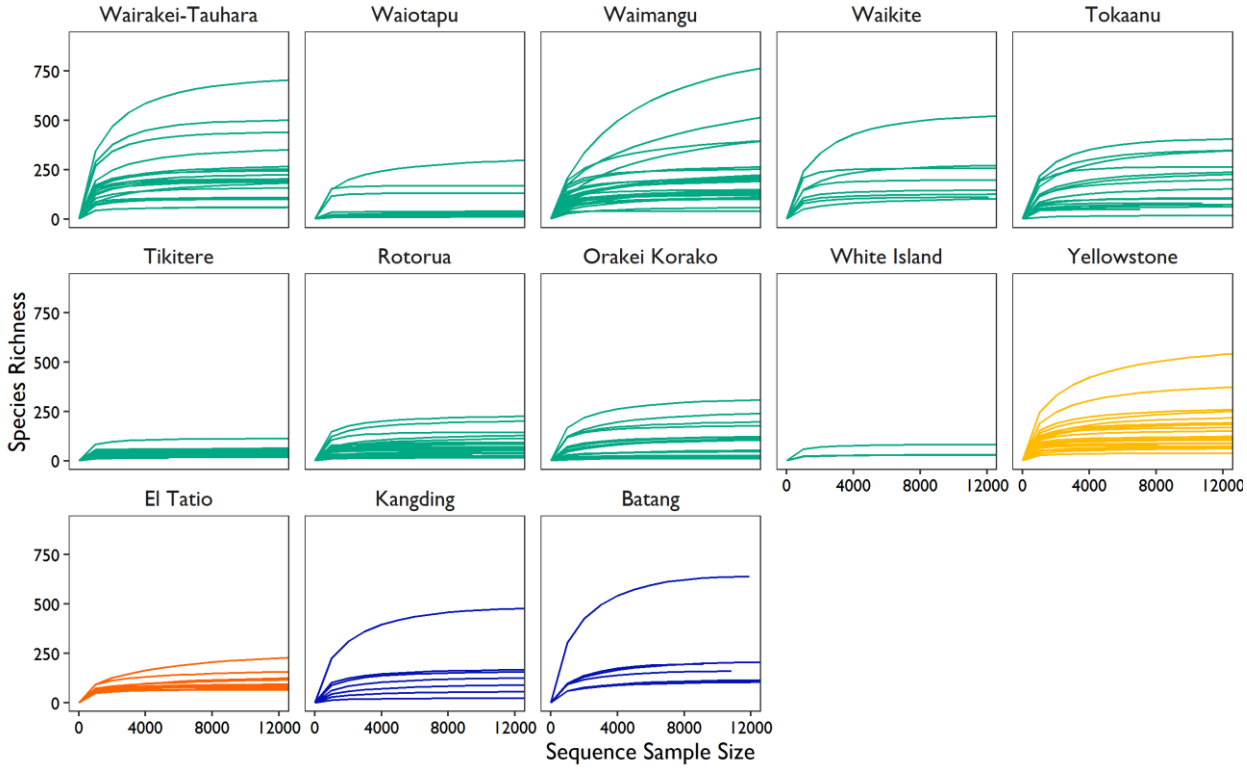

Supplementary Figure 3-3 Rarefaction curves of the samples by geothermal field.

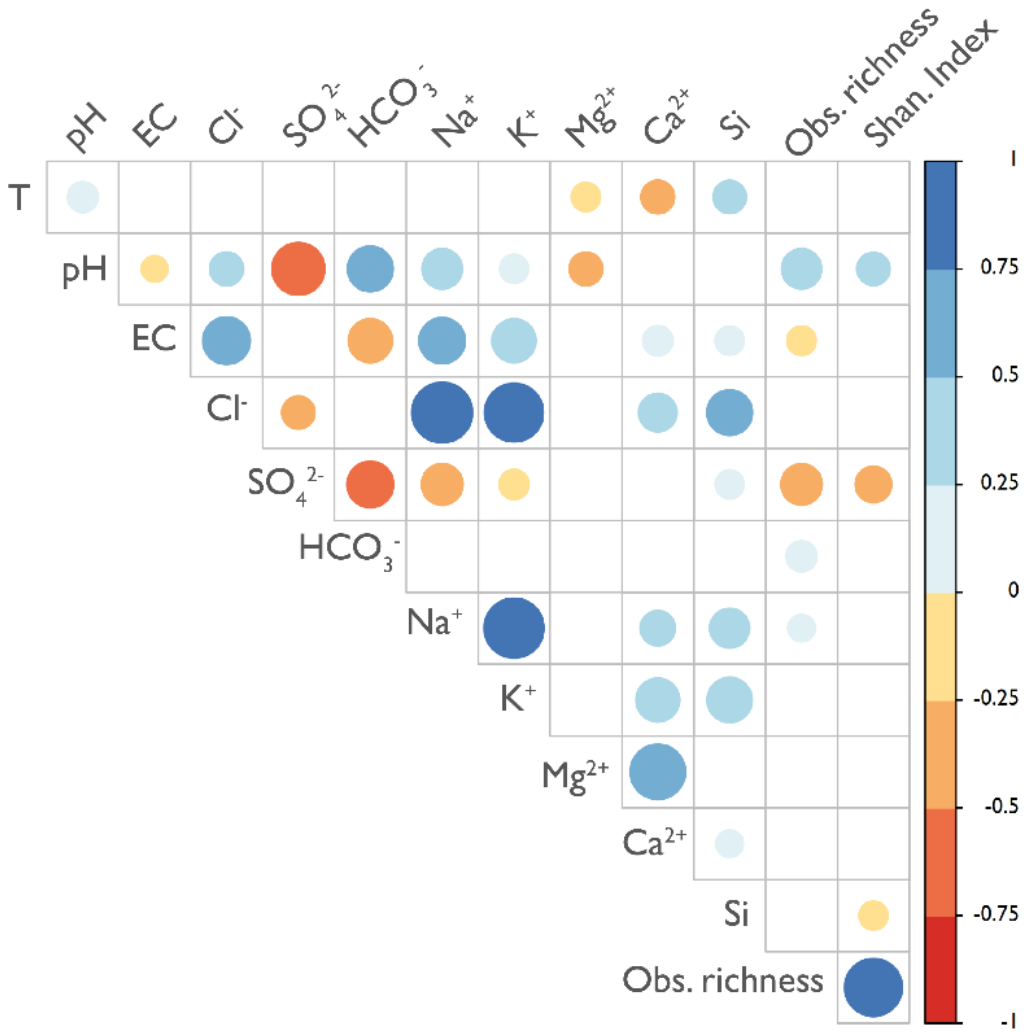

Supplementary Figure 3-4 Significant Spearman's correlations between environmental parameters, observed richness and Shannon indexes from all the analyzed hot springs.

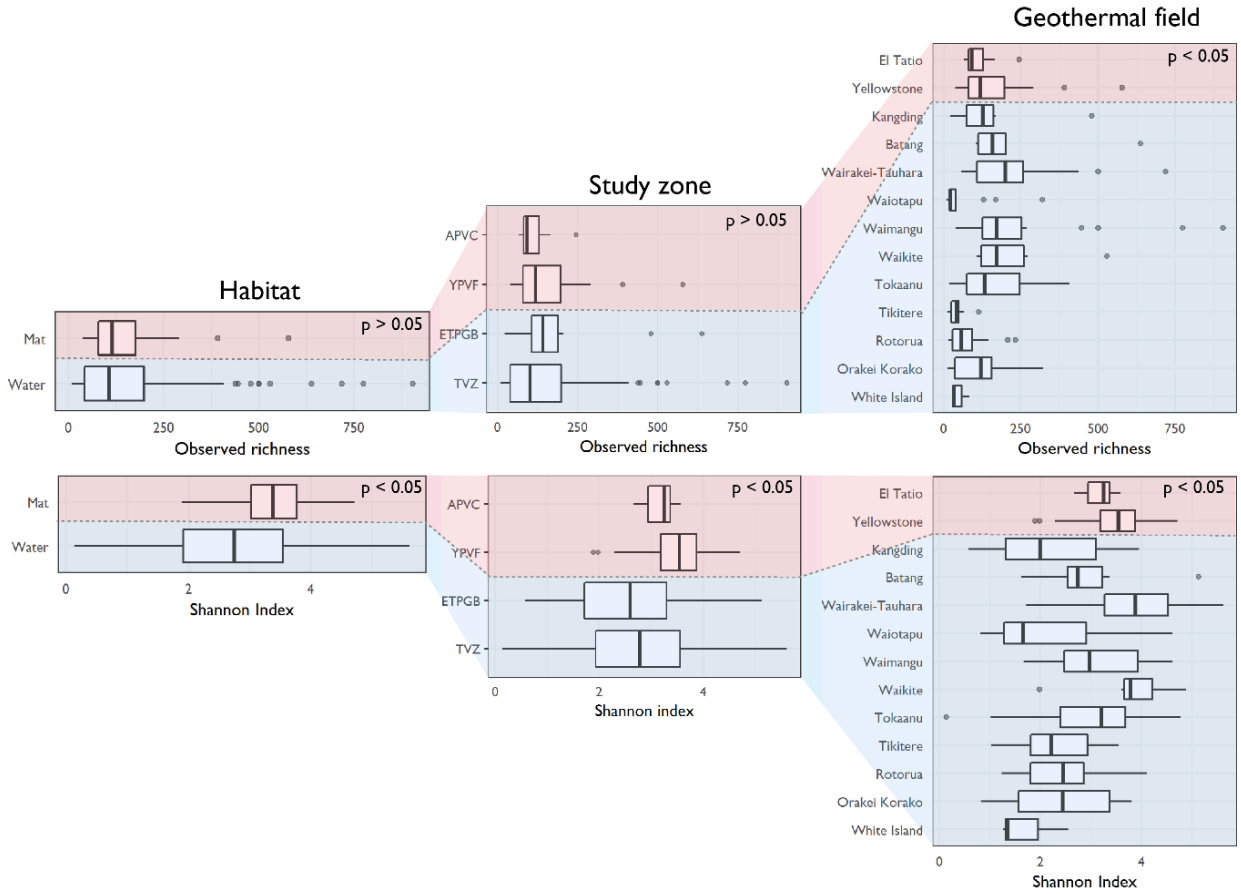

Supplementary Figure 3-5 Observed richness and Shannon indexes according to the habitat (water or microbial mat), geothermal area, and geothermal field (APVC: Altiplano-Puna Volcanic Complex; YPVF: Yellowstone Plateau Volcanic Field; ETPGB: Eastern Tibetan Plateau Geothermal Belt; TVZ: Taupo Volcanic Zone).

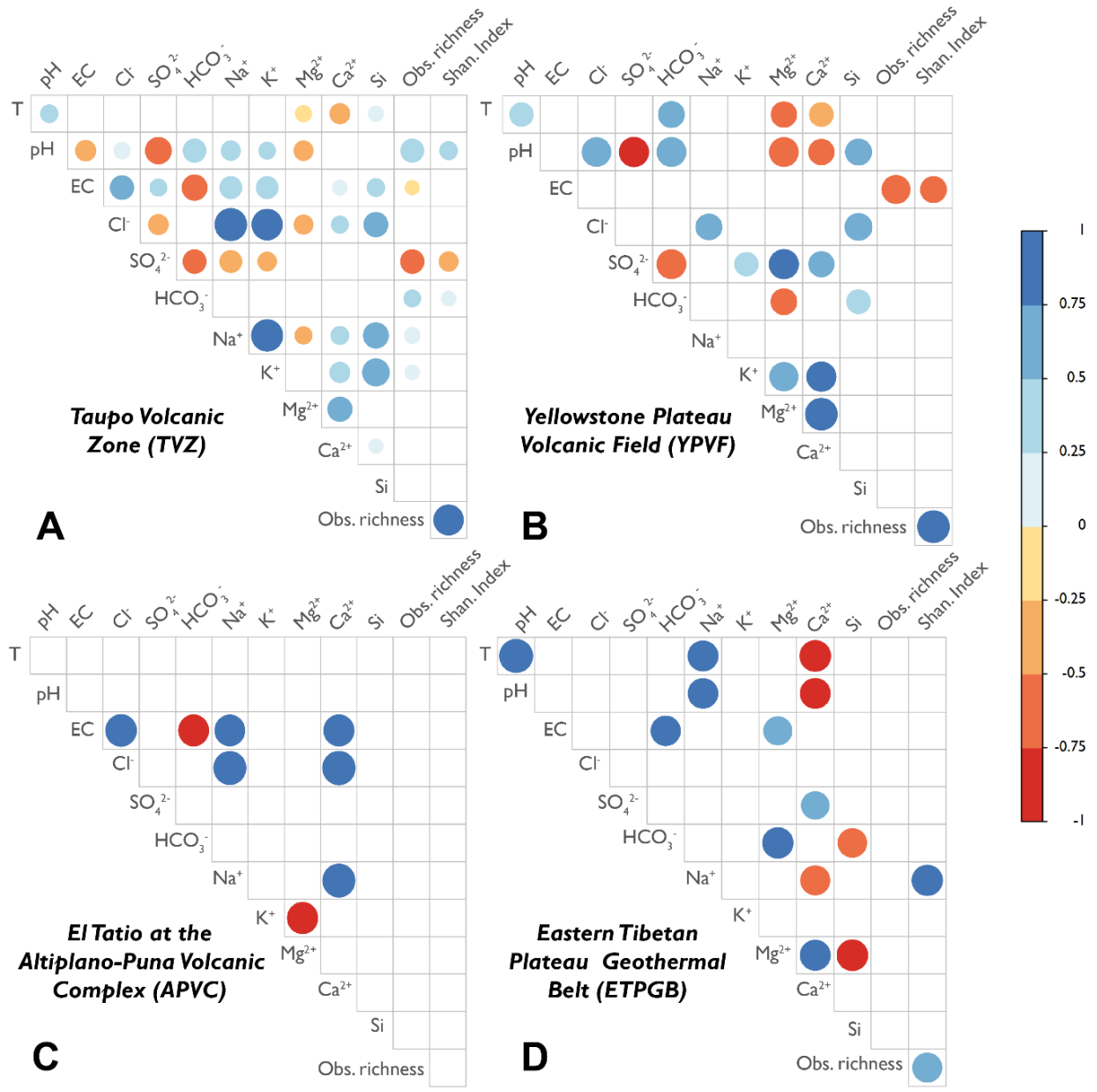

Supplementary Figure 3-6 Significant Spearman's correlations between environmental parameters, observed richness, and Shannon indexes at each study zone. T: temperature, EC: electrical conductivity, Obs.: observed, Shan: Shannon.

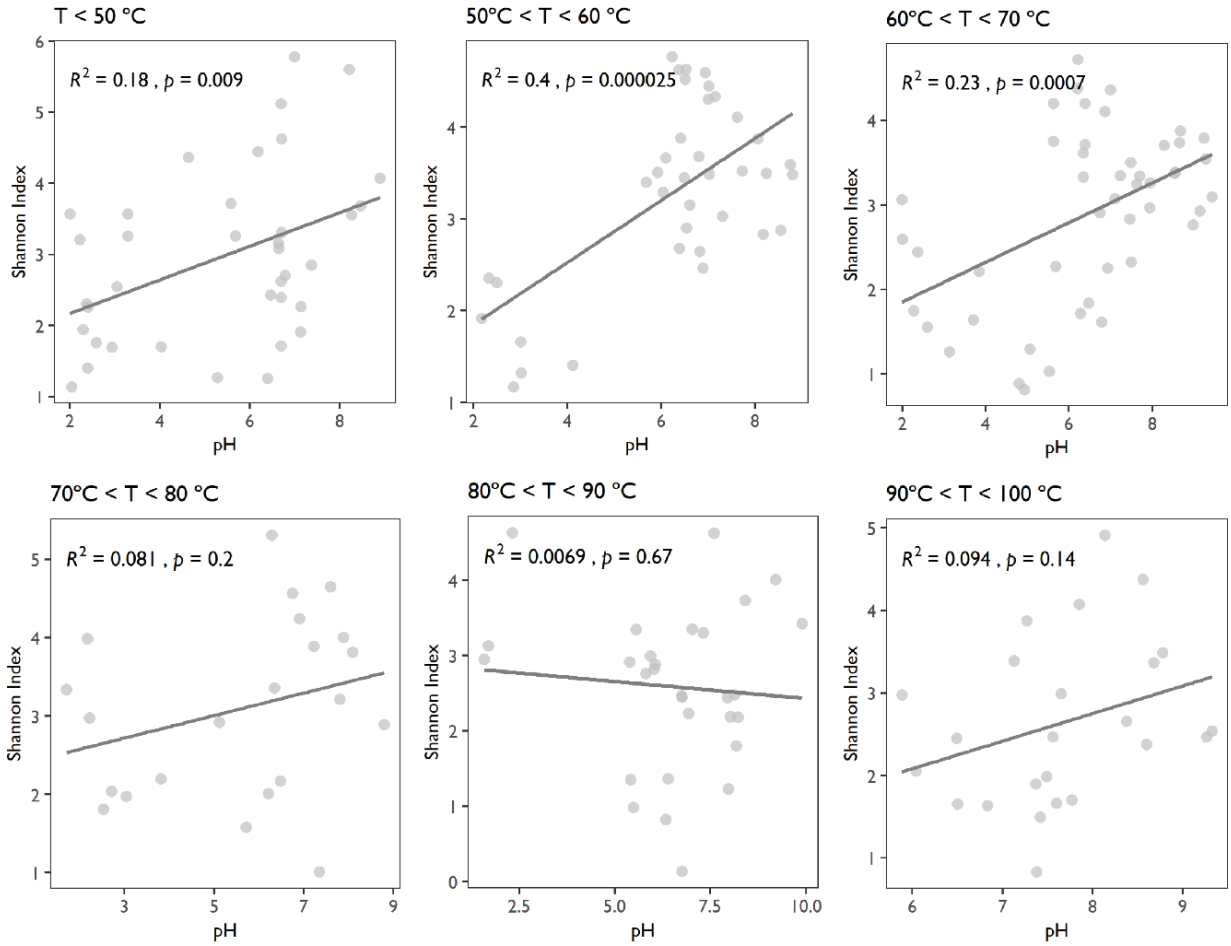

Supplementary Figure 3-7 Shannon diversity indexes plotted against pH. Samples were divided into six groups according to water temperature.

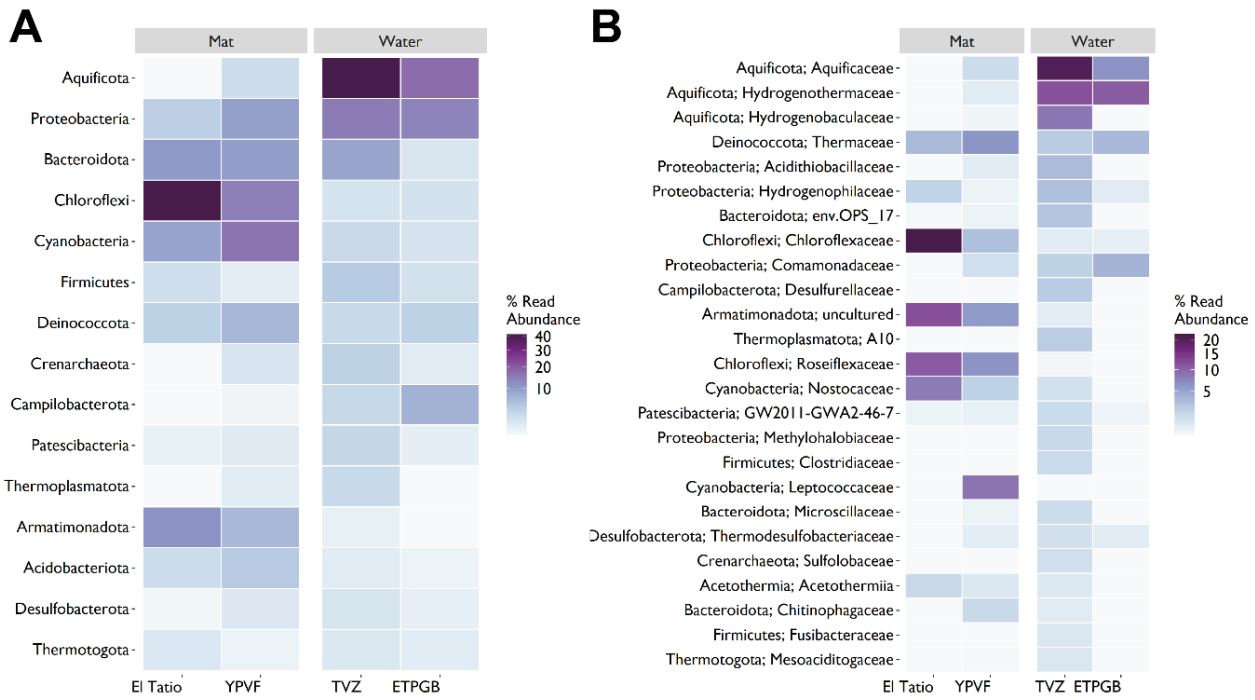

Supplementary Figure 3-8 Relative abundance of the microbial communities by study zone. A) Abundance of the 15 most abundant phyla. B) Abundance of the 30 most abundant families.

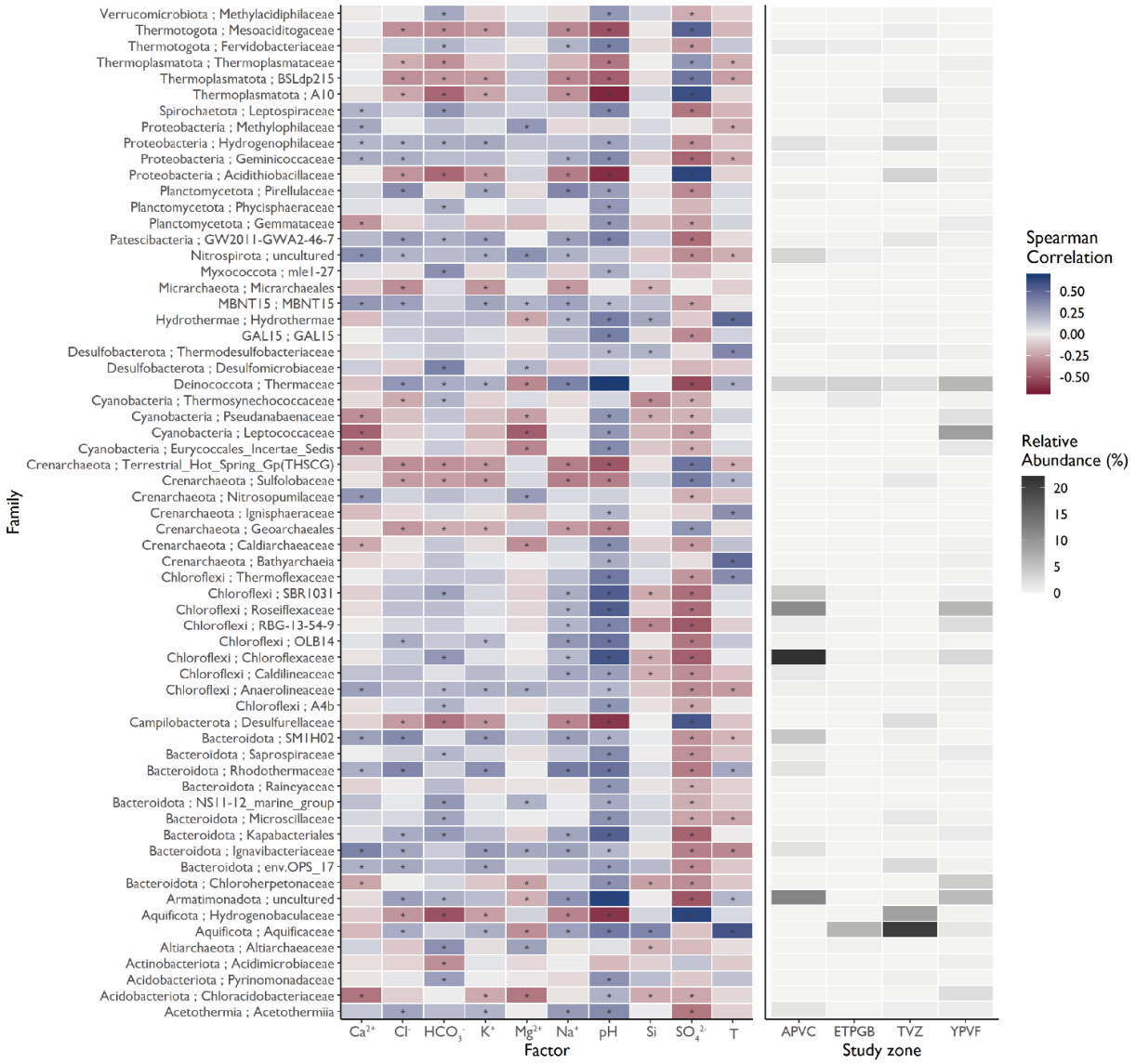

Supplementary Figure 3-9 Heatmap showing the highest Spearman correlations ($\rho > 0.3$; $p > 0.01$) between family abundance and hydrochemical variables. Sequences were previously filtered by relative abundance (<0.1%).

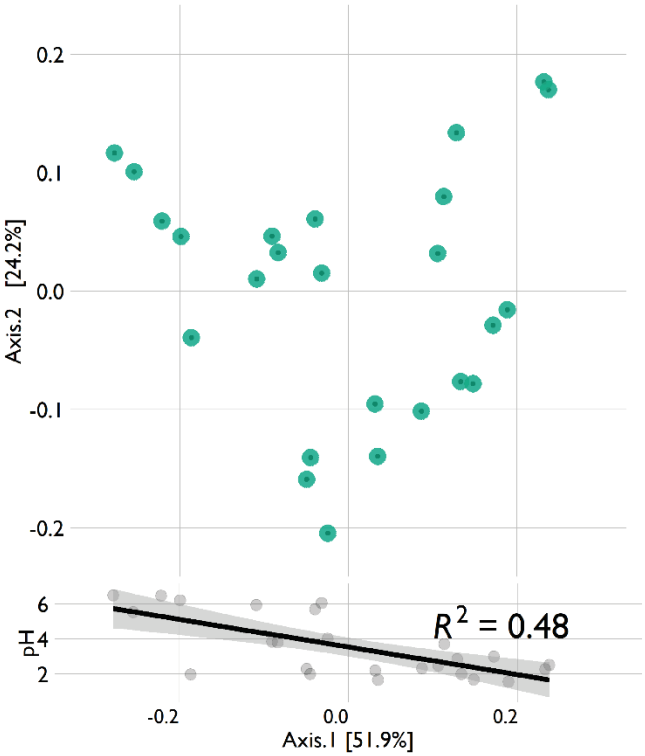

Supplementary Figure 3-10 Axis 1 and 2 resulted from the MDS analysis performed on the weighted Unifrac distances between thermal microbial communities in Tikitere. Correlation of Axis 1 with pH is also shown.

Supplementary Table 3-1 Strategies and analytical techniques used to obtain the 16S rRNA sequences and the chemical analysis of each set of samples.

	AREA	**Taupo Volcanic Zone**	**Yellowstone**	**Eastern Tibetan Plateau**	**El Tatio at APVC**
	PUBLICATION	**Power et al. (2018)**	**Hamilton et al. (2019)**	**Guo et al. (2020)**	**This article**
	Nº available SRA files	925	34	16	-
	Nº used samples	152	25	14	11
Genomic data	Source	ENA, NCBI (PRJEB24353)	NCBI (PRJNA513338)	NCBI (SRP234510)	This article
	Region of the 16S rRNA	V4	V4	V4	V4-V5
	Type of sample	Water	Microbial mat	Water	Microbial mat
	Technology of sequencing	Life Sciences Ion Torrent PGM	MiSeq Illumina 2 x 300-bp	MiSeq Illumina 2 x 250-bp	MiSeq Illumina 2 x 250-bp
Hydrochemical data	Source	1000springs.org.nz/	NCBI, Publication	NCBI, Publication	This article
	Anion quantification	Ion Chromatography (Cl, SO_4), tritation (HCO_3), potentiometric tritation (Cl)	Ion Chromatography	Ion Chromatography (Cl, SO_4), potentiometric tritation (HCO_3)	Ion Chromatography (Cl, SO_4), tritation (HCO_3)
	Cation quantification	Inductively coupled plasma mass spectroscopy (ICP-MS)	Inductively coupled plasma mass spectroscopy (ICP-MS)	Inductively Coupled Plasma Optical Emission Spectrometer (ICP-OES)	Flame Atomic Absorption Spectroscopy

Supplementary Table 3-2 Physicochemical parameters and concentration of major elements of the analyzed hot springs.

SRA number	Area	Geothermal field	N°	Latitude	Longitude	T (°C)	pH	EC (µS/cm)	Cl^- (mg/l)	SO_4^{2-} (mg/l)	HCO_3^- (mg/l)	Na^+ (mg/l)	K^+ (mg/l)	Mg^{2+} (mg/l)	Ca^{2+} (mg/l)	Si (mg/l)
TAT10_60.7_42	APVF	El Tatio	1	-22.346595	-68.00834	60.7	6.75	12350	3929.00	38.01	136.00	2460.00	118.00	11.03	163.40	99.50
TAT11_62.0_46	APVF	El Tatio	2	-22.336902	-68.018595	62.0	8.54	11700	3796.00	35.49	95.00	2250.00	229.00	5.93	141.90	70.99
TAT12_61.0_53	APVF	El Tatio	3	-22.337869	-68.01719	61.0	7.94	11500	3808.00	34.87	107.00	2260.00	230.00	5.22	141.00	66.32
TAT13_50.0_92	APVF	El Tatio	4	-22.356122	-68.022753	50.0	9.27	7700	1679.00	66.38	237.00	1130.00	96.00	11.34	77.50	126.66
TAT2_62.0_5	APVF	El Tatio	5	-22.337869	-68.01719	62.8	7.63	14600	4716.00	35.10	74.00	2890.00	286.00	4.94	169.40	86.00
TAT3_55.0_65	APVF	El Tatio	6	-22.34558	-68.012261	65.0	7.23	16500	5394.00	46.79	42.00	3270.00	149.00	6.77	238.40	109.79
TAT5_55.0_70	APVF	El Tatio	7	-22.337409	-68.017377	55.0	7.30	14500	4706.00	35.44	91.00	2790.00	287.00	4.91	168.50	79.87
TAT6_60.0_23	APVF	El Tatio	8	-22.336949	-68.0144	60.0	7.45	11650	3537.00	35.25	96.00	2270.00	212.00	5.03	140.30	96.37
TAT7_50.0_76	APVF	El Tatio	9	-22.333578	-68.012773	50.0	8.24	21000	7061.00	36.30	14.00	4260.00	508.00	1.72	239.60	113.01
TAT8_60.0_32	APVF	El Tatio	10	-22.347724	-68.011304	60.0	7.12	14400	5757.00	51.66	140.00	4580.00	152.00	10.48	258.80	84.08
TAT9_62.7_37	APVF	El Tatio	11	-22.350396	-68.007983	62.7	7.48	15000	5286.00	46.17	45.00	3210.00	150.00	4.98	230.60	95.34
SRR8420032	YPVF	Yellowstone	1	44.569662	-110.865018	55.0	8.24	1439	220.87	17.10	263.13	280.71	15.64	0.00	0.36	93.23
SRR8420033	YPVF	Yellowstone	8	44.687666	-110.727923	44.2	8.26	2481	449.54	123.92	5.74	392.44	28.54	0.24	4.81	112.60
SRR8420034	YPVF	Yellowstone	9	44.687602	-110.727684	59.9	7.62	3254	424.02	113.35	191.95	364.39	27.76	0.24	4.81	111.20
SRR8420035	YPVF	Yellowstone	10	44.532526	-110.797769	71.0	8.80	2910	246.04	15.37	0.02	346.69	21.50	0.00	0.52	130.01
SRR8420036	YPVF	Yellowstone	11	44.610054	-110.438726	63.7	6.21	1100	45.38	40.35	0.02	78.63	28.93	15.07	30.46	55.88
SRR8420037	YPVF	Yellowstone	12	44.61019	-110.438914	58.2	5.68	2539	278.31	213.25	9.61	296.34	37.53	0.97	6.41	78.34
SRR8420038	YPVF	Yellowstone	13	44.610107	-110.43865	31.5	4.64	556	31.91	138.33	5.74	63.68	17.59	6.81	15.63	44.65
SRR8420039	YPVF	Yellowstone	14	44.558769	-110.843889	68.5	8.68	2944	280.08	16.33	119.56	342.32	11.73	0.00	1.16	59.81
SRR8420040	YPVF	Yellowstone	15	44.532499	-110.797668	69.4	8.56	2751	244.27	14.41	127.41	337.95	20.72	0.00	0.60	111.20
SRR8420041	YPVF	Yellowstone	16	44.5684	-110.863623	51.4	8.05	2748	225.84	14.41	242.60	316.34	13.68	0.00	0.56	63.46
SRR8420042	YPVF	Yellowstone	2	44.517642	-110.806477	67.9	5.63	460	2.48	167.14	205.99	76.79	15.64	0.02	0.60	69.36
SRR8420043	YPVF	Yellowstone	3	44.700569	-110.765528	69.5	6.39	1925	232.93	314.12	63.01	383.01	27.37	0.02	3.25	71.60
SRR8420044	YPVF	Yellowstone	4	44.729157	-110.712676	38.4	3.29	2470	0.35	95.10	14.84	373.36	46.92	0.10	4.37	51.95
SRR8420045	YPVF	Yellowstone	17	44.569653	-110.865005	68.4	7.95	2969	216.97	16.33	129.75	287.83	14.08	0.00	0.44	101.09
SRR8420046	YPVF	Yellowstone	5	44.729157	-110.712676	38.4	3.29	2470	0.35	95.10	266.93	373.36	46.92	0.10	4.37	51.95
SRR8420047	YPVF	Yellowstone	6	44.699573	-110.767223	40.5	7.13	2310	565.48	206.53	257.68	404.85	35.19	0.07	5.17	61.50

SRA number	Area	Geothermal field	N°	Latitude	Longitude	T (°C)	pH	EC (µS/cm)	Cl^- (mg/l)	SO_4^{2-} (mg/l)	HCO_3^- (mg/l)	Na^+ (mg/l)	K^+ (mg/l)	Mg^{2+} (mg/l)	Ca^{2+} (mg/l)	Si (mg/l)
SRR8420048	YPVF	Yellowstone	7	44.517642	-110.806477	67.9	5.63	460	2.48	167.14	319.63	76.79	15.64	0.02	0.60	69.36
SRR8420049	YPVF	Yellowstone	18	44.516526	-110.806695	65.1	6.20	510	1.77	69.16	38.53	49.20	10.95	0.00	0.40	38.47
SRR8420050	YPVF	Yellowstone	19	44.520461	-110.812571	62.4	9.44	3756	324.75	15.37	137.99	371.75	17.20	0.00	0.40	117.66
SRR8420052	YPVF	Yellowstone	20	44.700081	-110.764873	52.8	2.17	4573	87.21	640.72	0.03	82.76	21.11	0.39	3.53	57.00
SRR8420053	YPVF	Yellowstone	21	44.700009	-110.764874	49.1	2.38	3804	128.69	529.29	0.08	109.89	23.85	0.49	4.33	71.04
SRR8420054	YPVF	Yellowstone	22	44.520407	-110.812558	62.3	9.29	3578	304.90	18.25	164.71	363.01	15.64	0.00	0.40	96.31
SRR8420055	YPVF	Yellowstone	23	44.5199	-110.8115	62.3	9.24	3584	305.25	18.25	174.04	361.17	15.25	0.00	0.40	69.64
SRR8420056	YPVF	Yellowstone	24	44.52091	-110.812154	68.4	9.14	3944	307.38	19.21	177.29	363.47	15.64	0.00	0.40	88.17
SRR8420057	YPVF	Yellowstone	25	44.700251	-110.764254	47.2	2.22	4133	93.95	644.56	0.00	94.03	22.68	0.39	3.61	76.94
SRR10580885	ETPGB	Batang	1	30.26	99.46	65.4	7.10	1200	16.80	5.10	692.50	278.30	21.40	1.70	4.10	27.58
SRR10580888	ETPGB	Batang	2	30.4	99.4	88.2	9.90	1430	50.90	22.60	176.50	359.00	29.30	0.00	0.60	70.36
SRR10580889	ETPGB	Batang	3	30.28	99.34	64.4	7.70	1580	14.40	99.00	876.10	294.20	20.00	17.80	26.60	29.91
SRR10580891	ETPGB	Batang	4	30.4	99.39	88.0	9.20	1530	53.20	24.60	560.80	368.80	30.10	0.10	0.50	56.30
SRR10580894	ETPGB	Batang	5	30.4	99.38	87.8	8.40	820	51.60	31.50	411.50	370.50	31.40	0.00	1.30	74.82
SRR10580896	ETPGB	Batang	6	30.15	99.19	45.5	7.00	1940	11.20	134.10	957.70	312.50	26.30	40.40	49.80	27.07
SRR10580898	ETPGB	Batang	7	29.96	99.08	43.3	6.70	1490	14.20	138.50	868.40	134.50	34.00	68.40	116.10	25.60
SRR10580884	ETPGB	Kangding	1	30.18	101.87	63.6	7.50	880	53.00	33.80	403.00	187.90	14.80	1.40	22.00	56.84
SRR10580886	ETPGB	Kangding	2	30.28	101.94	37.4	6.70	1240	53.50	1.60	738.40	262.00	18.90	5.10	24.50	40.09
SRR10580890	ETPGB	Kangding	3	29.98	101.96	72.2	7.60	2680	142.30	2.10	1228.10	510.60	53.80	32.80	17.90	34.98
SRR10580892	ETPGB	Kangding	4	30.12	101.94	40.4	6.40	2320	57.30	84.70	822.50	174.80	28.80	49.50	94.50	14.06
SRR10580895	ETPGB	Kangding	5	30.26	101.87	60.8	7.00	1750	75.60	2.40	899.40	316.00	30.30	15.10	20.50	40.66
SRR10580897	ETPGB	Kangding	6	30.18	101.87	44.8	6.70	960	58.60	35.40	455.30	200.20	15.90	2.00	33.70	60.22
SRR10580899	ETPGB	Kangding	7	29.95	101.96	79.5	7.80	2420	126.90	48.00	791.90	356.20	41.70	18.10	24.40	54.87
ERR2240344	TVZ	Orakei Korako	1	-38.4736	176.1467	50.6	8.80	1817	345.00	97.00	219.00	291.00	38.00	0.26	5.30	120.00
ERR2240345	TVZ	Orakei Korako	2	-38.4735	176.1468	75.8	8.09	1693	320.00	97.00	225.00	271.00	35.00	0.30	5.40	109.00
ERR2240346	TVZ	Orakei Korako	3	-38.4734	176.1469	82.3	7.94	1666	313.00	96.00	216.00	269.00	36.00	0.47	5.90	109.00
ERR2240347	TVZ	Orakei Korako	4	-38.4731	176.1475	99.0	7.42	1585	305.00	121.00	134.00	254.00	36.00	0.34	8.30	114.00

SRA number	Area	Geothermal field	N°	Latitude	Longitude	T (°C)	pH	EC (µS/cm)	Cl^- (mg/l)	SO_4^{2-} (mg/l)	HCO_3^- (mg/l)	Na^+ (mg/l)	K^+ (mg/l)	Mg^{2+} (mg/l)	Ca^{2+} (mg/l)	Si (mg/l)
ERR2240348	TVZ	Orakei Korako	5	-38.4732	176.1475	93.9	8.38	1637	319.00	101.00	168.00	263.00	36.00	0.34	6.80	120.00
ERR2240349	TVZ	Orakei Korako	6	-38.4732	176.1482	97.2	6.83	1731	328.00	114.00	223.00	297.00	39.00	0.34	8.70	115.00
ERR2241038	TVZ	Orakei Korako	7	-38.4733	176.1471	93.6	7.13	2028	283.00	90.00	230.00	340.00	43.00	1.50	7.00	124.00
ERR2241039	TVZ	Orakei Korako	8	-38.4735	176.1483	97.8	7.38	2270	308.00	99.00	265.00	365.00	51.00	1.10	7.50	144.00
ERR2241040	TVZ	Orakei Korako	9	-38.4736	176.1483	85.3	7.02	2154	278.00	149.00	192.00	327.00	48.00	0.99	8.40	140.00
ERR2241041	TVZ	Orakei Korako	10	-38.4735	176.1482	58.3	7.73	2375	318.00	104.00	264.00	356.00	52.00	0.98	10.60	133.00
ERR2241044	TVZ	Orakei Korako	11	-38.4735	176.1468	89.3	6.33	2165	287.00	90.00	294.00	333.00	40.00	0.84	6.60	138.00
ERR2241045	TVZ	Orakei Korako	12	-38.4737	176.1468	83.8	5.48	1908	279.00	152.00	67.00	276.00	33.00	1.10	7.60	127.00
ERR2241046	TVZ	Orakei Korako	13	-38.4742	176.1485	85.5	6.74	2100	321.00	120.00	206.00	457.00	52.00	3.80	7.40	173.00
ERR2241047	TVZ	Orakei Korako	14	-38.474	176.1485	96.0	7.77	2116	322.00	116.00	191.00	434.00	50.00	3.30	9.10	161.00
ERR2241048	TVZ	Orakei Korako	15	-38.4738	176.1471	95.0	7.37	1976	319.00	76.00	288.00	357.00	46.00	0.95	6.60	158.00
ERR2240422	TVZ	Rotorua	1	-38.1331	176.2454	81.3	6.03	1700	289.00	117.00	154.00	260.00	16.30	0.62	12.20	122.00
ERR2240473	TVZ	Rotorua	2	-38.1318	176.2453	87.1	6.92	1631	327.00	74.00	262.00	332.00	24.00	0.98	9.90	145.00
ERR2240483	TVZ	Rotorua	3	-38.1318	176.2443	49.2	2.94	2158	235.00	378.00	131.00	224.00	20.00	2.30	30.00	114.00
ERR2240508	TVZ	Rotorua	4	-38.1297	176.2445	54.2	8.17	1396	239.00	60.00	205.00	239.00	14.50	0.56	6.70	101.00
ERR2240516	TVZ	Rotorua	5	-38.1657	176.2505	56.8	8.55	1824	482.00	109.00	85.00	351.00	43.00	0.27	5.90	152.00
ERR2240588	TVZ	Rotorua	6	-38.1297	176.2443	46.8	7.37	1233	248.00	69.00	222.00	265.00	18.90	0.39	7.10	109.00
ERR2240589	TVZ	Rotorua	7	-38.1298	176.2438	53.2	6.89	1570	324.00	84.00	273.00	314.00	26.00	0.36	7.30	118.00
ERR2240629	TVZ	Rotorua	8	-38.164	176.2522	93.8	9.27	2252	563.00	52.00	84.00	418.00	29.00	0.39	6.40	105.00
ERR2240637	TVZ	Rotorua	9	-38.1309	176.2441	59.5	4.11	1359	208.00	158.00	44.00	172.00	19.70	0.82	10.10	136.00
ERR2240654	TVZ	Rotorua	10	-38.1641	176.253	73.2	2.71	4583	373.00	515.00	24.00	285.00	30.00	0.36	5.40	153.00
ERR2240662	TVZ	Rotorua	11	-38.1642	176.2528	72.0	3.04	3560	425.00	370.00	34.00	320.00	36.00	0.28	5.60	141.00
ERR2240672	TVZ	Rotorua	12	-38.1621	176.2555	79.6	6.35	2560	490.00	184.00	65.00	385.00	36.00	0.45	7.60	154.00
ERR2240680	TVZ	Rotorua	13	-38.1643	176.2528	55.9	3.01	3468	464.00	418.00	48.00	378.00	44.00	0.85	5.60	144.00
ERR2240707	TVZ	Rotorua	14	-38.1621	176.2565	67.5	7.46	2811	499.00	197.00	39.00	404.00	37.00	0.39	6.50	130.00
ERR2240712	TVZ	Rotorua	15	-38.1619	176.2565	94.1	6.04	2658	482.00	193.00	39.00	392.00	37.00	0.69	7.80	133.00
ERR2240716	TVZ	Rotorua	16	-38.1612	176.2579	58.9	7.02	2363	694.00	185.00	40.00	527.00	39.00	0.66	11.90	97.00

SRA number	Area	Geothermal field	N°	Latitude	Longitude	T (°C)	pH	EC (µS/cm)	Cl^- (mg/l)	SO_4^{2-} (mg/l)	HCO_3^- (mg/l)	Na^+ (mg/l)	K^+ (mg/l)	Mg^{2+} (mg/l)	Ca^{2+} (mg/l)	Si (mg/l)
ERR2240728	TVZ	Rotorua	17	-38.1611	176.258	61.5	6.87	2261	691.00	146.00	61.00	509.00	34.00	0.24	8.70	94.00
ERR2240756	TVZ	Rotorua	18	-38.1619	176.2592	79.3	5.72	2495	480.00	229.00	24.00	410.00	49.00	0.35	7.40	124.00
ERR2240786	TVZ	Rotorua	19	-38.1625	176.2583	86.5	8.18	2564	549.00	181.00	86.00	448.00	52.00	0.73	10.80	141.00
ERR2240797	TVZ	Rotorua	20	-38.1628	176.2545	86.8	6.39	2410	510.00	156.00	83.00	422.00	34.00	0.32	8.10	92.00
ERR2240800	TVZ	Rotorua	21	-38.1627	176.2581	88.0	7.97	2330	571.00	122.00	147.00	486.00	45.00	0.26	8.10	116.00
ERR2240809	TVZ	Rotorua	22	-38.1628	176.2582	92.1	8.60	2153	543.00	158.00	57.00	429.00	44.00	0.25	6.40	124.00
ERR2240825	TVZ	Rotorua	23	-38.1629	176.2548	58.9	6.54	2666	489.00	179.00	85.00	404.00	54.00	0.24	7.90	85.00
ERR2240865	TVZ	Rotorua	24	-38.163	176.2544	66.9	2.37	3216	330.00	428.00	51.00	270.00	38.00	0.44	6.40	119.00
ERR2240874	TVZ	Rotorua	25	-38.1638	176.2542	98.5	8.68	2492	607.00	111.00	186.00	512.00	70.00	0.13	5.00	186.00
ERR2240258	TVZ	Tikitere	1	-38.0611	176.3593	46.6	4.03	1120	2.20	403.00	213.00	11.70	5.10	2.30	12.50	80.00
ERR2240260	TVZ	Tikitere	2	-38.061	176.3592	57.0	3.00	1359	2.10	406.00	88.00	11.70	6.30	1.80	10.70	120.00
ERR2240270	TVZ	Tikitere	3	-38.0608	176.3587	88.4	1.57	12540	2.80	2418.00	33.00	10.70	6.50	1.80	10.30	107.00
ERR2240271	TVZ	Tikitere	4	-38.0608	176.3586	82.3	1.68	9265	2.60	1779.00	40.00	14.00	8.80	1.70	11.80	110.00
ERR2240272	TVZ	Tikitere	5	-38.0607	176.3587	73.4	1.70	8799	2.50	1708.00	43.00	13.40	9.10	1.70	9.90	113.00
ERR2240273	TVZ	Tikitere	6	-38.0608	176.3587	57.2	2.85	1473	1.10	390.00	70.00	14.70	9.20	1.10	10.60	117.00
ERR2240276	TVZ	Tikitere	7	-38.0609	176.3586	74.6	2.22	3265	0.90	700.00	105.00	13.00	7.40	0.83	6.90	132.00
ERR2240284	TVZ	Tikitere	8	-38.0608	176.3582	76.6	3.81	1827	1.80	695.00	117.00	14.60	8.50	5.10	18.20	98.00
ERR2240285	TVZ	Tikitere	9	-38.0607	176.3582	64.3	5.68	2182	2.20	819.00	94.00	10.10	4.10	2.00	7.60	75.00
ERR2240286	TVZ	Tikitere	10	-38.0607	176.3583	63.1	3.71	2337	2.30	904.00	51.00	7.80	5.90	0.77	6.00	94.00
ERR2240290	TVZ	Tikitere	11	-38.0606	176.3586	64.2	3.85	1287	1.60	462.00	38.00	9.60	5.30	1.30	6.20	94.00
ERR2240292	TVZ	Tikitere	12	-38.0612	176.3581	80.6	5.93	4794	1.10	1596.00	35.00	3.10	2.90	0.68	6.80	55.00
ERR2240393	TVZ	Tikitere	13	-38.0597	176.3591	54.7	2.33	3935	1.80	1231.00	104.00	5.70	4.30	0.68	6.90	88.00
ERR2240400	TVZ	Tikitere	14	-38.0593	176.359	69.0	1.99	5464	8.20	1393.00	36.00	12.90	6.40	1.30	7.00	106.00
ERR2240411	TVZ	Tikitere	15	-38.0593	176.3591	73.0	2.53	3050	0.09	834.00	48.00	9.30	9.30	1.90	10.90	100.00
ERR2240414	TVZ	Tikitere	16	-38.0592	176.3592	54.4	2.49	2994	0.06	780.00	39.00	10.00	9.40	2.00	12.50	93.00
ERR2240417	TVZ	Tikitere	17	-38.059	176.359	63.3	2.28	3208	0.05	808.00	22.00	15.80	7.30	3.90	16.10	131.00
ERR2240434	TVZ	Tikitere	18	-38.0589	176.3589	60.4	6.47	1059	1.80	478.00	119.00	7.70	5.00	1.10	6.90	81.00

SRA number	Area	Geothermal field	N°	Latitude	Longitude	T (°C)	pH	EC (µS/cm)	Cl^- (mg/l)	SO_4^{2-} (mg/l)	HCO_3^- (mg/l)	Na^+ (mg/l)	K^+ (mg/l)	Mg^{2+} (mg/l)	Ca^{2+} (mg/l)	Si (mg/l)
ERR2240436	TVZ	Tikitere	19	-38.0587	176.3594	86.8	6.05	2343	3.40	985.00	28.00	8.10	6.00	2.30	15.50	56.00
ERR2240439	TVZ	Tikitere	20	-38.0592	176.3604	78.5	6.48	489	4.60	33.00	359.00	41.00	7.20	0.35	6.80	100.00
ERR2240442	TVZ	Tikitere	21	-38.063	176.361	74.3	6.21	236	5.30	58.00	89.00	38.00	7.80	1.40	11.90	78.00
ERR2240444	TVZ	Tikitere	22	-38.063	176.3609	60.6	5.53	283	5.30	131.00	66.00	38.00	8.10	1.50	9.30	82.00
ERR2240462	TVZ	Tikitere	23	-38.0609	176.3594	66.8	2.00	3891	4.00	875.00	30.00	43.00	8.90	2.80	10.60	105.00
ERR2240495	TVZ	Tikitere	24	-38.0642	176.361	44.4	2.00	5297	3.90	1309.00	66.00	32.00	10.90	2.40	13.30	90.00
ERR2240498	TVZ	Tikitere	25	-38.0645	176.361	45.3	2.30	2816	4.30	660.00	34.00	27.00	7.00	3.10	21.00	69.00
ERR2240527	TVZ	Tokaanu	1	-38.9675	175.7645	46.0	7.14	10120	3234.00	66.00	33.00	1821.00	156.00	0.24	42.00	122.00
ERR2240528	TVZ	Tokaanu	2	-38.9676	175.7644	55.7	6.82	10420	3180.00	66.00	42.00	1827.00	156.00	0.29	41.00	121.00
ERR2240529	TVZ	Tokaanu	3	-38.9679	175.7646	87.1	6.75	10340	3152.00	67.00	95.00	1825.00	156.00	0.92	47.00	160.00
ERR2240530	TVZ	Tokaanu	4	-38.9679	175.7647	72.7	7.35	10650	3213.00	68.00	78.00	1817.00	159.00	0.80	45.00	160.00
ERR2240531	TVZ	Tokaanu	5	-38.968	175.7644	82.9	7.31	10350	3158.00	65.00	59.00	1875.00	165.00	0.14	44.00	161.00
ERR2240532	TVZ	Tokaanu	6	-38.9679	175.7644	41.0	6.47	9823	2954.00	65.00	96.00	1675.00	146.00	0.63	40.00	147.00
ERR2240533	TVZ	Tokaanu	7	-38.968	175.7644	66.7	6.79	10440	3228.00	69.00	90.00	1893.00	163.00	0.83	47.00	174.00
ERR2240578	TVZ	Tokaanu	8	-38.9683	175.7634	41.3	5.58	5443	1709.00	58.00	41.00	967.00	82.00	1.50	28.00	74.00
ERR2240579	TVZ	Tokaanu	9	-38.9684	175.7633	47.2	5.68	8115	2519.00	72.00	23.00	1411.00	125.00	0.50	34.00	125.00
ERR2240580	TVZ	Tokaanu	10	-38.9684	175.7631	48.0	6.79	9744	2953.00	63.00	52.00	1697.00	135.00	0.27	39.00	117.00
ERR2240581	TVZ	Tokaanu	11	-38.9684	175.763	53.1	6.09	10020	3042.00	74.00	60.00	1715.00	139.00	0.34	45.00	139.00
ERR2240584	TVZ	Tokaanu	12	-38.9686	175.7627	51.5	5.92	5753	2036.00	51.00	47.00	1132.00	83.00	0.97	35.00	97.00
ERR2240619	TVZ	Tokaanu	13	-38.9683	175.7622	51.9	6.23	5291	1563.00	28.00	48.00	841.00	68.00	1.10	22.00	72.00
ERR2240622	TVZ	Tokaanu	14	-38.9682	175.7624	49.4	6.71	6735	1989.00	49.00	56.00	1151.00	86.00	1.90	43.00	101.00
ERR2240623	TVZ	Tokaanu	15	-38.9688	175.7624	59.9	6.61	4010	1100.00	29.00	169.00	625.00	52.00	4.20	50.00	119.00
ERR2240625	TVZ	Tokaanu	16	-38.9682	175.7625	45.4	6.18	9044	2677.00	58.00	38.00	1551.00	121.00	1.70	39.00	116.00
ERR2240903	TVZ	Waikite	1	-38.3279	176.2978	48.8	8.47	873	125.00	27.00	244.00	199.00	11.80	0.92	11.00	92.00
ERR2240904	TVZ	Waikite	2	-38.3281	176.3014	65.1	8.29	1188	140.00	35.00	312.00	285.00	10.80	0.60	13.00	94.00
ERR2240905	TVZ	Waikite	3	-38.3269	176.3049	96.5	7.27	1247	140.00	34.00	354.00	283.00	11.40	0.52	14.60	97.00
ERR2240906	TVZ	Waikite	4	-38.3269	176.3049	93.3	7.49	1298	142.00	35.00	352.00	276.00	11.50	0.89	17.00	96.00

SRA number	Area	Geothermal field	N°	Latitude	Longitude	T (°C)	pH	EC (µS/cm)	Cl^- (mg/l)	SO_4^{2-} (mg/l)	HCO_3^- (mg/l)	Na^+ (mg/l)	K^+ (mg/l)	Mg^{2+} (mg/l)	Ca^{2+} (mg/l)	Si (mg/l)
ERR2240907	TVZ	Waikite	5	-38.3269	176.3045	88.8	7.59	1231	137.00	35.00	329.00	285.00	11.20	0.66	16.00	97.00
ERR2240908	TVZ	Waikite	6	-38.327	176.3037	93.2	8.14	1233	141.00	35.00	311.00	160.00	6.00	0.41	7.90	54.00
ERR2240909	TVZ	Waikite	7	-38.327	176.3035	55.6	8.75	1318	151.00	37.00	302.00	288.00	10.90	0.47	9.00	98.00
ERR2240910	TVZ	Waikite	8	-38.3272	176.3031	48.2	8.90	1330	153.00	38.00	298.00	292.00	11.00	0.44	9.00	99.00
ERR2240164	TVZ	Waimangu	1	-38.2829	176.3989	98.8	7.65	2155	471.00	150.00	103.00	670.00	89.00	2.10	28.00	283.00
ERR2240165	TVZ	Waimangu	2	-38.2828	176.3989	88.6	8.22	2218	483.00	152.00	88.00	576.00	79.00	1.30	23.00	250.00
ERR2240166	TVZ	Waimangu	3	-38.2829	176.3989	95.2	6.49	1873	371.00	164.00	133.00	530.00	74.00	4.20	37.00	236.00
ERR2240171	TVZ	Waimangu	4	-38.2827	176.3986	97.2	8.78	2699	595.00	123.00	75.00	790.00	113.00	0.21	19.40	368.00
ERR2240215	TVZ	Waimangu	5	-38.2828	176.3977	70.0	4.72	2678	678.00	178.00	31.00	746.00	85.00	6.10	29.00	245.00
ERR2240218	TVZ	Waimangu	6	-38.2828	176.3976	89.5	6.76	2888	775.00	105.00	45.00	690.00	78.00	1.90	21.00	240.00
ERR2240221	TVZ	Waimangu	7	-38.2829	176.3974	86.9	5.81	2422	551.00	219.00	51.00	677.00	60.00	2.90	16.40	217.00
ERR2240234	TVZ	Waimangu	8	-38.2826	176.3989	62.0	6.35	2173	563.00	70.00	58.00	648.00	106.00	12.70	35.00	269.00
ERR2240235	TVZ	Waimangu	9	-38.2826	176.3989	51.9	6.53	2022	462.00	171.00	50.00	526.00	97.00	17.80	61.00	233.00
ERR2240236	TVZ	Waimangu	10	-38.2825	176.399	59.7	6.04	2042	510.00	68.00	91.00	550.00	87.00	13.90	42.00	215.00
ERR2240237	TVZ	Waimangu	11	-38.283	176.3994	89.1	8.02	2402	528.00	135.00	174.00	729.00	100.00	0.20	17.20	301.00
ERR2240300	TVZ	Waimangu	12	-38.283	176.3997	70.2	6.75	1445	278.00	90.00	148.00	217.00	31.00	1.00	7.20	121.00
ERR2240307	TVZ	Waimangu	13	-38.2833	176.3999	62.1	8.66	1923	465.00	133.00	96.00	326.00	43.00	0.36	7.10	104.00
ERR2240314	TVZ	Waimangu	14	-38.2831	176.3968	90.5	5.88	2256	550.00	205.00	52.00	388.00	33.00	1.50	8.20	130.00
ERR2240337	TVZ	Waimangu	15	-38.2784	176.4085	93.6	7.60	2355	583.00	94.00	160.00	416.00	45.00	0.19	5.60	191.00
ERR2240342	TVZ	Waimangu	16	-38.2785	176.4087	70.7	7.23	2546	615.00	99.00	172.00	413.00	43.00	0.33	7.00	167.00
ERR2240356	TVZ	Waimangu	17	-38.2793	176.4094	60.6	8.98	2595	704.00	79.00	115.00	474.00	41.00	0.19	8.70	136.00
ERR2240360	TVZ	Waimangu	18	-38.2802	176.4074	88.1	8.13	1408	189.00	97.00	298.00	239.00	27.00	2.70	14.10	139.00
ERR2240361	TVZ	Waimangu	19	-38.2801	176.4074	73.6	7.89	1673	286.00	106.00	220.00	259.00	32.00	0.28	13.80	125.00
ERR2240535	TVZ	Waimangu	20	-38.2828	176.3987	97.6	7.85	2446	536.00	151.00	89.00	355.00	48.00	3.00	17.10	144.00
ERR2240537	TVZ	Waimangu	21	-38.2828	176.3986	91.0	7.56	2572	556.00	164.00	72.00	404.00	49.00	2.30	17.60	147.00
ERR2240836	TVZ	Waimangu	22	-38.27	176.4175	98.0	9.33	3343	691.00	133.00	137.00	620.00	35.00	0.20	5.00	204.00
ERR2240837	TVZ	Waimangu	23	-38.2686	176.4195	90.0	6.88	2112	336.00	92.00	221.00	312.00	29.00	4.00	11.30	107.00

SRA number	Area	Geothermal field	N°	Latitude	Longitude	T (°C)	pH	EC (µS/cm)	Cl^- (mg/l)	SO_4^{2-} (mg/l)	HCO_3^- (mg/l)	Na^+ (mg/l)	K^+ (mg/l)	Mg^{2+} (mg/l)	Ca^{2+} (mg/l)	Si (mg/l)
ERR2240839	TVZ	Waimangu	24	-38.2641	176.4188	96.9	8.56	315	42.00	23.00	32.00	48.00	3.70	0.56	6.20	40.00
ERR2240176	TVZ	Waiotapu	1	-38.3582	176.3695	67.2	4.80	5007	1313.00	209.00	76.00	1069.00	139.00	0.69	36.00	158.00
ERR2240206	TVZ	Waiotapu	2	-38.3611	176.3688	48.8	2.41	3660	490.00	512.00	28.00	522.00	97.00	5.60	38.00	179.00
ERR2240318	TVZ	Waiotapu	3	-38.3618	176.3684	74.8	5.12	2340	586.00	260.00	61.00	345.00	34.00	0.61	18.20	126.00
ERR2240319	TVZ	Waiotapu	4	-38.3618	176.3685	66.0	5.06	2361	594.00	265.00	74.00	353.00	35.00	0.47	15.00	127.00
ERR2240320	TVZ	Waiotapu	5	-38.3618	176.3685	89.5	5.38	2229	564.00	254.00	57.00	337.00	33.00	0.46	14.40	121.00
ERR2240322	TVZ	Waiotapu	6	-38.3618	176.3683	41.3	2.59	3824	661.00	458.00	189.00	401.00	42.00	0.57	18.20	124.00
ERR2240327	TVZ	Waiotapu	7	-38.3618	176.3683	43.0	5.28	2802	769.00	123.00	226.00	456.00	40.00	1.10	25.00	135.00
ERR2240334	TVZ	Waiotapu	8	-38.362	176.368	45.8	2.04	6345	330.00	1420.00	61.00	217.00	28.00	2.60	22.00	138.00
ERR2240380	TVZ	Waiotapu	9	-38.3622	176.3679	75.2	2.17	5681	609.00	822.00	26.00	375.00	37.00	2.50	25.00	140.00
ERR2240384	TVZ	Waiotapu	10	-38.3619	176.3694	62.3	4.93	2486	673.00	83.00	44.00	369.00	60.00	0.36	15.80	191.00
ERR2240388	TVZ	Waiotapu	11	-38.3629	176.3688	40.8	2.40	4196	510.00	526.00	43.00	296.00	49.00	2.80	26.00	121.00
ERR2240389	TVZ	Waiotapu	12	-38.3613	176.3705	66.1	2.60	2730	228.00	518.00	110.00	183.00	33.00	2.70	24.00	104.00
ERR2240563	TVZ	Waiotapu	13	-38.3506	176.377	82.3	2.31	3426	357.00	512.00	24.00	230.00	41.00	1.60	14.60	140.00
ERR2240924	TVZ	Waiotapu	14	-38.3622	176.3699	92.8	6.50	1361	1.90	367.00	26.00	23.00	11.80	2.20	40.00	70.00
ERR2240925	TVZ	Waiotapu	15	-38.3622	176.3701	83.4	5.55	2340	0.32	613.00	44.00	1.70	1.60	0.32	4.60	36.00
ERR2240129	TVZ	Wairakei-Tauhara	1	-38.6325	176.0981	44.6	6.65	1935	477.00	6.40	214.00	590.00	90.00	27.00	51.00	157.00
ERR2240519	TVZ	Wairakei-Tauhara	2	-38.7002	176.0845	63.1	6.39	1069	105.00	128.00	251.00	153.00	27.00	3.90	23.00	113.00
ERR2240520	TVZ	Wairakei-Tauhara	3	-38.7002	176.0844	55.3	6.80	1120	106.00	126.00	241.00	229.00	30.00	5.40	25.00	114.00
ERR2240521	TVZ	Wairakei-Tauhara	4	-38.7003	176.0842	45.4	6.64	1179	127.00	112.00	262.00	163.00	31.00	3.70	24.00	105.00
ERR2240522	TVZ	Wairakei-Tauhara	5	-38.7003	176.0843	61.6	6.93	1274	143.00	112.00	287.00	176.00	35.00	3.90	26.00	114.00
ERR2240523	TVZ	Wairakei-Tauhara	6	-38.7003	176.0843	57.0	7.00	1232	140.00	112.00	274.00	172.00	35.00	4.50	28.00	117.00
ERR2240524	TVZ	Wairakei-Tauhara	7	-38.7003	176.0842	51.9	7.01	1163	129.00	115.00	249.00	163.00	32.00	3.70	23.00	115.00
ERR2240525	TVZ	Wairakei-Tauhara	8	-38.7003	176.0842	60.5	6.35	1141	122.00	114.00	276.00	156.00	32.00	3.80	25.00	113.00
ERR2240526	TVZ	Wairakei-Tauhara	9	-38.7017	176.085	67.0	6.28	1376	163.00	100.00	343.00	188.00	35.00	4.10	26.00	118.00
ERR2240543	TVZ	Wairakei-Tauhara	10	-38.702	176.0852	45.0	6.71	1350	167.00	100.00	327.00	199.00	37.00	4.00	27.00	123.00
ERR2240544	TVZ	Wairakei-Tauhara	11	-38.7032	176.0865	51.2	6.38	1682	224.00	72.00	470.00	255.00	36.00	4.70	28.00	120.00

SRA number	Area	Geothermal field	N°	Latitude	Longitude	T (°C)	pH	EC (µS/cm)	Cl^- (mg/l)	SO_4^{2-} (mg/l)	HCO_3^- (mg/l)	Na^+ (mg/l)	K^+ (mg/l)	Mg^{2+} (mg/l)	Ca^{2+} (mg/l)	Si (mg/l)
ERR2240545	TVZ	Wairakei-Tauhara	12	-38.7044	176.087	56.7	6.49	1997	343.00	73.00	355.00	306.00	32.00	4.50	24.00	128.00
ERR2240546	TVZ	Wairakei-Tauhara	13	-38.7045	176.087	59.8	6.37	1927	325.00	71.00	354.00	286.00	31.00	4.70	25.00	113.00
ERR2240547	TVZ	Wairakei-Tauhara	14	-38.7045	176.087	54.7	6.51	2022	368.00	74.00	353.00	310.00	33.00	4.90	23.00	126.00
ERR2240548	TVZ	Wairakei-Tauhara	15	-38.7056	176.0865	55.0	7.15	1777	298.00	81.00	280.00	267.00	27.00	4.80	22.00	115.00
ERR2240549	TVZ	Wairakei-Tauhara	16	-38.7058	176.0867	59.9	6.41	1753	284.00	82.00	321.00	271.00	26.00	5.30	23.00	113.00
ERR2240550	TVZ	Wairakei-Tauhara	17	-38.708	176.0875	56.2	6.93	1857	318.00	53.00	329.00	278.00	29.00	4.80	22.00	119.00
ERR2240553	TVZ	Wairakei-Tauhara	18	-38.6706	176.0894	41.7	6.70	770	14.20	235.00	96.00	109.00	19.80	6.00	20.00	109.00
ERR2240555	TVZ	Wairakei-Tauhara	19	-38.6741	176.0998	71.6	6.90	1164	8.30	427.00	62.00	155.00	34.00	7.80	30.00	168.00
ERR2240990	TVZ	Wairakei-Tauhara	20	-38.7065	176.0874	72.5	6.28	1899	344.00	56.00	336.00	307.00	34.00	3.60	22.00	126.00
ERR2240991	TVZ	Wairakei-Tauhara	21	-38.7064	176.0876	40.3	8.21	1867	336.00	70.00	267.00	314.00	35.00	5.00	29.00	118.00
ERR2240513	TVZ	White Island	1	-37.5253	177.1904	84.0	5.41	1471	73.00	804.00	57.00	42.00	12.40	51.00	63.00	101.00
ERR2240565	TVZ	White Island	2	-37.5257	177.1903	68.0	3.13	4151	128.00	1969.00	60.00	240.00	29.00	171.00	381.00	125.00
ERR2240567	TVZ	White Island	3	-37.5256	177.1902	41.4	3.05	4299	126.00	2131.00	104.00	140.00	25.00	173.00	381.00	133.00

Supplementary Table 3-3 Observed richness, Shannon and Pielou indexes of the analyzed hot springs.

SRA number	Area	Geothermal field	N°	Observed	Shannon	Pielou
TAT10_60.7_42	APVF	El Tatio	1	66	2.91	0.69
TAT11_62.0_46	APVF	El Tatio	2	128	3.37	0.70
TAT12_61.0_53	APVF	El Tatio	3	78	2.97	0.68
TAT13_50.0_92	APVF	El Tatio	4	85	2.66	0.60
TAT2_62.0_5	APVF	El Tatio	5	91	3.25	0.72
TAT3_55.0_65	APVF	El Tatio	6	129	3.35	0.69
TAT5_55.0_70	APVF	El Tatio	7	84	3.03	0.68
TAT6_60.0_23	APVF	El Tatio	8	94	3.58	0.79
TAT7_50.0_76	APVF	El Tatio	9	65	2.81	0.67
TAT8_60.0_32	APVF	El Tatio	10	245	3.33	0.61
TAT9_62.7_37	APVF	El Tatio	11	166	3.50	0.68
SRR8420032	YPVF	Yellowstone	1	129	3.50	0.72
SRR8420033	YPVF	Yellowstone	8	222	3.55	0.66
SRR8420034	YPVF	Yellowstone	9	197	4.11	0.78
SRR8420035	YPVF	Yellowstone	10	63	2.90	0.70
SRR8420036	YPVF	Yellowstone	11	578	4.71	0.74
SRR8420037	YPVF	Yellowstone	12	199	3.39	0.64
SRR8420038	YPVF	Yellowstone	13	391	4.39	0.73
SRR8420039	YPVF	Yellowstone	14	118	3.88	0.81
SRR8420040	YPVF	Yellowstone	15	89	3.39	0.76
SRR8420041	YPVF	Yellowstone	16	156	3.87	0.77
SRR8420042	YPVF	Yellowstone	2	291	4.20	0.74
SRR8420043	YPVF	Yellowstone	3	170	4.20	0.82
SRR8420044	YPVF	Yellowstone	4	104	3.18	0.68
SRR8420045	YPVF	Yellowstone	17	79	3.26	0.75
SRR8420046	YPVF	Yellowstone	5	117	3.76	0.79
SRR8420047	YPVF	Yellowstone	6	63	1.98	0.48

SRA number	Area	Geothermal field	N°	Observed	Shannon	Pielou
SRR8420048	YPVF	Yellowstone	7	192	3.75	0.71
SRR8420049	YPVF	Yellowstone	18	266	4.38	0.78
SRR8420050	YPVF	Yellowstone	19	71	3.10	0.73
SRR8420052	YPVF	Yellowstone	20	38	1.89	0.52
SRR8420053	YPVF	Yellowstone	21	74	2.28	0.53
SRR8420054	YPVF	Yellowstone	22	111	3.54	0.75
SRR8420055	YPVF	Yellowstone	23	122	3.79	0.79
SRR8420056	YPVF	Yellowstone	24	63	2.93	0.71
SRR8420057	YPVF	Yellowstone	25	87	3.23	0.72
SRR10580885	ETPGB	Batang	1	115	2.37	0.50
SRR10580888	ETPGB	Batang	2	110	2.74	0.58
SRR10580889	ETPGB	Batang	3	105	2.70	0.58
SRR10580891	ETPGB	Batang	4	159	3.37	0.67
SRR10580894	ETPGB	Batang	5	204	3.06	0.57
SRR10580896	ETPGB	Batang	6	638	5.14	0.80
SRR10580898	ETPGB	Batang	7	196	1.63	0.31
SRR10580884	ETPGB	Kangding	1	127	1.61	0.33
SRR10580886	ETPGB	Kangding	2	91	1.99	0.44
SRR10580890	ETPGB	Kangding	3	479	3.95	0.64
SRR10580892	ETPGB	Kangding	4	22	0.58	0.19
SRR10580895	ETPGB	Kangding	5	167	3.69	0.72
SRR10580897	ETPGB	Kangding	6	55	1.00	0.25
SRR10580899	ETPGB	Kangding	7	155	2.50	0.50
ERR2240344	TVZ	Orakei Korako	1	180	3.49	0.67
ERR2240345	TVZ	Orakei Korako	2	322	3.81	0.66
ERR2240346	TVZ	Orakei Korako	3	121	2.44	0.51
ERR2240347	TVZ	Orakei Korako	4	27	1.50	0.46
ERR2240348	TVZ	Orakei Korako	5	131	2.66	0.55

SRA number	Area	Geothermal field	N°	Observed	Shannon	Pielou
ERR2240349	TVZ	Orakei Korako	6	47	1.63	0.42
ERR2241038	TVZ	Orakei Korako	7	249	3.39	0.61
ERR2241039	TVZ	Orakei Korako	8	16	0.83	0.30
ERR2241040	TVZ	Orakei Korako	9	127	3.35	0.69
ERR2241041	TVZ	Orakei Korako	10	205	3.52	0.66
ERR2241044	TVZ	Orakei Korako	11	12	0.82	0.33
ERR2241045	TVZ	Orakei Korako	12	24	0.98	0.31
ERR2241046	TVZ	Orakei Korako	13	112	2.46	0.52
ERR2241047	TVZ	Orakei Korako	14	61	1.70	0.41
ERR2241048	TVZ	Orakei Korako	15	122	1.90	0.40
ERR2240422	TVZ	Rotorua	1	65	2.82	0.68
ERR2240473	TVZ	Rotorua	2	94	2.23	0.49
ERR2240483	TVZ	Rotorua	3	15	1.70	0.63
ERR2240508	TVZ	Rotorua	4	85	2.83	0.64
ERR2240516	TVZ	Rotorua	5	71	2.88	0.67
ERR2240588	TVZ	Rotorua	6	132	2.85	0.58
ERR2240589	TVZ	Rotorua	7	38	2.46	0.68
ERR2240629	TVZ	Rotorua	8	122	2.45	0.51
ERR2240637	TVZ	Rotorua	9	44	1.40	0.37
ERR2240654	TVZ	Rotorua	10	52	1.99	0.50
ERR2240662	TVZ	Rotorua	11	43	1.97	0.52
ERR2240672	TVZ	Rotorua	12	145	3.32	0.67
ERR2240680	TVZ	Rotorua	13	24	1.32	0.42
ERR2240707	TVZ	Rotorua	14	67	2.83	0.67
ERR2240712	TVZ	Rotorua	15	23	2.05	0.66
ERR2240716	TVZ	Rotorua	16	208	3.49	0.65
ERR2240728	TVZ	Rotorua	17	233	4.11	0.75
ERR2240756	TVZ	Rotorua	18	15	1.58	0.58

SRA number	Area	Geothermal field	N°	Observed	Shannon	Pielou
ERR2240786	TVZ	Rotorua	19	37	1.80	0.50
ERR2240797	TVZ	Rotorua	20	18	1.36	0.47
ERR2240800	TVZ	Rotorua	21	28	1.23	0.37
ERR2240809	TVZ	Rotorua	22	58	2.37	0.58
ERR2240825	TVZ	Rotorua	23	93	2.90	0.64
ERR2240865	TVZ	Rotorua	24	29	2.44	0.73
ERR2240874	TVZ	Rotorua	25	85	3.34	0.75
ERR2240258	TVZ	Tikitere	1	41	1.71	0.46
ERR2240260	TVZ	Tikitere	2	28	1.66	0.50
ERR2240270	TVZ	Tikitere	3	50	2.95	0.76
ERR2240271	TVZ	Tikitere	4	45	3.13	0.82
ERR2240272	TVZ	Tikitere	5	114	3.34	0.70
ERR2240273	TVZ	Tikitere	6	22	1.17	0.38
ERR2240276	TVZ	Tikitere	7	47	2.94	0.76
ERR2240284	TVZ	Tikitere	8	18	2.20	0.76
ERR2240285	TVZ	Tikitere	9	19	2.27	0.77
ERR2240286	TVZ	Tikitere	10	20	1.64	0.55
ERR2240290	TVZ	Tikitere	11	43	2.21	0.59
ERR2240292	TVZ	Tikitere	12	60	2.93	0.72
ERR2240393	TVZ	Tikitere	13	37	2.35	0.65
ERR2240400	TVZ	Tikitere	14	42	3.02	0.81
ERR2240411	TVZ	Tikitere	15	53	1.81	0.46
ERR2240414	TVZ	Tikitere	16	30	2.30	0.68
ERR2240417	TVZ	Tikitere	17	12	1.75	0.70
ERR2240434	TVZ	Tikitere	18	44	1.84	0.49
ERR2240436	TVZ	Tikitere	19	44	2.83	0.75
ERR2240439	TVZ	Tikitere	20	36	2.17	0.61
ERR2240442	TVZ	Tikitere	21	49	2.01	0.52

SRA number	Area	Geothermal field	N°	Observed	Shannon	Pielou
ERR2240444	TVZ	Tikitere	22	26	1.03	0.32
ERR2240462	TVZ	Tikitere	23	66	2.59	0.62
ERR2240495	TVZ	Tikitere	24	49	3.54	0.91
ERR2240498	TVZ	Tikitere	25	17	1.94	0.69
ERR2240527	TVZ	Tokaanu	1	80	2.27	0.52
ERR2240528	TVZ	Tokaanu	2	48	2.65	0.68
ERR2240529	TVZ	Tokaanu	3	18	0.14	0.05
ERR2240530	TVZ	Tokaanu	4	75	1.01	0.23
ERR2240531	TVZ	Tokaanu	5	102	3.30	0.71
ERR2240532	TVZ	Tokaanu	6	107	2.44	0.52
ERR2240533	TVZ	Tokaanu	7	61	1.62	0.39
ERR2240578	TVZ	Tokaanu	8	361	3.72	0.63
ERR2240579	TVZ	Tokaanu	9	239	3.26	0.59
ERR2240580	TVZ	Tokaanu	10	159	2.71	0.53
ERR2240581	TVZ	Tokaanu	11	209	3.67	0.69
ERR2240584	TVZ	Tokaanu	12	241	3.51	0.64
ERR2240619	TVZ	Tokaanu	13	264	4.77	0.86
ERR2240622	TVZ	Tokaanu	14	353	4.62	0.79
ERR2240623	TVZ	Tokaanu	15	72	3.15	0.74
ERR2240625	TVZ	Tokaanu	16	408	4.44	0.74
ERR2240903	TVZ	Waikite	1	271	3.68	0.66
ERR2240904	TVZ	Waikite	2	125	3.71	0.77
ERR2240905	TVZ	Waikite	3	198	3.85	0.73
ERR2240906	TVZ	Waikite	4	108	1.98	0.42
ERR2240907	TVZ	Waikite	5	529	4.61	0.73
ERR2240908	TVZ	Waikite	6	257	4.89	0.88
ERR2240909	TVZ	Waikite	7	110	3.59	0.76
ERR2240910	TVZ	Waikite	8	145	4.07	0.82

SRA number	Area	Geothermal field	N°	Observed	Shannon	Pielou
ERR2240164	TVZ	Waimangu	1	101	2.97	0.64
ERR2240165	TVZ	Waimangu	2	130	2.10	0.43
ERR2240166	TVZ	Waimangu	3	500	2.35	0.38
ERR2240171	TVZ	Waimangu	4	904	3.39	0.50
ERR2240215	TVZ	Waimangu	5	115	2.79	0.59
ERR2240218	TVZ	Waimangu	6	218	2.45	0.46
ERR2240221	TVZ	Waimangu	7	117	2.76	0.58
ERR2240234	TVZ	Waimangu	8	197	3.32	0.63
ERR2240235	TVZ	Waimangu	9	446	4.62	0.76
ERR2240236	TVZ	Waimangu	10	256	3.28	0.59
ERR2240237	TVZ	Waimangu	11	143	2.18	0.44
ERR2240300	TVZ	Waimangu	12	252	4.57	0.83
ERR2240307	TVZ	Waimangu	13	126	3.74	0.77
ERR2240314	TVZ	Waimangu	14	40	2.98	0.81
ERR2240337	TVZ	Waimangu	15	61	1.67	0.41
ERR2240342	TVZ	Waimangu	16	147	3.89	0.78
ERR2240356	TVZ	Waimangu	17	138	2.77	0.56
ERR2240360	TVZ	Waimangu	18	221	2.47	0.46
ERR2240361	TVZ	Waimangu	19	221	4.01	0.74
ERR2240535	TVZ	Waimangu	20	774	4.07	0.61
ERR2240537	TVZ	Waimangu	21	146	2.47	0.50
ERR2240836	TVZ	Waimangu	22	121	2.53	0.53
ERR2240837	TVZ	Waimangu	23	198	4.28	0.81
ERR2240839	TVZ	Waimangu	24	269	4.36	0.78
ERR2240176	TVZ	Waiotapu	1	39	0.89	0.24
ERR2240206	TVZ	Waiotapu	2	24	2.26	0.71
ERR2240318	TVZ	Waiotapu	3	39	2.92	0.80
ERR2240319	TVZ	Waiotapu	4	9	1.30	0.59

SRA number	Area	Geothermal field	N°	Observed	Shannon	Pielou
ERR2240320	TVZ	Waiotapu	5	23	2.88	0.92
ERR2240322	TVZ	Waiotapu	6	15	1.76	0.65
ERR2240327	TVZ	Waiotapu	7	18	1.27	0.44
ERR2240334	TVZ	Waiotapu	8	21	1.14	0.37
ERR2240380	TVZ	Waiotapu	9	130	3.98	0.82
ERR2240384	TVZ	Waiotapu	10	11	0.82	0.34
ERR2240388	TVZ	Waiotapu	11	23	1.40	0.45
ERR2240389	TVZ	Waiotapu	12	33	1.56	0.44
ERR2240563	TVZ	Waiotapu	13	169	4.61	0.90
ERR2240924	TVZ	Waiotapu	14	21	1.66	0.54
ERR2240925	TVZ	Waiotapu	15	319	3.33	0.58
ERR2240129	TVZ	Wairakei-Tauhara	1	191	3.09	0.59
ERR2240519	TVZ	Wairakei-Tauhara	2	108	3.72	0.79
ERR2240520	TVZ	Wairakei-Tauhara	3	188	3.68	0.70
ERR2240521	TVZ	Wairakei-Tauhara	4	194	3.16	0.60
ERR2240522	TVZ	Wairakei-Tauhara	5	58	2.25	0.55
ERR2240523	TVZ	Wairakei-Tauhara	6	200	4.31	0.81
ERR2240524	TVZ	Wairakei-Tauhara	7	202	4.45	0.84
ERR2240525	TVZ	Wairakei-Tauhara	8	104	3.62	0.78
ERR2240526	TVZ	Wairakei-Tauhara	9	60	1.72	0.42
ERR2240543	TVZ	Wairakei-Tauhara	10	101	3.27	0.71
ERR2240544	TVZ	Wairakei-Tauhara	11	107	2.68	0.57
ERR2240545	TVZ	Wairakei-Tauhara	12	159	3.45	0.68
ERR2240546	TVZ	Wairakei-Tauhara	13	244	4.63	0.84
ERR2240547	TVZ	Wairakei-Tauhara	14	257	4.52	0.82
ERR2240548	TVZ	Wairakei-Tauhara	15	273	4.34	0.77
ERR2240549	TVZ	Wairakei-Tauhara	16	208	3.88	0.73
ERR2240550	TVZ	Wairakei-Tauhara	17	366	4.60	0.78

SRA number	Area	Geothermal field	N°	Observed	Shannon	Pielou
ERR2240553	TVZ	Wairakei-Tauhara	18	438	5.12	0.84
ERR2240555	TVZ	Wairakei-Tauhara	19	225	4.24	0.78
ERR2240990	TVZ	Wairakei-Tauhara	20	500	5.31	0.85
ERR2240991	TVZ	Wairakei-Tauhara	21	718	5.61	0.85
ERR2240513	TVZ	White Island	1	28	1.35	0.41
ERR2240565	TVZ	White Island	2	33	1.27	0.36
ERR2240567	TVZ	White Island	3	82	2.55	0.58

CHAPTER 4: FINAL REMARKS

The main objective of this study was to evaluate the possibility to relate geological settings and geothermal processes to the microbial ecology of terrestrial hot springs on a global scale. Novel and pre-existing data were analyzed on the basis that hydrothermal water chemistry is conditioned by the geological setting and geothermal processes that occur before the water reaches the surface and that microbial communities are influenced by the physicochemical conditions and chemistry of this aqueous medium.

A database of 202 hot springs with a wide range of temperature and pH, as well as great compositional variability, was created through a field campaign to El Tatio geothermal field and bibliographic compilation of hydrochemical data and 16S rRNA amplicon sequences from the Taupo Volcanic Zone, the Yellowstone Plateau Volcanic field, and the Eastern Tibetan Plateau Geothermal Belt. This allowed the comparison of alpha diversity, beta diversity, and composition of microbial communities in different hydrochemical scenarios.

The most relevant results and contributions of this thesis were as follows:

- No statistically significant correlations were found between temperature and alpha diversity in any study zone. In contrast, observed richness and Shannon index were correlated with pH and SO_4^{2-} concentrations at temperatures below 70 ºC. This implies that acid-sulfate waters have lower diversity indexes compared to bicarbonate and NaCl water, at temperatures below 70 ºC.
- The structure of the thermal microbial community was partially influenced by temperature and pH gradients. SO_4^{2-}, Mg^{2+}, HCO_3^- and Si concentrations also showed a significant influence on beta diversity, although only 25% of the structure of the microbial communities was explained by water chemistry. This suggested that many other factors were also influencing these populations of microorganisms. Among them, 1) chemical parameters not analyzed in this study, such as dissolved oxygen, trace, and metal concentrations, and availability of carbon and nitrogen; 2) environmental parameters other than water chemistry, such as solar radiation and humidity; and 3) biotic interactions and viral activity. It is thought that a stronger relationship between hydrochemistry and microbial communities would be found in thermal communities dominated by chemolithotrophs, where inorganic compounds are used as energy sources.
- Microbial communities in the TVZ and the ETPGB were mainly composed of Aquificota and Proteobacteria phyla. More specifically, the dominant families in the TVZ were Aquificaceae, Hydrogenothermaceae, and Hydrogenobaculaceae. The two former Aquificota families also dominated the ETPGB along with the Thermaceae and Comamonadaceae families. In contrast, the El Tatio communities were mainly composed of the phyla Chloroflexota, Bacteroidota, and Cyanobacteria. The dominant families in this field were Chloroflexaceae, an uncultured member of Armatimonadota, Roseiflexaceae, and Nostocaceae. Similarly, Chloroflexota, Bacteroidota, and Cyanobacteria dominated in YPVF communities. The dominant families in the YPVF were Leptococcaceae, Roseiflexaceae, and Thermaceae.
- The highest correlations between hydrochemical gradients and abundance of dominant taxa (> 0.1%) were related to temperature, pH, and SO_4^{2-} variations. Some of the most relevant correlations were found between pH, SO_4^{2-} and members of Chloroflexaceae (Chloroflexota), Thermaceae (Deinococcota) families, and a family with uncultured members of Armatimonadota and pH. In contrast, memberes of Desulfurellaceae (Campilobacterota), a family with uncultured members of the phylum Thermoplasmatota and members of the family Acidithiobacillaceae (Proteobacteria) were negatively correlated with SO_4^{2-} and positively correlated with pH.

- Geographic distance did not explain the change in community composition across hydrothermal regions. Moreover, intercontinental microbial communities were taxonomically related. This might suggest a potential ancient divergence in the same taxonomic groups between globally distant thermal zones and thus with time, some endemic character in each of them.

Studying microorganisms inhabiting terrestrial hot springs has helped to understand biogeochemical cycles, the origin of life on Earth, and the potential existence of life beyond Earth. The approach proposed in this thesis contributes to elucidating how geological settings and geothermal processes have shaped the evolutionary history of these communities and how microorganisms have influenced their habitat. To further investigate this relationship between geological processes and microbial ecology would require a conceptual model of each geothermal system under study. It would be necessary to incorporate concentrations and speciations of metals and trace elements, in addition to the isotopic composition of the thermal fluids to characterize the sources of the fluid components and potential secondary processes occurring in the system such as phase separation, mixing fluids, water-rock interactions or evaporation. Once geothermal systems are well described, it would be necessary to recognize the taxonomic groups forming microbial communities and identify the metabolic pathway they use and their ecological role within the community.

BIBLIOGRAPHY

Alcamán, M.E., Fernandez, C., Delgado, A., Bergman, B., Díez, B., 2015. The cyanobacterium Mastigocladus fulfills the nitrogen demand of a terrestrial hot spring microbial mat. ISME J. 9, 2290–2303. https://doi.org/10.1038/ismej.2015.63

Alcorta, J., Espinoza, S., Viver, T., Alcamán-Arias, M.E., Trefault, N., Rosselló-Móra, R., Díez, B., 2018. Temperature modulates Fischerella thermalis ecotypes in Porcelana Hot Spring. Syst. Appl. Microbiol. 41, 531–543. https://doi.org/10.1016/j.syapm.2018.05.006

Alsop, E.B., Boyd, E.S., Raymond, J., 2014. Merging metagenomics and geochemistry reveals environmental controls on biological diversity and evolution. BMC Ecol. 14, 1–12. https://doi.org/10.1186/1472-6785-14-16

Amin, A., Ahmed, I., Salam, N., Kim, B.Y., Singh, D., Zhi, X.Y., Xiao, M., Li, W.J., 2017. Diversity and Distribution of Thermophilic Bacteria in Hot Springs of Pakistan. Microb. Ecol. 74, 116–127. https://doi.org/10.1007/s00248-017-0930-1

Arnórsson, S., Stefánsson, A., Bjarnason, J.Ö., 2007. Fluid-fluid interactions in geothermal systems. Rev. Mineral. Geochemistry 65, 259–312. https://doi.org/10.2138/rmg.2007.65.9

Baker-Austin, C., Dopson, M., 2007. Life in acid: pH homeostasis in acidophiles. Trends Microbiol. 15, 165–171. https://doi.org/10.1016/j.tim.2007.02.005

Bender, Madigan, Buckley, Sattley, Stahl, 2019. Brock Biology of Microorganisms, Fifteen edition.

Brock, T., 1978. Thermophilic microorganisms and life at high temperatures, Springer Series in Microbiology.

Callahan, B.J., McMurdie, P.J., Holmes, S.P., 2017. Exact sequence variants should replace operational taxonomic units in marker-gene data analysis. ISME J. 11, 2639–2643. https://doi.org/10.1038/ismej.2017.119

Chan, C.S., Chan, K.G., Ee, R., Hong, K.W., Urbieta, M.S., Donati, E.R., Shamsir, M.S., Goh, K.M., 2017. Effects of physiochemical factors on prokaryotic Biodiversity in Malaysian circumneutral hot springs. Front. Microbiol. 8. https://doi.org/10.3389/fmicb.2017.01252

Cole, J.K., Peacock, J.P., Dodsworth, J.A., Williams, A.J., Thompson, D.B., Dong, H., Wu, G., Hedlund, B.P., 2013. Sediment microbial communities in Great Boiling Spring are controlled by temperature and distinct from water communities. ISME J. 7, 718–729.

Colman, D.R., Feyhl-Buska, J., Fecteau, K.M., Xu, H., Shock, E.L., Boyd, E.S., 2016. Ecological differentiation in planktonic and sediment-associated chemotrophic microbial populations in Yellowstone hot springs. FEMS Microbiol. Ecol. 92. https://doi.org/10.1093/femsec/fiw137

Cox, A., Shock, E.L., Havig, J.R., 2011. The transition to microbial photosynthesis in hot spring ecosystems. Chem. Geol. 280, 344–351. https://doi.org/10.1016/j.chemgeo.2010.11.022

Daniele, L., Taucare, M., Viguier, B., Arancibia, G., Aravena, D., Roquer, T., Sepúlveda, J., Molina, E., Delgado, A., Muñoz, M., Morata, D., 2020. Exploring the shallow geothermal resources in the Chilean Southern Volcanic Zone: Insight from the Liquiñe thermal springs. J. Geochemical Explor. 218, 106611. https://doi.org/10.1016/j.gexplo.2020.106611

Djokic, T., VanKranendonk, M.J., Campbel, K.A., Walter, M.R., Ward, C.R., 2017. Earliest signs of life on land preserved in ca. 3.5 Ga hot spring deposits. Nat. Commun. 8, 1–8.

https://doi.org/10.1038/ncomms15263

Druschel, G.K., Kappler, A., 2015. Geomicrobiology and microbial geochemistry. Elements 11, 389–394. https://doi.org/10.2113/gselements.11.6.389

Giggenbach, W.F., 1991. Chemical techniques in geothermal exploration. Appl. Geochemistry Geotherm. Reserv. Dev. 119–144.

Giggenbach, W.F., 1988. Geothermal solute equilibria. Derivation of Na-K-Mg-Ca geoindicators. Geochim. Cosmochim. Acta 52, 2749–2765. https://doi.org/10.1016/0016-7037(88)90143-3

Gupta, Roy, 2005. Geothermal Energy: An alternative resource for the 21st century.

Hamilton, T.L., Bennett, A.C., Murugapiran, S.K., Havig, J.R., 2019. Anoxygenic Phototrophs Span Geochemical Gradients and Diverse Morphologies in Terrestrial Geothermal Springs. mSystems 4, 1–25. https://doi.org/10.1128/msystems.00498-19

Hedenquist, J.W., 1991. Boiling and dilution in the shallow portion of the Waiotapu geothermal system, New Zealand. Geochim. Cosmochim. Acta 55, 2753–2765. https://doi.org/10.1016/0016-7037(91)90442-8

Hou, W., Wang, S., Dong, H., Jiang, H., Briggs, B.R., Peacock, J.P., Huang, Q., Huang, L., Wu, G., Zhi, X., Li, W., Dodsworth, J.A., Hedlund, B.P., Zhang, C., Hartnett, H.E., Dijkstra, P., Hungate, B.A., 2013. A Comprehensive Census of Microbial Diversity in Hot Springs of Tengchong, Yunnan Province China Using 16S rRNA Gene Pyrosequencing. PLoS One 8. https://doi.org/10.1371/journal.pone.0053350

Inskeep, W.P., Jay, Z.J., Herrgard, M.J., Kozubal, M.A., Rusch, D.B., Tringe, S.G., Macur, R.E., Jennings, R. de M., Boyd, E.S., Spear, J.R., Roberto, F.F., 2013a. Phylogenetic and functional analysis of metagenome sequence from high-temperature archaeal habitats demonstrate linkages between metabolic potential and geochemistry. Front. Microbiol. 4. https://doi.org/10.3389/fmicb.2013.00095

Inskeep, W.P., Jay, Z.J., Tringe, S.G., Herrgård, M.J., Rusch, D.B., 2013b. The YNP metagenome project: Environmental parameters responsible for microbial distribution in the yellowstone geothermal ecosystem. Front. Microbiol. 4, 1–15. https://doi.org/10.3389/fmicb.2013.00067

Ionescu, D., Hindiyeh, M., Malkawi, H., Oren, A., 2010. Biogeography of thermophilic cyanobacteria: Insights from the Zerka Ma'in hot springs (Jordan). FEMS Microbiol. Ecol. 72, 103–113. https://doi.org/10.1111/j.1574-6941.2010.00835.x

Jolie, E., Scott, S., Faulds, J., Chambefort, I., Axelsson, G., Gutiérrez-Negrín, L.C., Regenspurg, S., Ziegler, M., Ayling, B., Richter, A., Zemedkun, M.T., 2021. Geological controls on geothermal resources for power generation. Nat. Rev. Earth Environ. 2, 324–339. https://doi.org/10.1038/s43017-021-00154-y

Kaasalainen, H., Stefánsson, A., 2012. The chemistry of trace elements in surface geothermal waters and steam, Iceland. Chem. Geol. 330–331, 60–85. https://doi.org/10.1016/j.chemgeo.2012.08.019

Kozubal, M.A., Macur, R.E., Jay, Z.J., Beam, J.P., Malfatti, S.A., Tringe, S.G., Kocar, B.D., Borch, T., Inskeep, W.P., 2012. Microbial iron cycling in acidic geothermal springs of Yellowstone National Park: Integrating molecular surveys, geochemical processes, and isolation of novel Fe-active microorganisms. Front. Microbiol. 3, 1–16. https://doi.org/10.3389/fmicb.2012.00109

Li, L., Ma, Z., 2019. Global microbiome diversity scaling in hot springs with DAR (Diversity-area relationship) profiles. Front. Microbiol. 10. https://doi.org/10.3389/fmicb.2019.00118

Li, S.J., Hua, Z.S., Huang, L.N., Li, J., Shi, S.H., Chen, L.X., Kuang, J.L., Liu, J., Hu, M., Shu, W.S., 2014. Microbial communities evolve faster in extreme environments. Sci. Rep. 4, 1–9. https://doi.org/10.1038/srep06205

Lutz, H., Newman, D.K., Kappler, A., 2016. Ehrlich's Geomicrobiology Sixth Edition, Ehrlich's Geomicrobiology. https://doi.org/10.1201/b19121

Mackenzie, R., Pedrós-Alió, C., Díez, B., 2013. Bacterial composition of microbial mats in hot springs in Northern Patagonia: Variations with seasons and temperature. Extremophiles 17, 123–136. https://doi.org/10.1007/s00792-012-0499-z

Massello, F.L., Chan, C.S., Chan, K.G., Goh, K.M., Donati, E., Urbieta, M.S., 2020. Meta-analysis of microbial communities in hot springs: Recurrent taxa and complex shaping factors beyond ph and temperature. Microorganisms 8, 1–18. https://doi.org/10.3390/microorganisms8060906

Moeck, I.S., 2014. Catalog of geothermal play types based on geologic controls. Renew. Sustain. Energy Rev. 37, 867–882. https://doi.org/10.1016/j.rser.2014.05.032

Nicholson, K., 1993. Geothermal fluids: Chemistry and exploration techniques, Journal of Geochemical Exploration. https://doi.org/10.1016/0375-6742(95)90013-6

Nordstrom, K.D., Blaine McCleskey, R., Ball, J.W., 2009. Sulfur geochemistry of hydrothermal waters in Yellowstone National Park: IV Acid-sulfate waters. Appl. Geochemistry 24, 191–207. https://doi.org/10.1016/j.apgeochem.2008.11.019

Papke, R.T., Ramsing, N.B., Bateson, M.M., Ward, D.M., 2003. Geographical isolation in hot spring cyanobacteria. Environ. Microbiol. 5, 650–659. https://doi.org/10.1046/j.1462-2920.2003.00460.x

Podar, P.T., Yang, Z., Björnsdóttir, S.H., Podar, M., 2020. Comparative Analysis of Microbial Diversity Across Temperature Gradients in Hot Springs From Yellowstone and Iceland. Front. Microbiol. 11, 1–16. https://doi.org/10.3389/fmicb.2020.01625

Power, J.F., Carere, C.R., Lee, C.K., Wakerley, G.L.J., Evans, D.W., Button, M., White, D., Climo, M.D., Hinze, A.M., Morgan, X.C., McDonald, I.R., Cary, S.C., Stott, M.B., 2018. Microbial biogeography of 925 geothermal springs in New Zealand. Nat. Commun. 9. https://doi.org/10.1038/s41467-018-05020-y

Prieto-Barajas, C.M., Valencia-Cantero, E., Santoyo, G., 2018. Microbial mat ecosystems: Structure types, functional diversity, and biotechnological application. Electron. J. Biotechnol. 31, 48–56. https://doi.org/10.1016/j.ejbt.2017.11.001

Quatrini, R., Johnson, D.B., 2019. Acidithiobacillus ferrooxidans. Trends Microbiol. 27, 282–283. https://doi.org/10.1016/j.tim.2018.11.009

Rampelotto, P.H., 2010. Resistance of microorganisms to extreme environmental conditions and its contribution to astrobiology. Sustainability 2, 1602–1623. https://doi.org/10.3390/su2061602

Reysenbach, A.L., Shock, E., 2002. Merging genomes with geochemistry in hydrothermal ecosystems. Science (80-.). 296, 1077–1082. https://doi.org/10.1126/science.1072483

Roulleau, E., Tardani, D., Sano, Y., Takahata, N., Vinet, N., Bravo, F., Muñoz, C., Sanchez, J., 2016. New insight from noble gas and stable isotopes of geothermal/hydrothermal fluids at Caviahue-Copahue Volcanic Complex: Boiling steam separation and water-rock interaction at shallow depth. J. Volcanol. Geotherm. Res. 328, 70–83. https://doi.org/10.1016/j.jvolgeores.2016.10.007

Schleper, C., Puehler, G., Holz, I., Gambacorta, A., Janekovic, D., Santarius, U., Klenk, H.P., Zillig, W., 1995. Picrophilus gen. nov., fam. nov.: A novel aerobic, heterotrophic, thermoacidophilic genus and

family comprising archaea capable of growth around pH 0. J. Bacteriol. 177, 7050–7059. https://doi.org/10.1128/jb.177.24.7050-7059.1995

Seckbach, Oren, 2010. Microbial mats: modern an ancient microorganisms in stratified systems, Cellular Origin, Life in Extreme Habitats and Astrobiology.

Sharp, C.E., Brady, A.L., Sharp, G.H., Grasby, S.E., Stott, M.B., Dunfield, P.F., 2014. Humboldt's spa: Microbial diversity is controlled by temperature in geothermal environments. ISME J. 8, 1166–1174. https://doi.org/10.1038/ismej.2013.237

Shock, E.L., Boyd, E.S., 2015. Principles of geobiochemistry. Elements 11, 395–401. https://doi.org/10.2113/gselements.11.6.395

Shock, E.L., Holland, M., Meyer-Dombard, D.R., Amend, J.P., 2005. Geochemical sources of energy for microbial metabolism in hydrothermal ecosystems: Obsidian Pool, Yellowstone National Park. Geotherm. Biol. Geochemistry Yellowstone Natl. Park 95–112.

Stewart, M.K., Hulston, J.R., 1975. Stable isotope ratios of volcanic steam from White Island, New Zealand. Bull. Volcanol. 39, 28–46. https://doi.org/10.1007/BF02596944

Takai, K., Nakamura, K., Toki, T., Tsunogai, U., Miyazaki, M., Miyazaki, J., Hirayama, H., Nakagawa, S., Nunoura, T., Horikoshi, K., 2008. Cell proliferation at 122°C and isotopically heavy CH4 production by a hyperthermophilic methanogen under high-pressure cultivation. Proc. Natl. Acad. Sci. U. S. A. 105, 10949–10954. https://doi.org/10.1073/pnas.0712334105

Tringe, S.G., Hugenholtz, P., 2018. A renaissance for the pioneering 16S rRNA gene. J. Volcanol. Geotherm. Res. 4, 1–15. https://doi.org/10.1073/pnas.1000080107

Urbieta, M.S., Donati, E.R., Chan, K.G., Shahar, S., Sin, L.L., Goh, K.M., 2015. Thermophiles in the genomic era: Biodiversity, science, and applications. Biotechnol. Adv. 33, 633–647. https://doi.org/10.1016/j.biotechadv.2015.04.007

Uribe-Lorío, L., Brenes-Guillén, L., Hernández-Ascencio, W., Mora-Amador, R., González, G., Ramírez-Umaña, C.J., Díez, B., Pedrós-Alió, C., 2019. The influence of temperature and pH on bacterial community composition of microbial mats in hot springs from Costa Rica. Microbiologyopen 8. https://doi.org/10.1002/mbo3.893

Wakai, S., 2019. Biochemical and thermodynamic analyses of energy conversion in extremophiles. Biosci. Biotechnol. Biochem. 83, 49–64. https://doi.org/10.1080/09168451.2018.1538769

Wang, S., Hou, W., Dong, H., Jiang, H., Huang, L., Wu, G., Zhang, C., Song, Z., Zhang, Y., Ren, H., Zhang, J., Zhang, L., 2013. Control of Temperature on Microbial Community Structure in Hot Springs of the Tibetan Plateau. PLoS One 8. https://doi.org/10.1371/journal.pone.0062901

White, W.M., 2005. Geochemistry W . M . White.

Winogradsky, 1887. Über schwefelbakterien. Bot. Zeitung 45, 488–610.

Wrage, J., Tardani, D., Reich, M., Daniele, L., Arancibia, G., Cembrano, J., Sánchez-Alfaro, P., Morata, D., Pérez-Moreno, R., 2017. Geochemistry of thermal waters in the Southern Volcanic Zone, Chile – Implications for structural controls on geothermal fluid composition. Chem. Geol. 466, 545–561. https://doi.org/10.1016/j.chemgeo.2017.07.004

Zhang, Y., Wu, G., Jiang, H., Yang, J., She, W., Khan, I., Li, W., 2018. Abundant and rare microbial biospheres respond differently to environmental and spatial factors in tibetan hot springs. Front. Microbiol. 9, 1–16. https://doi.org/10.3389/fmicb.2018.02096